
Recent Developments in $\gamma\gamma$ Collider Concepts from 125 GeV to 100 TeV

Physics At The Highest Energies With Colliders

Tim Barklow

SLAC National Accelerator Laboratory

July 29, 2025

Outline

- $\gamma\gamma$ Collider Introduction
- $\gamma\gamma$ Collider Higgs Factories
- Higgs Self Coupling Measurement at 280/380 GeV
- Accelerator and MDI
- Major Technical Challenges
- Multi-TeV $\gamma\gamma$ Colliders

Introduction

Compton $\gamma\gamma$ colliders -- where laser photons are up-converted to the energy of colliding e^- beams -- have been studied for more than 40 years, usually in the context of initial, supplemental, or follow-on stages of e^+e^- colliders. Recent innovations in photon science, particularly in XFEL technology, can lead to enhanced $\gamma\gamma$ collider capabilities beyond those of previous concepts

- Previous $\gamma\gamma$ collider concepts were limited to optical wavelength lasers due to the nascent status of XFEL's and an underappreciation of the particle physics advantages of $\gamma\gamma$ colliders with shorter wavelength lasers.
- e^+e^- collider proposals continue to be bedeviled by cost. As an alternative, $\gamma\gamma$ Higgs factories are of interest. They have a smaller footprint than any e^+e^- Higgs factory because there is no need to produce an associated Z boson \Rightarrow lower cost. Physics case for XFEL versions is more compelling than previous optical laser $\gamma\gamma$ colliders.
- If a 10 TeV WFA e^+e^- collider is not feasible due to e^+ acceleration issues, then the XFEL Compton $\gamma\gamma$ configuration of a 10 TeV WFA e^-e^- collider may provide the optimum particle physics environment for such a machine. An XFEL $\gamma\gamma$ collider Higgs factory would serve as a prototype for such a collider.

COLLIDING ge AND gg BEAMS BASED ON THE SINGLE-PASS e^-e^- COLLIDERS (VLEPP TYPE)

Ilya F. GINZBURG

Institute of Mathematics, Novosibirsk 90, U.S.S.R.

Gleb L. KOTKIN and Valery G. SERBO

Novosibirsk State University, Novosibirsk 90, U.S.S.R.

Valery I. TELNOV

Institute of Nuclear Physics, Novosibirsk 90, U.S.S.R.

Received 14 April 1982

CERN-TH/2001-235
CLIC-Note 500
NUHEP-EXP/01-050
UCRL-JC-145692

Higgs Physics with a $\gamma\gamma$ Collider Based on CLIC 1

D. Asner¹, H. Burkhardt², A. De Roeck², J. Ellis², J. Gronberg¹, S. Heinemeyer³,
M. Schmitt⁴, D. Schulte², M. Velasco⁴ and F. Zimmermann²

¹ Lawrence Livermore National Laboratory, Livermore, California 94550, USA

² CERN, CH-1211 Geneva 23, Switzerland

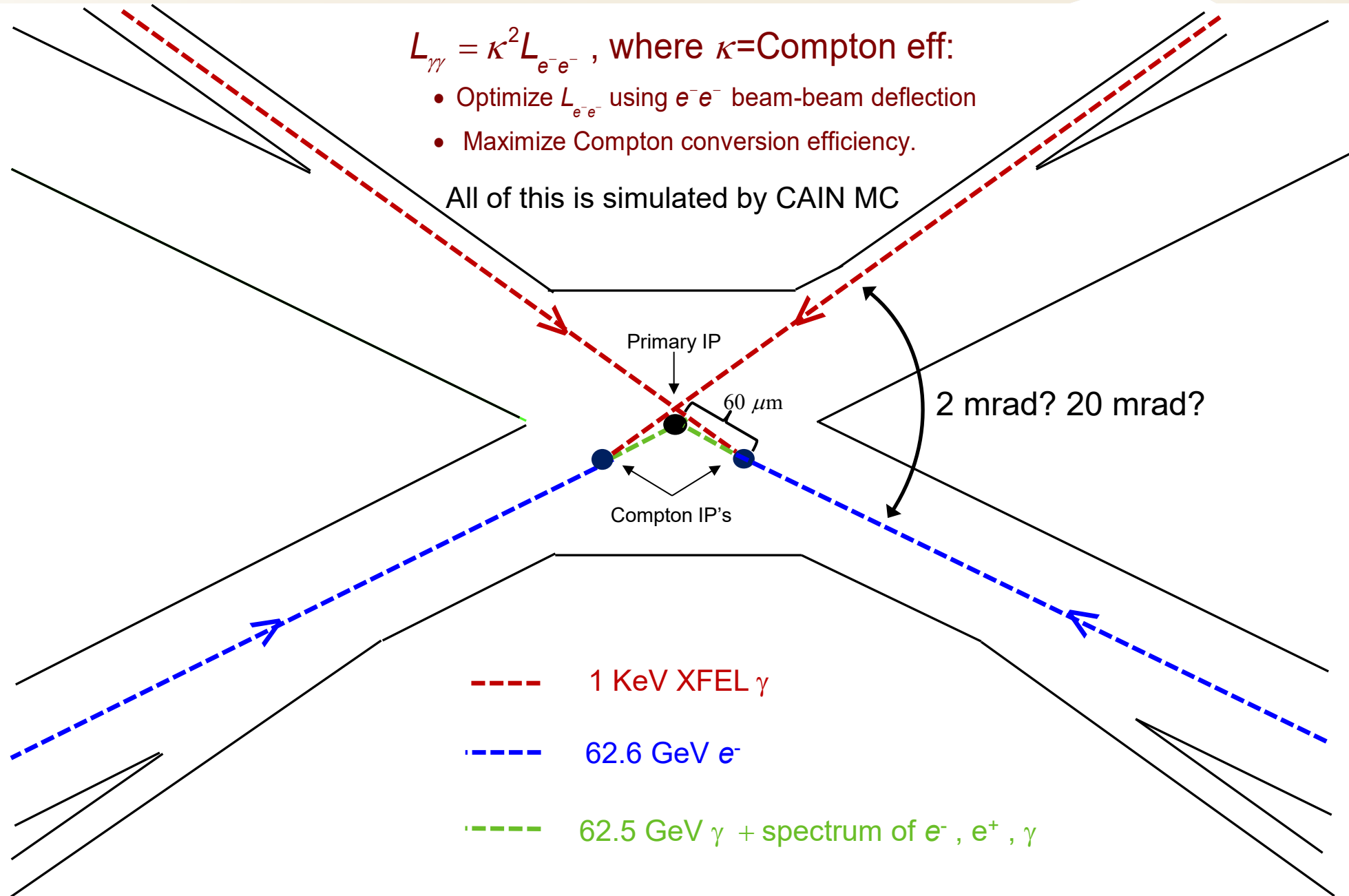
³ Brookhaven National Laboratory, Upton, New York, USA

⁴ Northwestern University, Evanston, Illinois 60201, USA

1 The Photon Collider at TESLA

B. Badelek⁴³, C. Blöchliger⁴⁴, J. Blümlein¹², E. Boos²⁸, R. Brinkmann¹²,
H. Burkhardt¹¹, P. Bussey¹⁷, C. Carimalo³³, J. Chyla³⁴, A.K. Çiftçi⁴, W. Decking,
A. De Roeck¹¹, V. Fadin¹⁰, M. Ferrario¹⁵, A. Finch²⁴, H. Fraas⁴⁴, F. Franke⁴⁴,
M. Galynskii²⁷, A. Gamp¹², I. Ginzburg³¹, R. Godbole⁶, D.S. Gorbunov²⁸,
G. Gounaris³⁹, K. Hagiwara²², L. Han¹⁹, R.-D. Heuer¹⁸, C. Heusch³⁶, J. Illana¹²,
V. Ilyin²⁸, P. Jankowski⁴³, Yi Jiang¹⁹, G. Jikia¹⁶, L. Jönsson²⁶, M. Kalachnikow⁸,
F. Kapusta³³, R. Klanner^{12,18}, M. Klasen¹², K. Kobayashi⁴¹, T. Kon⁴⁰, G. Kotkin,
M. Krämer¹⁴, M. Krawczyk⁴³, Y.P. Kuang⁷, E. Kuraev¹³, J. Kwiecinski²³,
M. Leenen¹², M. Levchuk²⁷, W.F. Ma¹⁹, H. Martyn¹, T. Mayer⁴⁴, M. Melles³⁵,
D.J. Miller²⁵, S. Mtingwa²⁹, M. Mühlleitner¹², B. Muryn²³, P.V. Nickles⁸, R. Oras

Layout of **laser** , **e⁻** beams near interaction point of $\gamma\gamma$ collider -- x=1000, XFEL Higgs Factory Example



The x variable in $\gamma\gamma$ colliders

$$x = \frac{4E_{e^-}\omega_0}{m_e^2} \quad \text{determines luminosity spectra}$$

ω_0 = laser photon energy

maximum Compton photon energy $\omega_m = \frac{x}{x+1} E_{e^-}$

angular divergence of photons $\theta_0 = \frac{m_e}{E_{e^-}} \sqrt{x+1}$

Important thresholds in x :

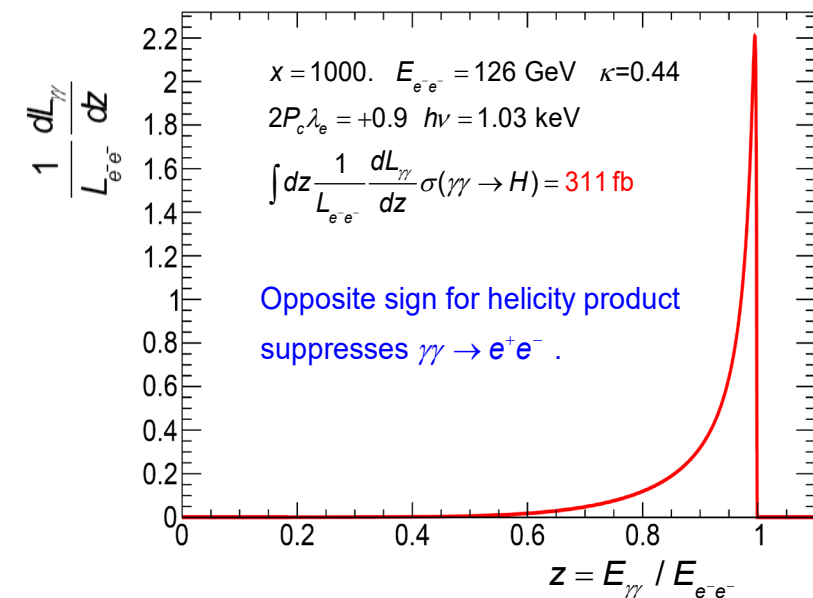
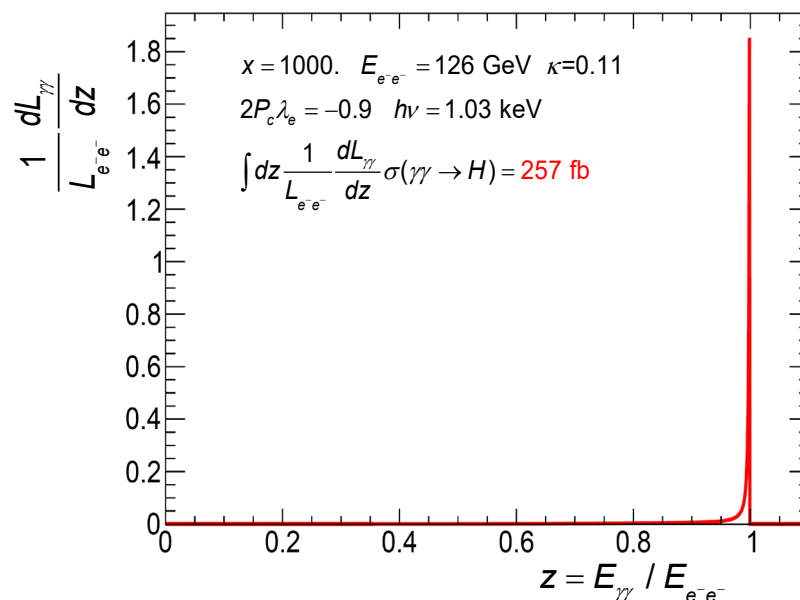
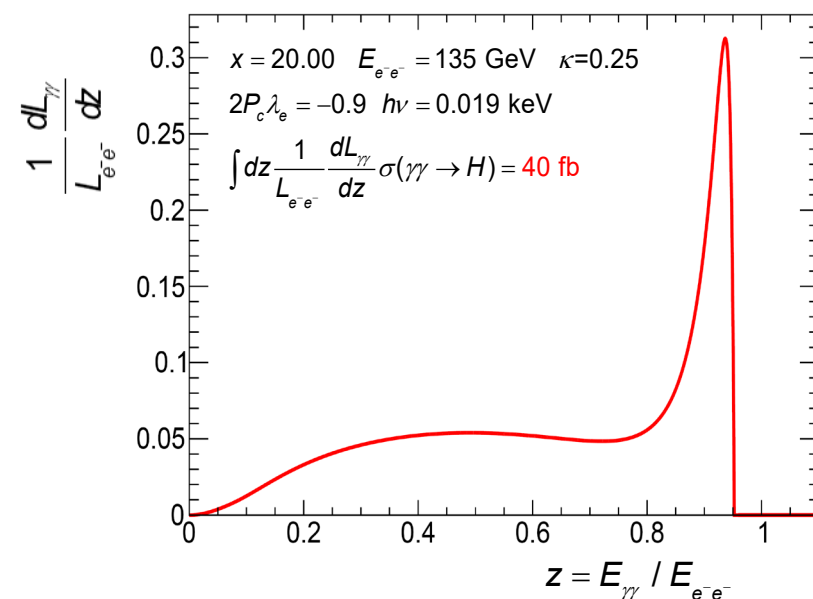
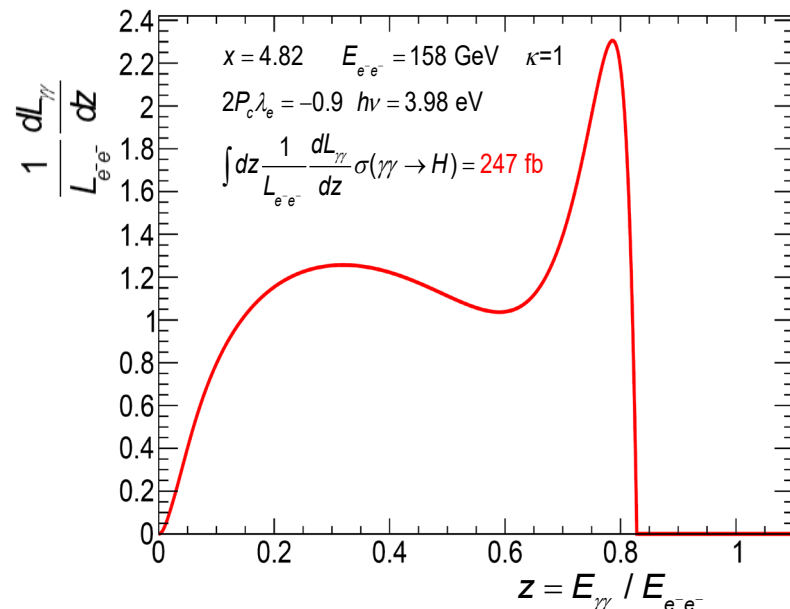
At $x = 4.82$ $\gamma\gamma_{\text{laser}} \rightarrow e^+e^-$ opens up which depletes the high energy photon beam and adds e^+ to mix of particles exiting Compton IP

At $x = 8$ $e^-\gamma_{\text{laser}} \rightarrow e^+e^-e^-$ opens up, with interesting consequences at different $\gamma\gamma \sqrt{s}$

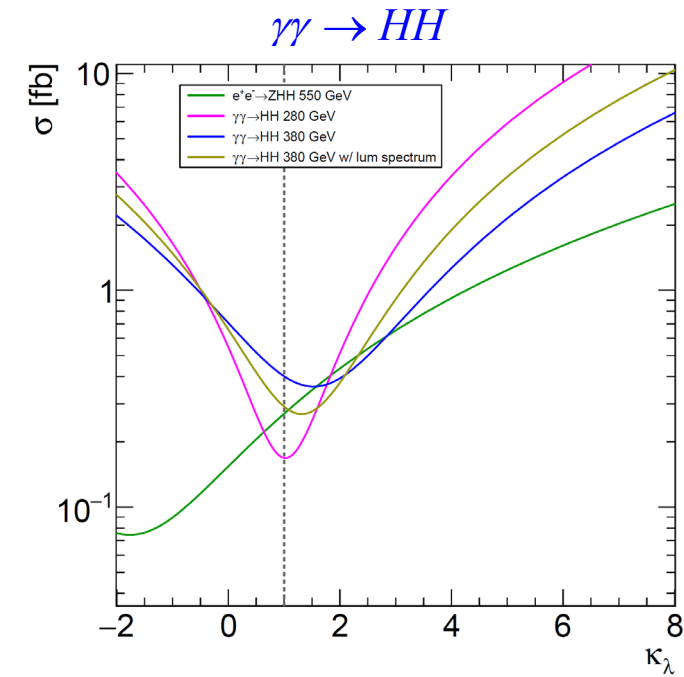
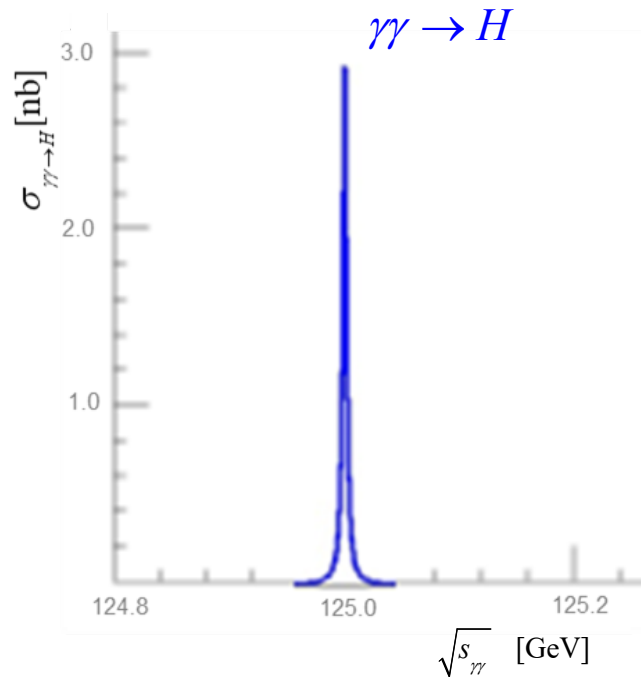
$\kappa = 1$ – prob that Compton γ annihilates with laser γ parameterizes depletion of high energy γ 's.

$$\sigma(\gamma\gamma \rightarrow H) = \frac{8\pi\Gamma_{\gamma\gamma}\Gamma_{\text{tot}}}{(s-M_H^2)^2 + \Gamma_{\text{tot}}^2 M_H^2} (1 + \xi_1 \xi_2)$$

$$\approx \frac{4\pi^2\Gamma_{\gamma\gamma}}{M_H^3} (1 + \xi_1 \xi_2) z_H \delta(z - z_H)$$



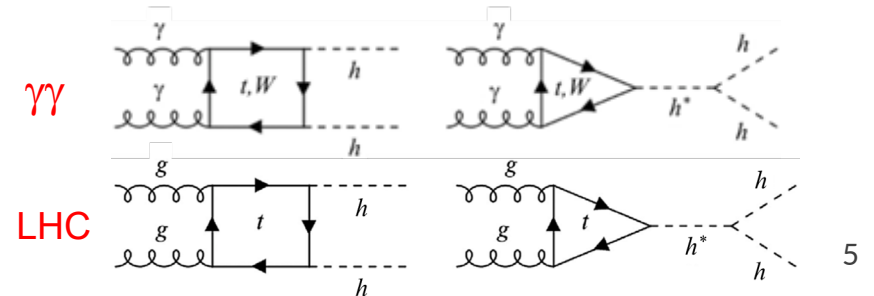
Higgs Production Cross Sections for $\gamma\gamma$, e^+e^- , $\mu^+\mu^-$ Initial States



	\sqrt{s} (GeV)	polarization	σ (fb)
$e^+e^- \rightarrow ZH$	250	-80% e^- +30% e^+	310
$\gamma\gamma \rightarrow H$	125	+100% γ +100% γ	3×10^6 [†]
$\mu^+\mu^- \rightarrow H$	125	0% μ^- 0% μ^+	7×10^4
$e^+e^- \rightarrow H$	125	0% e^- 0% e^+	1.64

[†] Can't take full advantage of $\sigma_{\gamma\gamma} = 3$ nb because $\gamma\gamma$ beam width < 4 MeV is impossible. But in general, narrower $\gamma\gamma$ beam width \Rightarrow higher Higgs rate

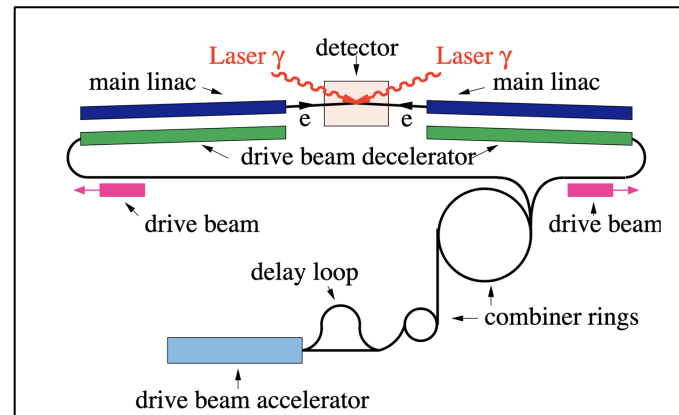
	\sqrt{s} (GeV)	polarization	σ (fb)
$\gamma\gamma \rightarrow HH$	380	+100% γ +100% γ	0.40
$e^+e^- \rightarrow ZHH$	500 / 550	-80% e^- +30% e^+	0.20 / 0.22



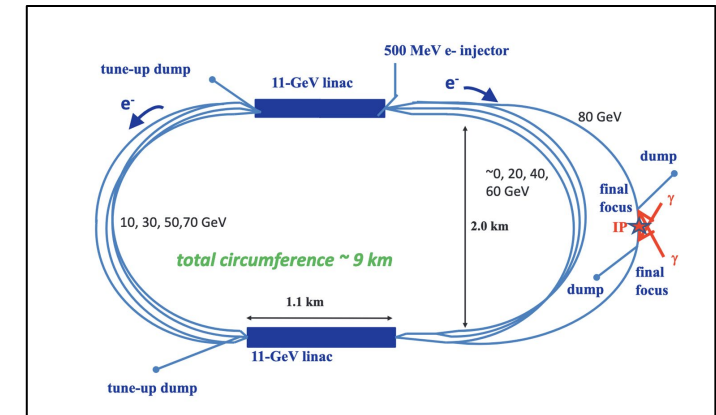
Photon Collider Concepts

- Optical photon colliders concepts developed in the 2000's can produce similar number of Higgs bosons per year than e^+e^- , but with higher backgrounds
- Recent innovation in photon science, particularly in XFELs can lead to enhanced capabilities

CLICHE



SAPPHiRE



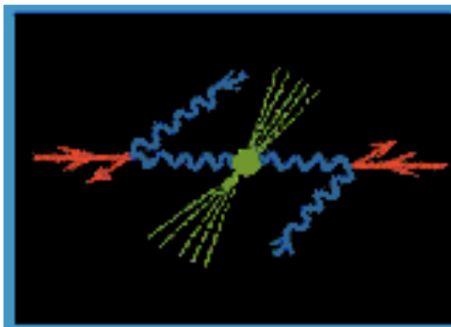
TESLA

The Superconducting Electron Positron Linear Collider with an Integrated X-Ray Laser Laboratory

Technical Design Report

Part VI: Appendices

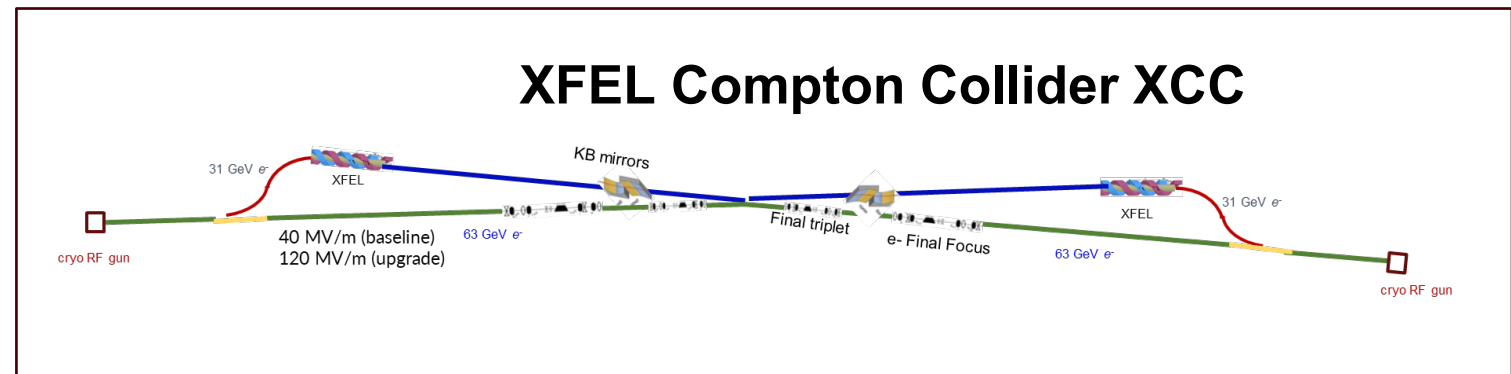
Chapter 1: Photon Collider at TESLA



DESY-2001-011, ECFA-2001-209
TESLA-2001-23, TESLA-FEL-2001-05

March
2001

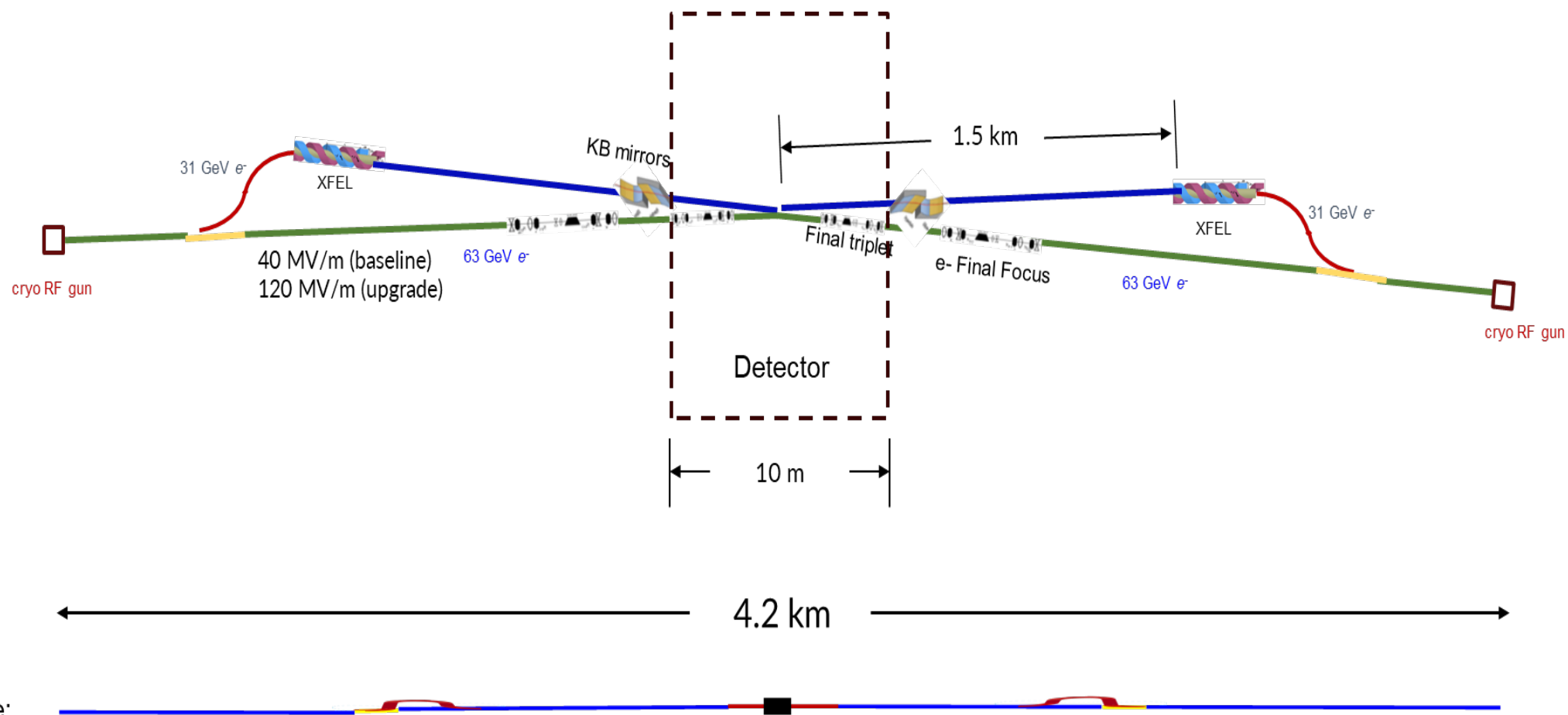
XFEL Compton Collider XCC



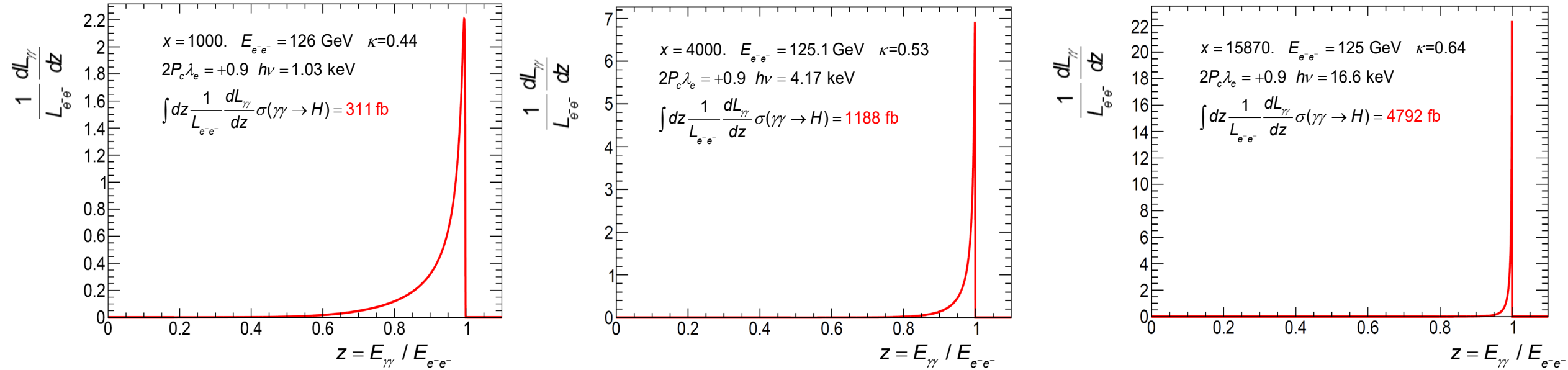
XFEL Compton Collider (XCC) Schematic

XCC s-channel $\gamma\gamma \rightarrow H$ @ $\sqrt{s} = 125$ GeV

$\gamma\gamma \rightarrow HH$ @ $\sqrt{s} = 380$ GeV



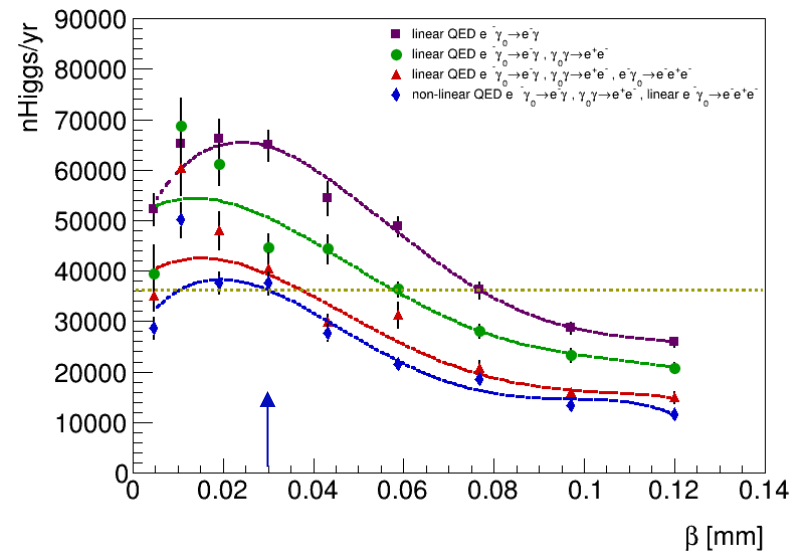
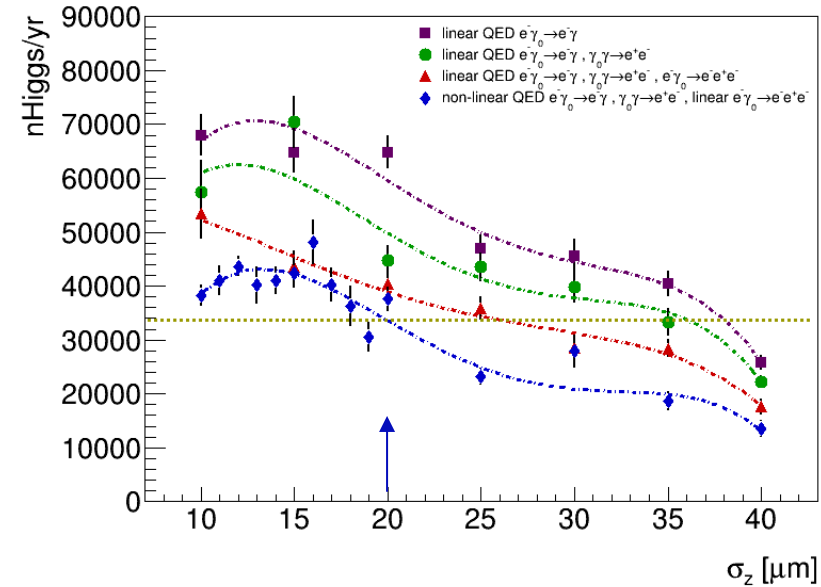
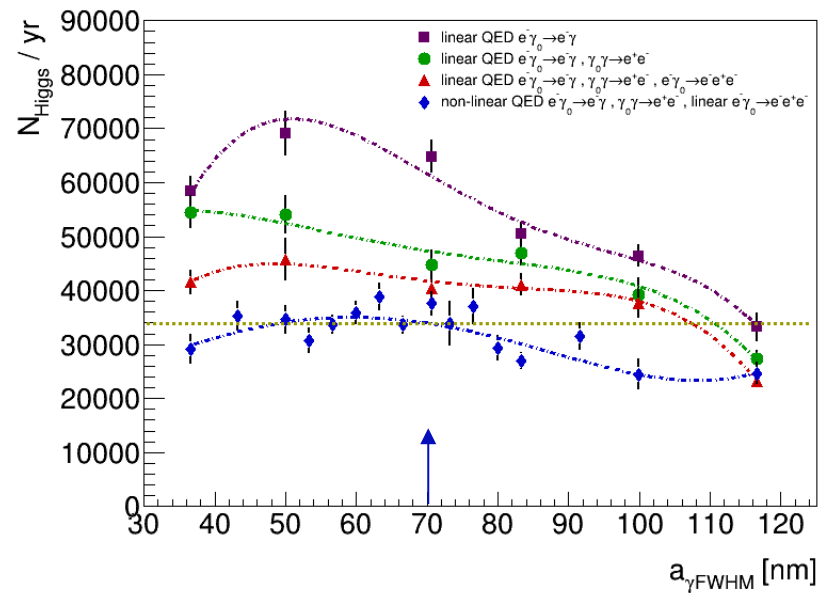
Choice of XCC Design Parameters - what value of x ?



The Higgs rate continues to grow with increasing x . What value of x should be used?

- Impose condition that XCC Higgs rate be comparable to ILC at $\sqrt{s} = 250$ GeV
- Iterate with XFEL experts on what photon wavelengths and pulse energies are possible using an e^- beam with $E < 62$ GeV to drive the XFEL. CAIN MC used to calculate Higgs rate.
- To maximize geometric luminosity, assume round beam focusing for the 62.5 GeV e^- beam \Rightarrow beamspot is a \sim few nm in both horizontal and vertical.

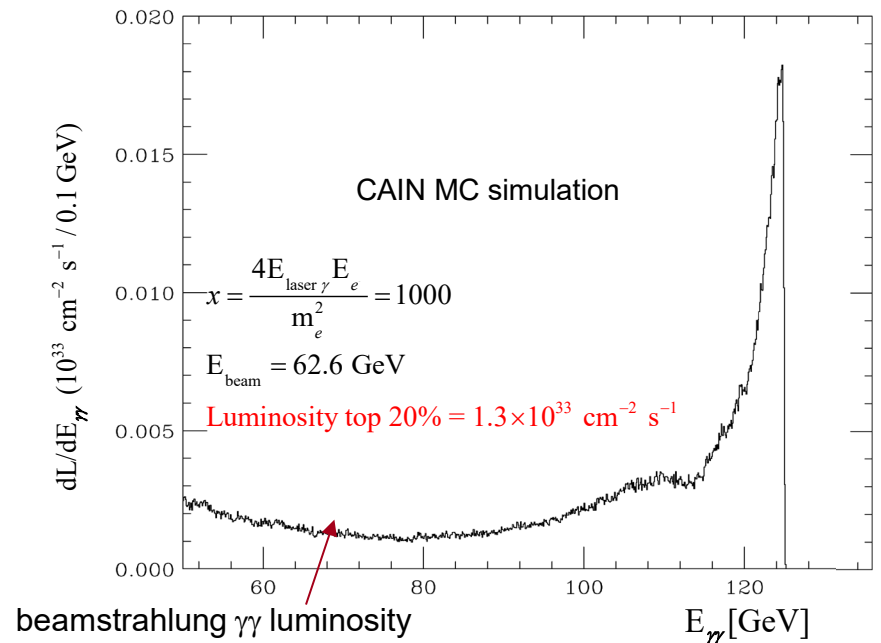
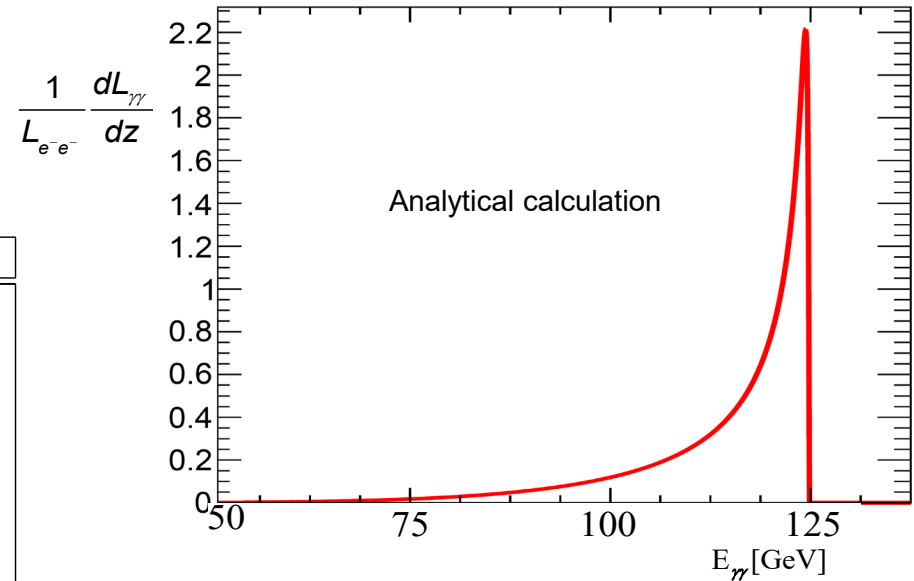
Choice of XCC Design Parameters - laser waist, bunch length , β^* , ...



XCC Design Parameters, Full Cain Simulation

$$x=1000, \quad \omega_0 = 1 \text{ keV}$$

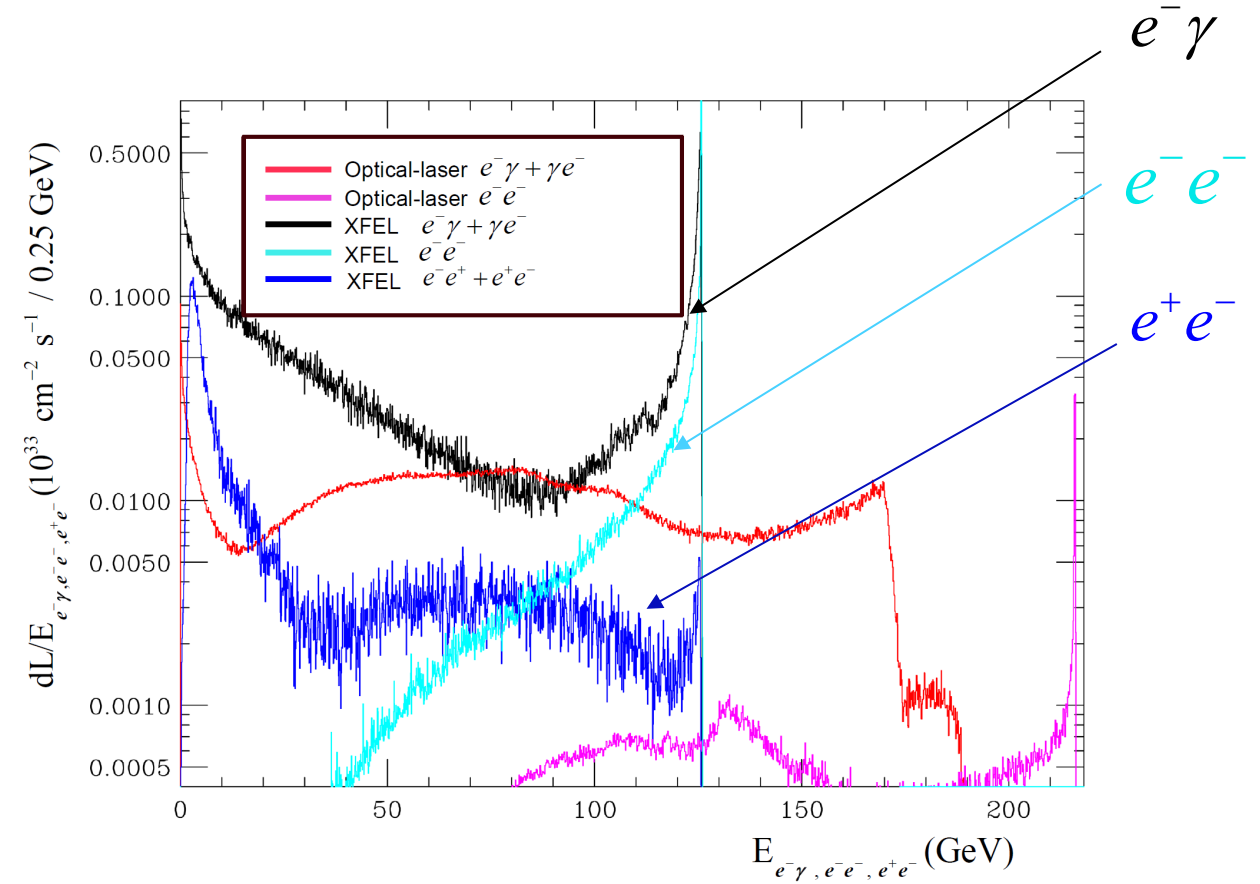
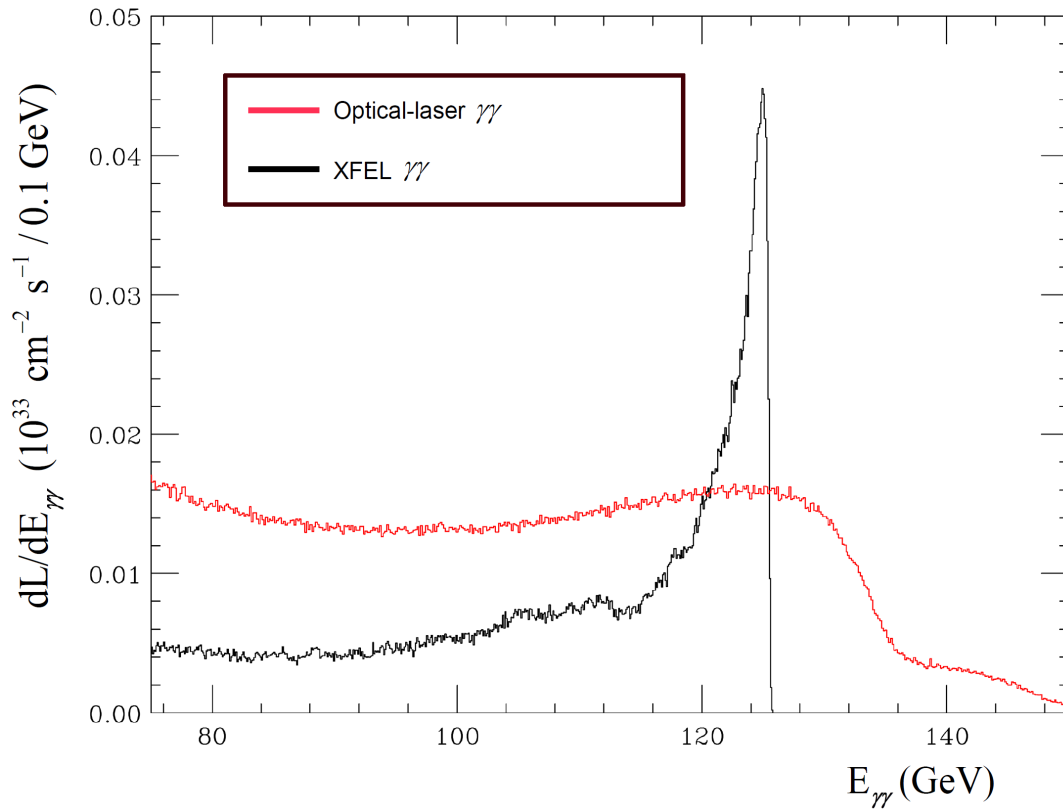
Final Focus parameters	Approx. value	XFEL parameters	Approx. value
Electron energy	62.8 GeV	Electron energy	31 GeV
Electron beam power	0.57 MW	Electron beam power	0.28 MW
β_x/β_y	0.03/0.03 mm	normalized emittance	120 nm
$\gamma\epsilon_x/\gamma\epsilon_y$	120/120 nm	RMS energy spread $\langle\Delta\gamma/\gamma\rangle$	0.05%
σ_x/σ_y at e^-e^- IP	5.4/5.4 nm	bunch charge	1 nC
σ_z	20 μm	Linac-to-XFEL curvature radius	133 km
bunch charge	1 nC	Undulator B field	$\gtrsim 1 \text{ T}$
Rep. Rate at IP	$240 \times 38 \text{ Hz}$	Undulator period λ_u	9 cm
σ_x/σ_y at IPC	12.1/12.12 nm	Average β function	12 m
$\mathcal{L}_{\text{geometric}}$	$9.7 \times 10^{34} \text{ cm}^2 \text{ s}^{-1}$	x-ray λ (energy)	1.2 nm (1 keV)
δ_E/E	0.05%	x-ray pulse energy	0.7 J
L^* (QD0 exit to e^- IP)	1.5m	pulse length	40 μm
d_{cp} (IPC to IP)	60 μm	$a_{\gamma x}/a_{\gamma y}$ (x/y waist)	21.2/21.2 nm
QD0 aperture	9 cm diameter	non-linear QED ξ^2	0.10
Site parameters	Approx. value		
crossing angle	2 mrad		
total site power	85 MW		
total length	3.0 km		



X-ray vs. Optical Laser $\gamma\gamma$ Higgs Factories $\sqrt{s} \approx 125 \text{ GeV}$ ($\gamma\gamma \rightarrow H$)

Laser E_γ (eV)	$\sqrt{s_{ee}}$ (GeV)	$N_{\text{bunch}} / \text{train}$	Rep Rate (Hz)	$L_{\gamma\gamma} (\text{cm}^{-2}\text{s}^{-1})^\dagger$	$N_H / 1.0 \times 10^7 \text{s}$
1.17	216	2820	5	3.5×10^{34}	25,000
1.04×10^3	126	165	120	3.5×10^{34}	72,200

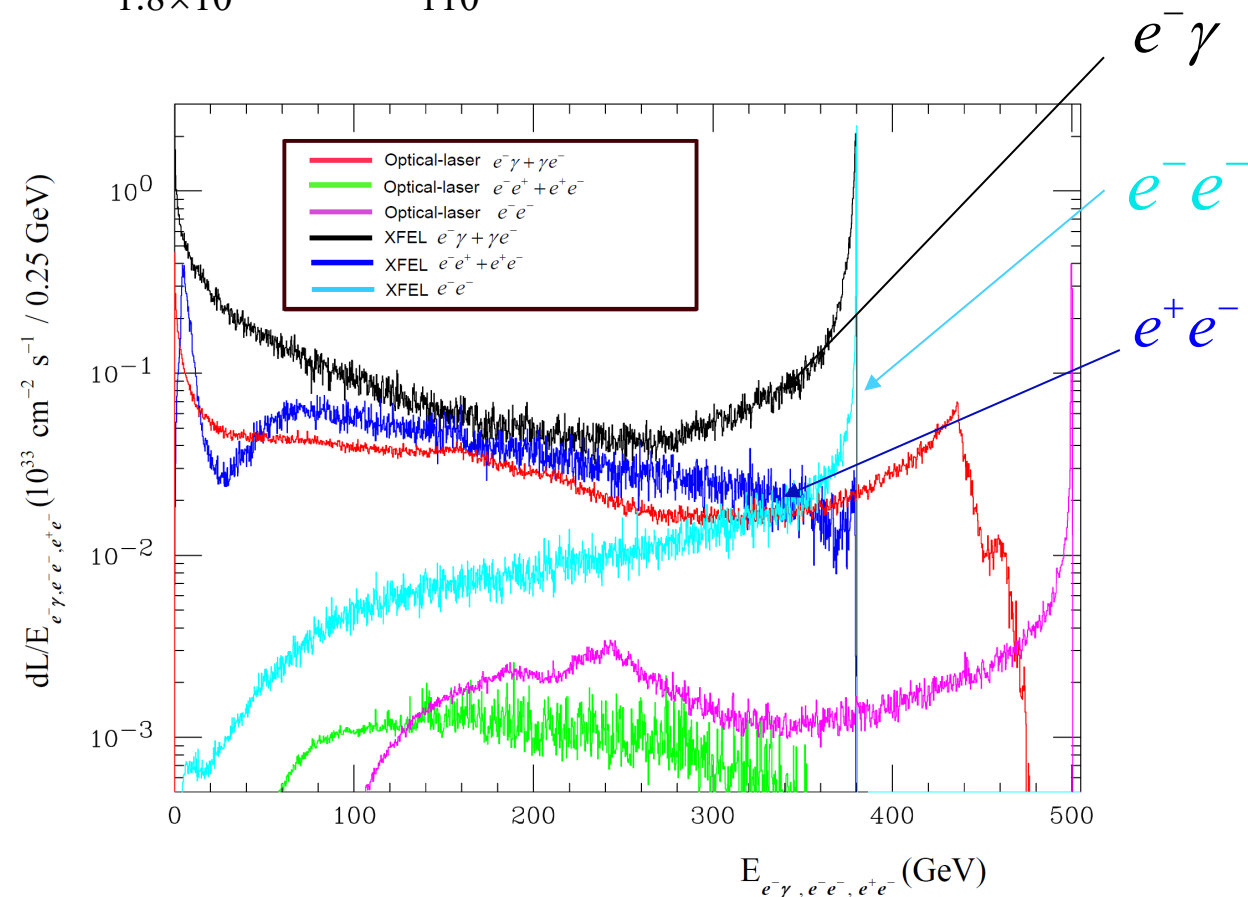
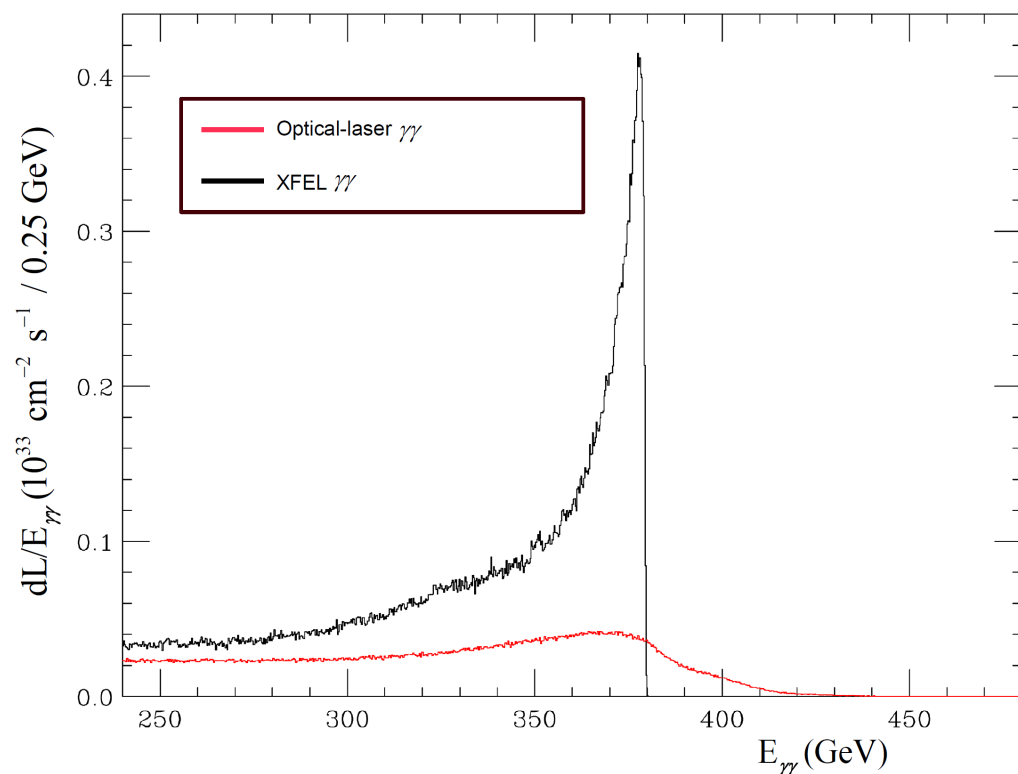
$$^\dagger 0 < \sqrt{s_{\gamma\gamma}} < \sqrt{s_{ee}}$$



X-ray vs. Optical Laser $\gamma\gamma$ Higgs Factories $\sqrt{s} \approx 380$ GeV ($\gamma\gamma \rightarrow HH$)

Laser E_γ (eV)	$\sqrt{s_{ee}}$ (GeV)	$N_{\text{bunch}} / \text{train}$	Rep Rate (Hz)	$L_{\gamma\gamma}$ ($\text{cm}^{-2}\text{s}^{-1}$) [†]	$N_{HH} / 1.0 \times 10^7 \text{s}$
1.17	500	2820	5	0.73×10^{35}	20
0.52×10^3	380	93	120	1.8×10^{35}	110

$$^\dagger 0 < \sqrt{s_{\gamma\gamma}} < \sqrt{s_{ee}}$$



Delphes Analysis of $\gamma\gamma \rightarrow HH$ assuming SiD Detector and Full Suite of Backgrounds

Higgs self-coupling analysis

of $\gamma\gamma \rightarrow HH$ at $\sqrt{s} = 380$ GeV

Data sets were produced using

WHIZARD MC & Cain $\sqrt{\hat{s}}$ spectra:

Signal main channel:

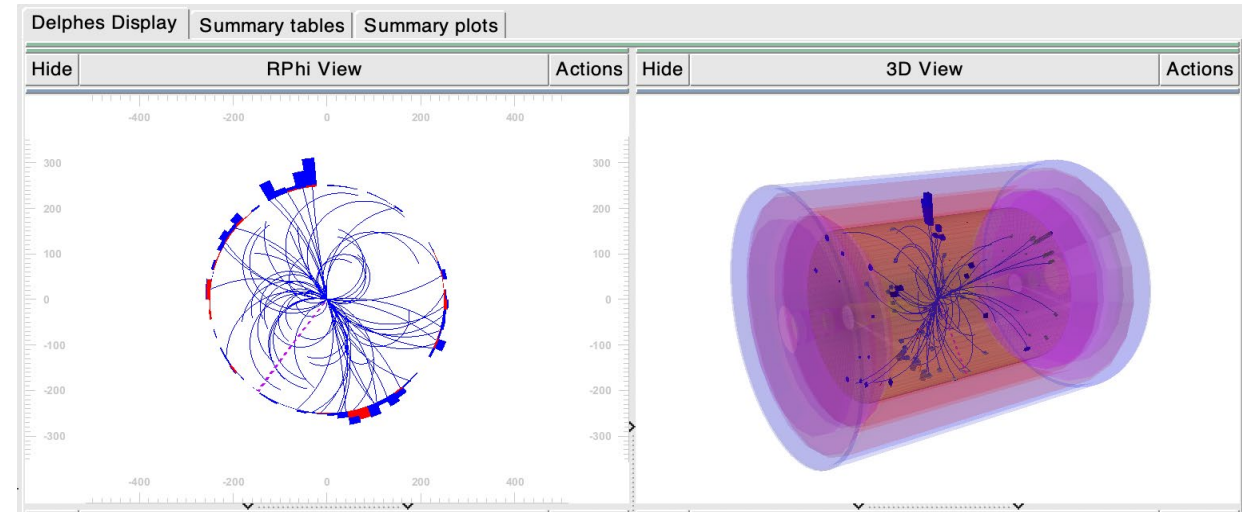
• $\gamma\gamma \rightarrow HH \rightarrow b\bar{b}b\bar{b}$

All with variable Ecm at around
380 GeV; luminosity = 4900 fb⁻¹
for 10 years

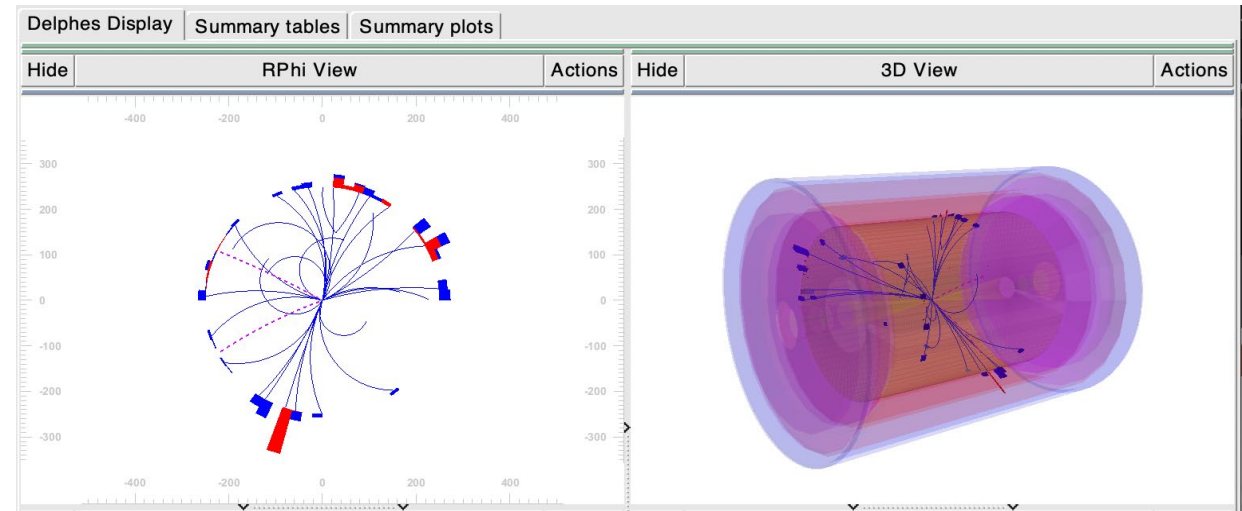
Backgrounds:

- $\gamma\gamma \rightarrow q\bar{q}$
- $\gamma\gamma \rightarrow ZZ$
- $\gamma\gamma \rightarrow ZH$
- $e\gamma \rightarrow q\bar{q}q\bar{q}$
- $e^+e^- \rightarrow b\bar{b}$
- $e^+e^- \rightarrow ZH$
- $\gamma\gamma \rightarrow t\bar{t}$
- $\gamma\gamma \rightarrow W^+W^-$
- $e\gamma \rightarrow q\bar{q}$
- $e\gamma \rightarrow q\bar{q}H$
- $e^+e^- \rightarrow b\bar{b}q\bar{q}$
- $e^+e^- \rightarrow t\bar{t}$

$e^+e^- \rightarrow ZHH$
 $\rightarrow qqbbbb$
 $\sqrt{s} = 550$ GeV



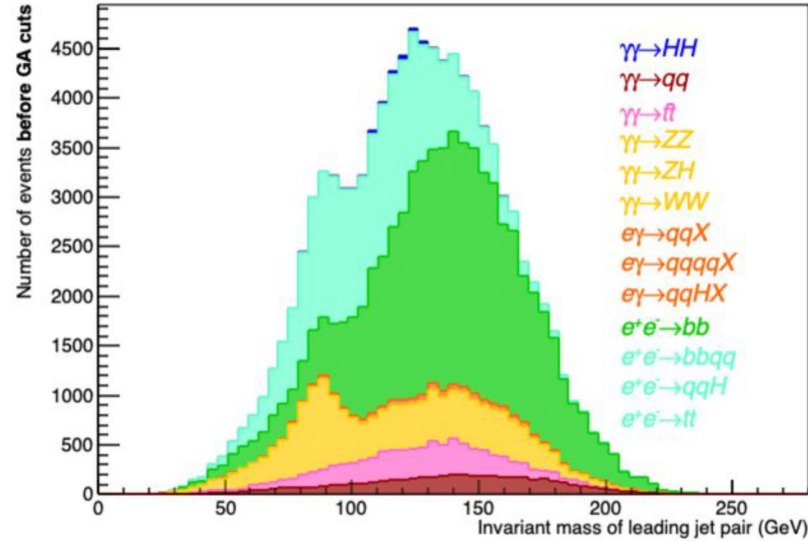
$\gamma\gamma \rightarrow HH$
 $\rightarrow b\bar{b}b\bar{b}$
 $\sqrt{s} = 380$ GeV



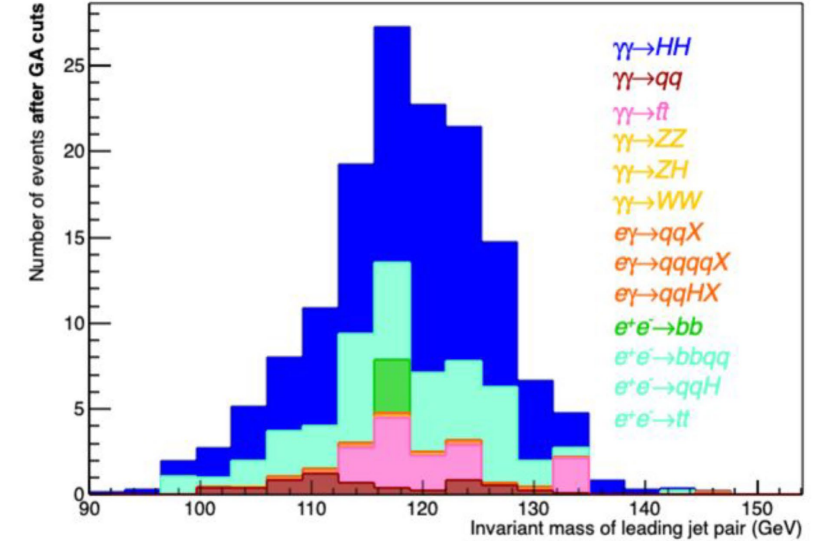
Delphes Event Displays of $e^+e^- \rightarrow ZHH \rightarrow qqbbbb$ and $\gamma\gamma \rightarrow HH \rightarrow b\bar{b}b\bar{b}$

Higgs Self-Coupling Analysis of $\gamma\gamma \rightarrow HH$

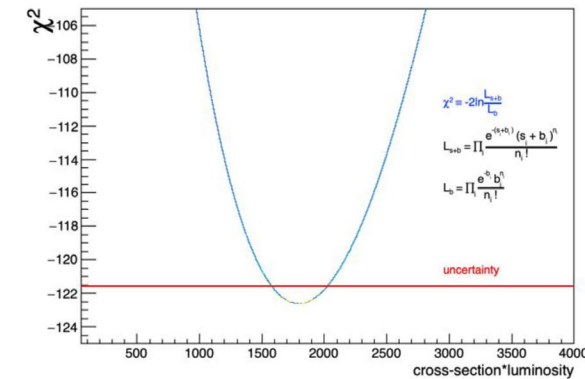
Before NN cuts



After NN cuts



	XCC
Ecm:	380 GeV
Channel(s):	$\gamma\gamma \rightarrow HH \rightarrow b\bar{b}b\bar{b}$
Cross-Section :	~ 0.365
Uncertainty:	10.8%
Significance:	8.5σ

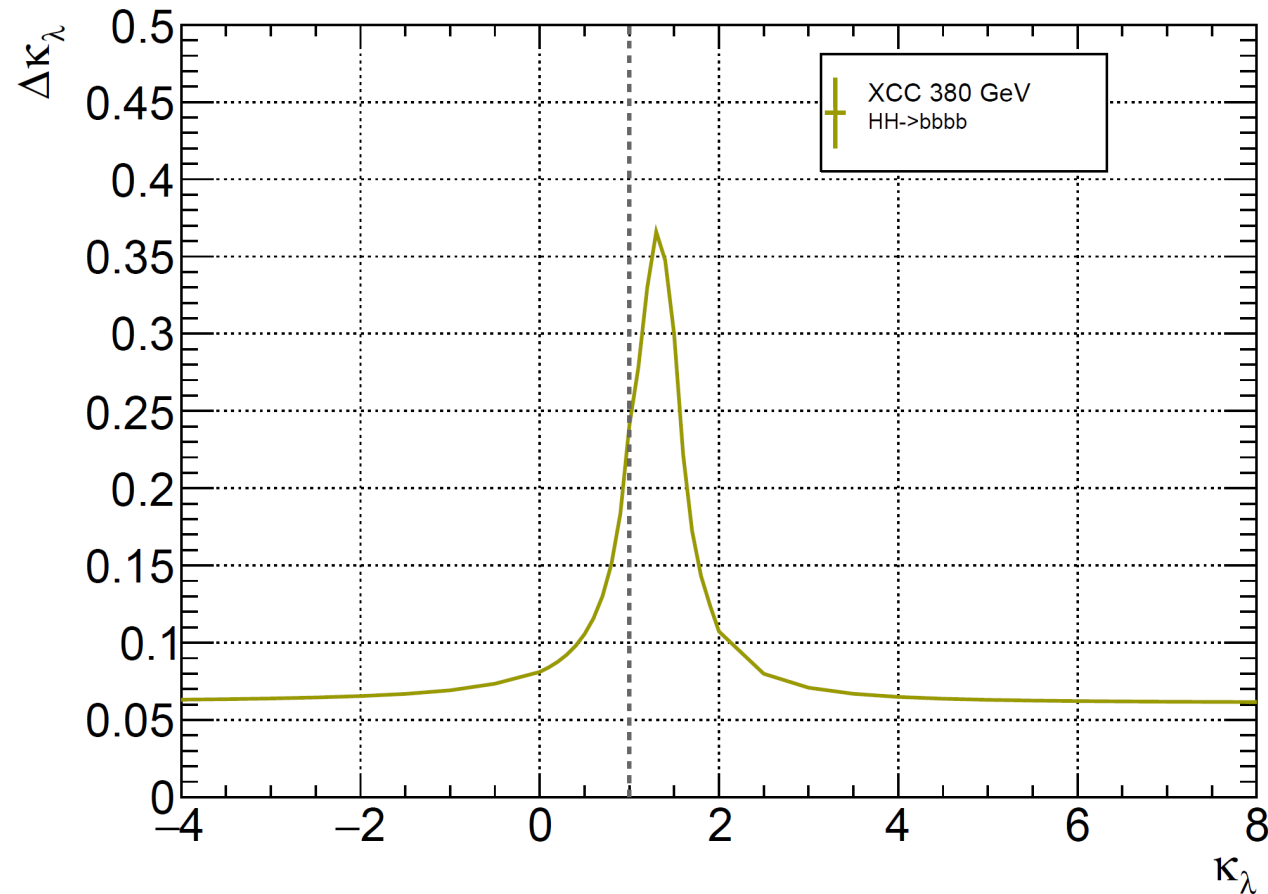


S. Ampudia Castelazo

Error on κ_λ from $\gamma\gamma \rightarrow HH$ cross section at $\sqrt{s} = 380$ GeV

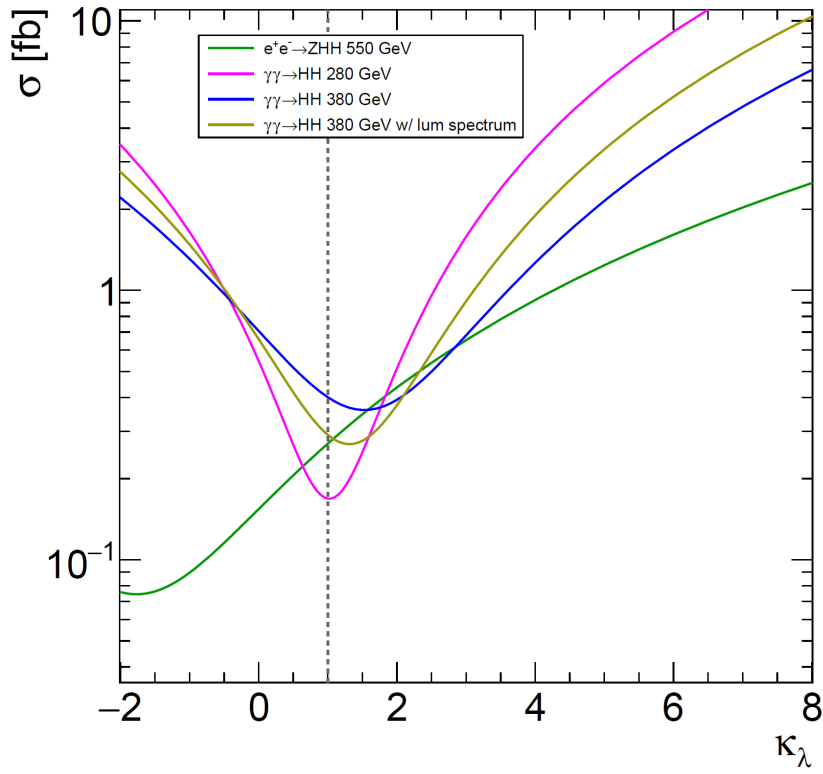
Delphes simulation of $HH \rightarrow bbbb$ signal and full suite of

backgrounds at $\sqrt{s}=380$ GeV gives $\frac{\Delta\sigma}{\sigma} = 0.11$ for 5 ab^{-1} and $\kappa_\lambda = 1$

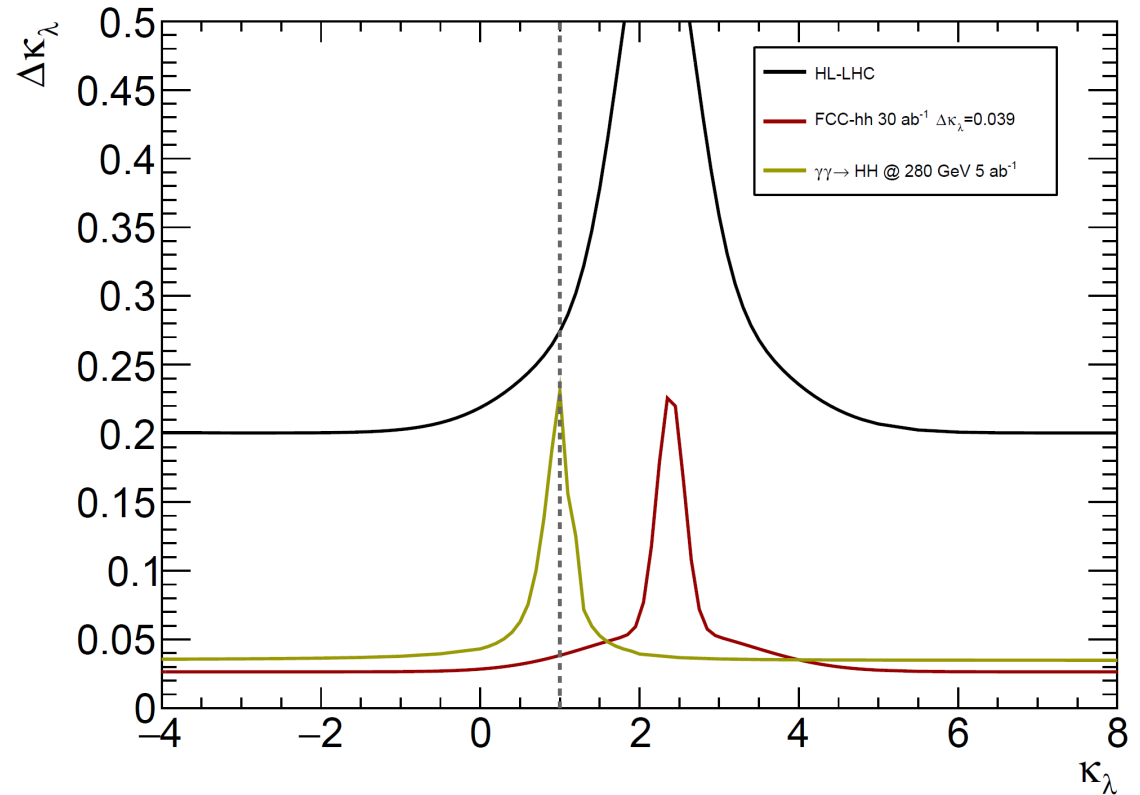


Projected error on κ_λ from $\gamma\gamma \rightarrow HH$ cross section at $\sqrt{s} = 280$ GeV

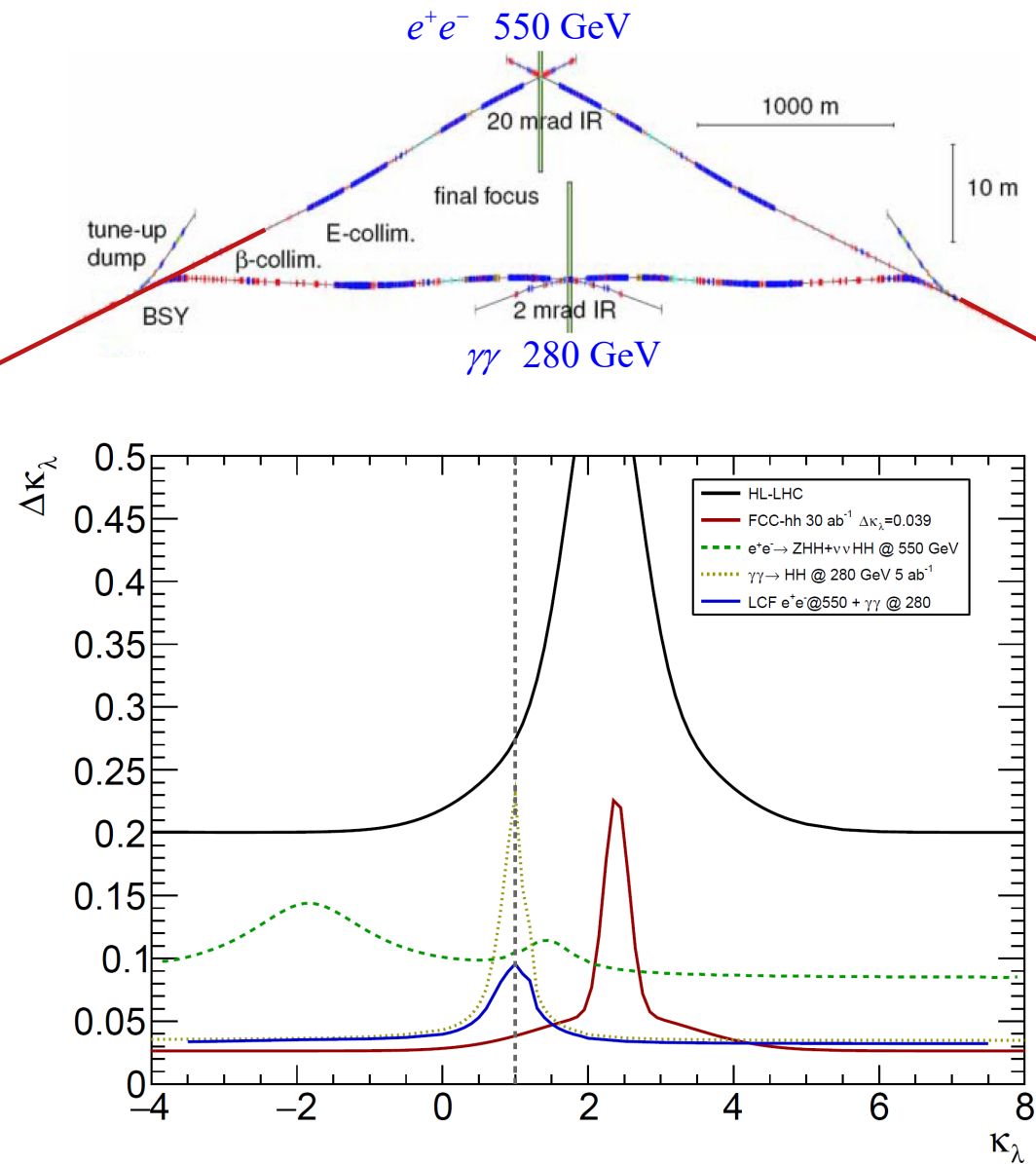
The σ vs. κ_λ curve at $\sqrt{s}=280$ GeV has a narrow valley at $\kappa_\lambda = 1$ and steeply rising walls which provide great leverage in converting cross-section error to κ_λ error.



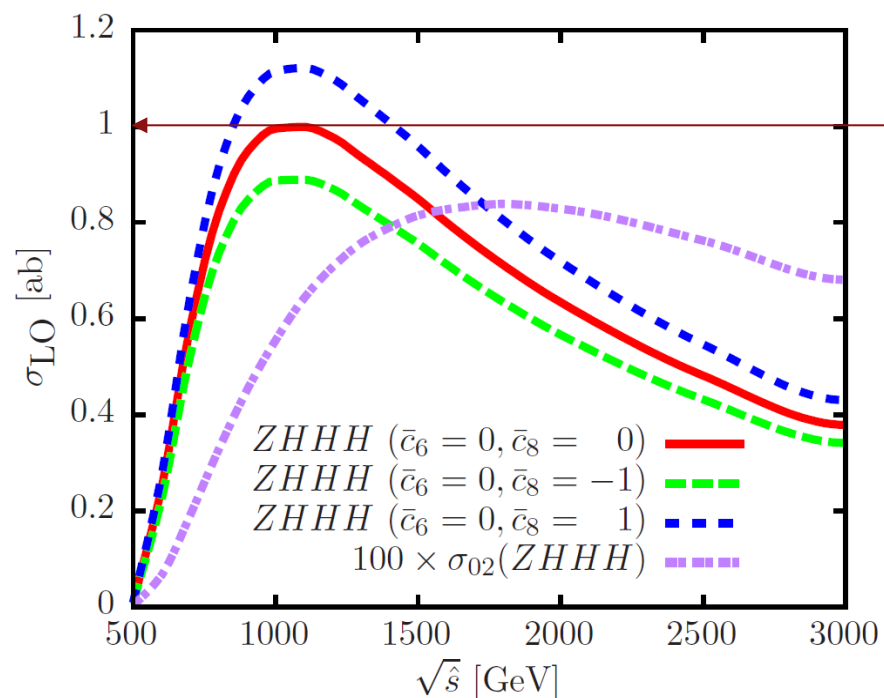
$\Delta\kappa_\lambda$ calculated assuming 11% cross-section error at $\sqrt{s} = 280$ GeV. The 11% error is an extrapolation of a 6.4% error at $\sqrt{s} = 380$ GeV which in turn is an extrapolation of the 11% error for $\gamma\gamma \rightarrow HH \rightarrow b\bar{b}b\bar{b}$ to an analysis of all HH decay topologies.



LCF κ_λ sensitivity: $e^+e^- \rightarrow ZHH @ 550 + \gamma\gamma \rightarrow HH @ 280$ GeV



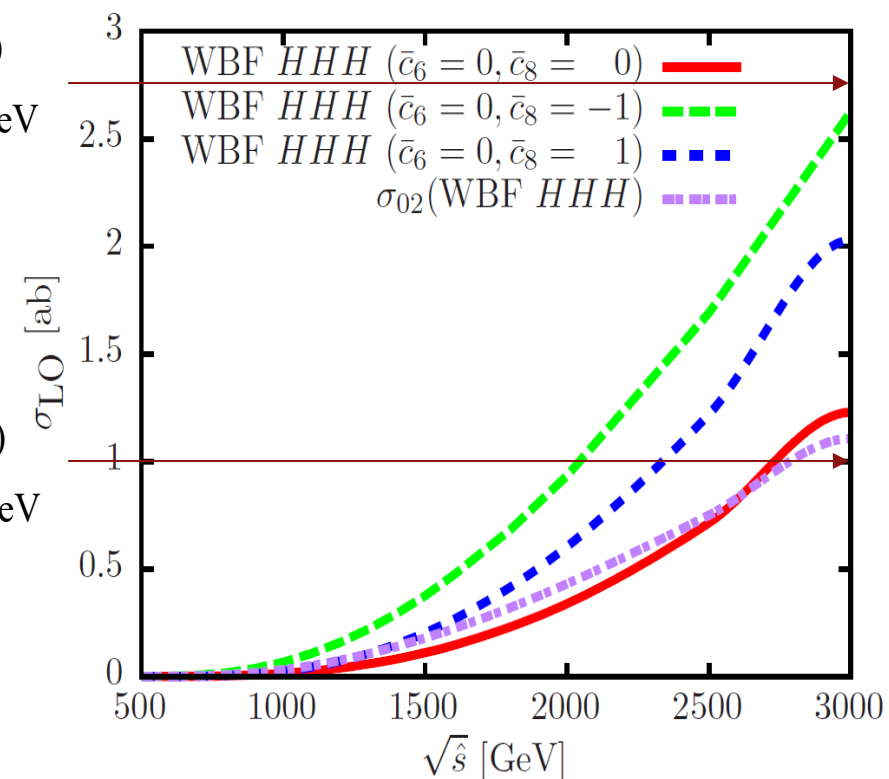
$$\sigma(\gamma\gamma \rightarrow HHH) @ 500 \text{ GeV} \approx \sigma(e^+e^- \rightarrow \nu\nu HHH) @ 3 \text{ TeV}$$



$\sigma(\gamma\gamma \rightarrow HHH)$
@ $\sqrt{s} = 505 \text{ GeV}$

$\sigma(\gamma\gamma \rightarrow HHH)$
@ $\sqrt{s} = 750 \text{ GeV}$

$\sigma(\gamma\gamma \rightarrow HHH)$
@ $\sqrt{s} = 505 \text{ GeV}$



Other $\gamma\gamma$ Studies to be Explored

- Ability to control the photon polarizations provides a powerful tool for the **exploration of CP properties** of any single neutral Higgs boson
 - The $J_z=0$ $\gamma\gamma$ initial state can form a CP-even or a CP-odd state using linear polarizations of the laser beams
 - CP-even Higgs bosons (h^0, H^0) couple to linearly polarized photons with maximum strength for parallel polarisation vectors
 - CP-odd Higgs boson (A^0) couple to linearly polarized photons with perpendicular polarization vectors

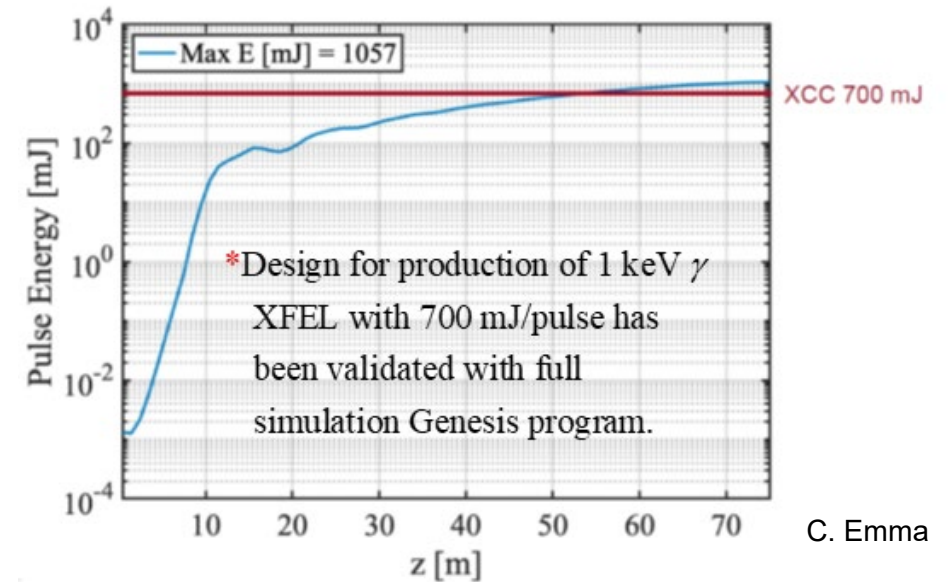
Reaction	Remarks
$\gamma\gamma \rightarrow h^0 \rightarrow b\bar{b}$	SM (or MSSM) Higgs, $M_{h^0} < 160$ GeV
$\gamma\gamma \rightarrow h^0 \rightarrow WW(WW^*)$	SM Higgs, $140 \text{ GeV} < M_{h^0} < 190$ GeV
$\gamma\gamma \rightarrow h^0 \rightarrow ZZ(ZZ^*)$	SM Higgs, $180 \text{ GeV} < M_{h^0} < 350$ GeV
$\gamma\gamma \rightarrow H, A \rightarrow b\bar{b}$	MSSM heavy Higgs, for intermediate $\tan\beta$
$\gamma\gamma \rightarrow \tilde{f}\tilde{f}^*, \tilde{\chi}_i^+ \tilde{\chi}_i^-, H^+ H^-$	large cross sections, possible observations of FCNC
$\gamma\gamma \rightarrow S[\tilde{t}\tilde{t}]$	$\tilde{t}\tilde{t}$ stoponium
$\gamma e \rightarrow \tilde{e}^- \tilde{\chi}_1^0$	$M_{\tilde{e}^-} < 0.9 \times 2E_0 - M_{\tilde{\chi}_1^0}$
$\gamma\gamma \rightarrow W^+ W^-$	anomalous W interactions, extra dimensions
$\gamma e^- \rightarrow W^- \nu_e$	anomalous W couplings
$\gamma\gamma \rightarrow WWWW, WWZZ$	strong WW scatt., quartic anomalous W, Z couplings
$\gamma\gamma \rightarrow t\bar{t}$	anomalous top quark interactions
$\gamma e^- \rightarrow \bar{t} b \nu_e$	anomalous Wtb coupling
$\gamma\gamma \rightarrow \text{hadrons}$	total $\gamma\gamma$ cross section
$\gamma e^- \rightarrow e^- X$ and $\nu_e X$	\mathcal{NC} and \mathcal{CC} structure functions (polarised and unpolarised)
$\gamma g \rightarrow q\bar{q}, c\bar{c}$	gluon distribution in the photon
$\gamma\gamma \rightarrow J/\psi J/\psi$	QCD Pomeron

Beam Parameter Table for $\sqrt{s}=125$ GeV

Final Focus parameters	Approx. value	XFEL parameters	Approx. value
Electron energy	62.8 GeV	Electron energy	31 GeV
Electron beam power	1.24 MW	Electron beam power	0.61 MW
β_x/β_y	0.030/0.030 mm	Normalized emittance	120 nm
$\gamma\epsilon_x/\gamma\epsilon_y$	120/120 nm	RMS energy spread $\langle\Delta\gamma/\gamma\rangle$	0.05%
σ_x/σ_y at e^-e^- IP	5.4/5.4 nm	Bunch charge	1 nC
σ_z	20 μm	Linac-to-XFEL CSR	0.017%
Bunch charge	1 nC	Undulator B field	$\gtrsim 1$ T
Bunches/train at IP	165	Undulator period λ_u	9 cm
Train Rep. Rate at IP	120 Hz	Average β function	12 m
Bunch spacing at IP	4.2 ns	x-ray λ (energy)	1.2 nm (1 keV)
σ_x/σ_y at IPC	12.1/12.1 nm	x-ray pulse energy	0.7 J
$\mathcal{L}_{\text{geometric}}$	$2.1 \times 10^{35} \text{ cm}^2 \text{ s}^{-1}$	rms pulse length	20 μm
δ_E/E	0.1%	$a_{\gamma x}/a_{\gamma y}$ (x/y waist)	21.2/21.2 nm
L^* (QD0 exit to e^- IP)	1.5m	non-linear QED ξ^2	0.10
d_{cp} (IPC to IP)	60 μm		
QD0 aperture	12 cm diameter		
Accel. gradient	70 MV/m		Z. Huang
Site parameters	Approx. value		
crossing angle	2 mrad		
total site power	115 MW		
total length	4.2 km		

Aggressive emittance, β^* , bunch length
Round beam FF distinct from usual flat FF
And the e- beam must be 80 to 90% pol.

SASE followed by self-seeded section
Helical permanent magnet undulator
Negligible quantum diffusion



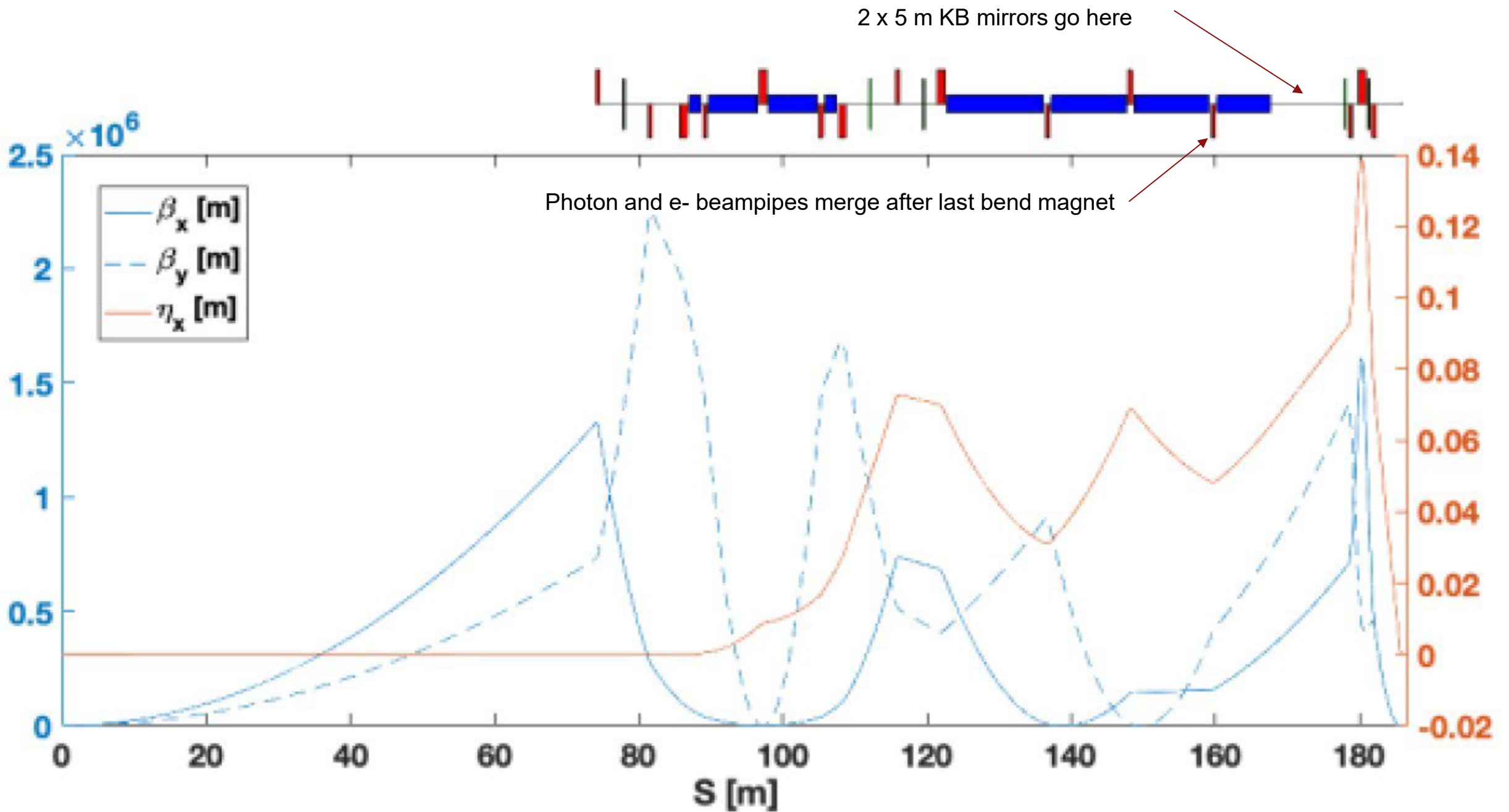
C. Emma

Beam Parameter Table for $\sqrt{s}=380$ GeV

Final Focus parameters	Approx. value	XFEL parameters	Approx. value
Electron energy	190 GeV	Electron energy	31 GeV
Electron beam power	2.13 MW	Electron beam power	0.34 MW
β_x/β_y	0.010/0.010 mm	Normalized emittance	60 nm
$\gamma\epsilon_x/\gamma\epsilon_y$	60/60 nm	RMS energy spread $\langle\Delta\gamma/\gamma\rangle$	0.05%
σ_x/σ_y at e^-e^- IP	1.3/1.3 nm	Bunch charge	1 nC
σ_z	10 μm	Linac-to-XFEL CSR	0.017%
Bunch charge	1 nC	Undulator B field	-
Bunches/train at IP	93	Undulator period λ_u	-
Train Rep. Rate at IP	120 Hz	Average β function	-
Bunch spacing at IP	5.2 ns	x-ray λ (energy)	2.4 nm (0.52 keV)
σ_x/σ_y at IPC	5.2/5.2 nm	x-ray pulse energy	1.0 J
$\mathcal{L}_{\text{geometric}}$	$1.8 \times 10^{36} \text{ cm}^2 \text{ s}^{-1}$	rms pulse length	10 μm
$\delta E/E$	0.1%	$a_{\gamma x}/a_{\gamma y}$ (x/y waist)	64.4/64.4 nm
L^* (QD0 exit to e^- IP)	1.5m	non-linear QED ξ^2	0.40
d_{cp} (IPC to IP)	40 μm		
QD0 aperture	12 cm diameter		
Accel. gradient	120 MV/m		
Site parameters	Approx. value		
crossing angle	2 mrad		
total site power	140 MW		
total length	4.2 km		

Even more aggressive emittance, β^* , bunch length.
Unattainable now, but assume can be reached
once 125 GeV design is realized, in spirit of an upgrade

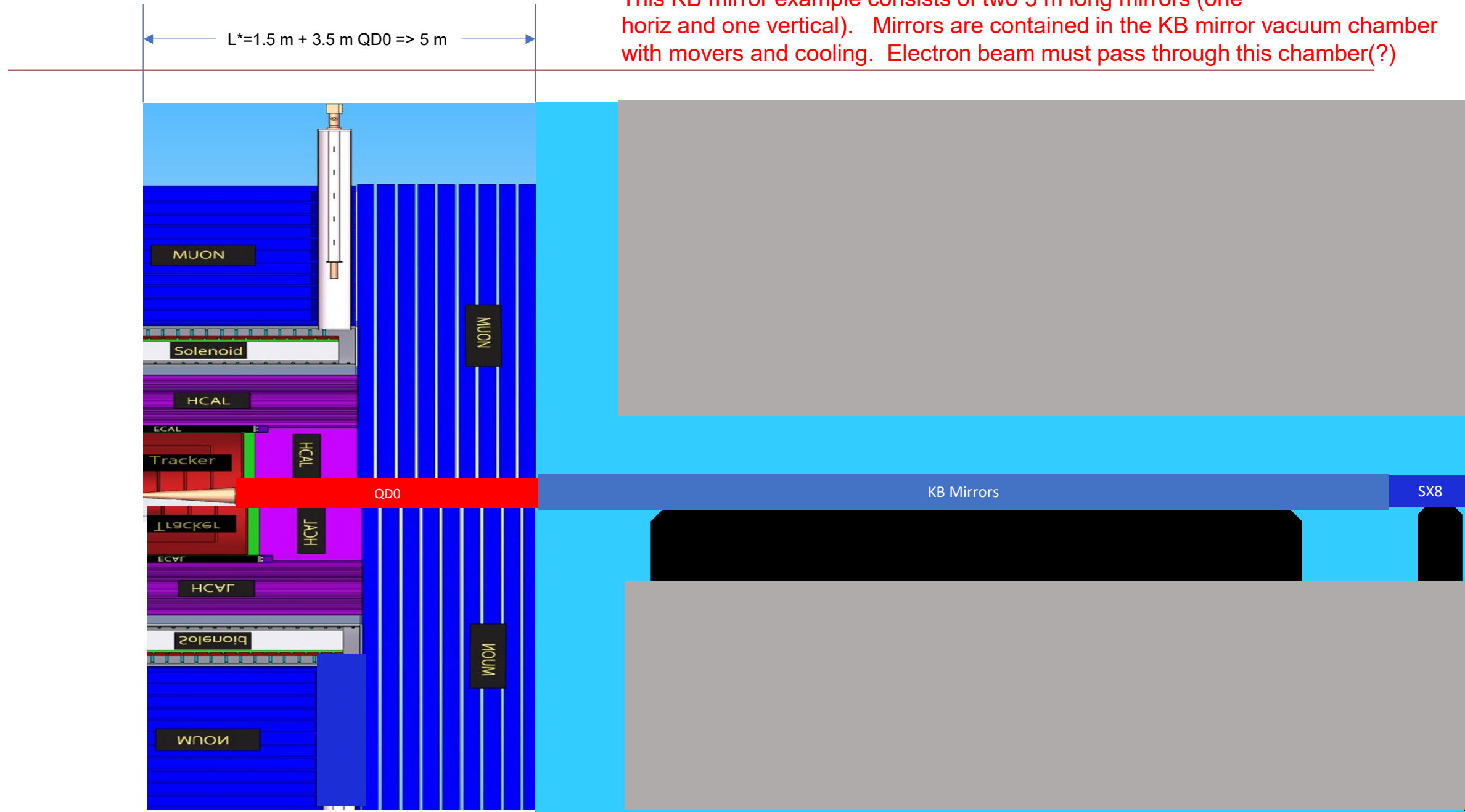
0.5 keV instead of 1 keV photons
1.0 Joule instead of 0.7 Joule
No design yet



First attempt at XCC round beam FF design

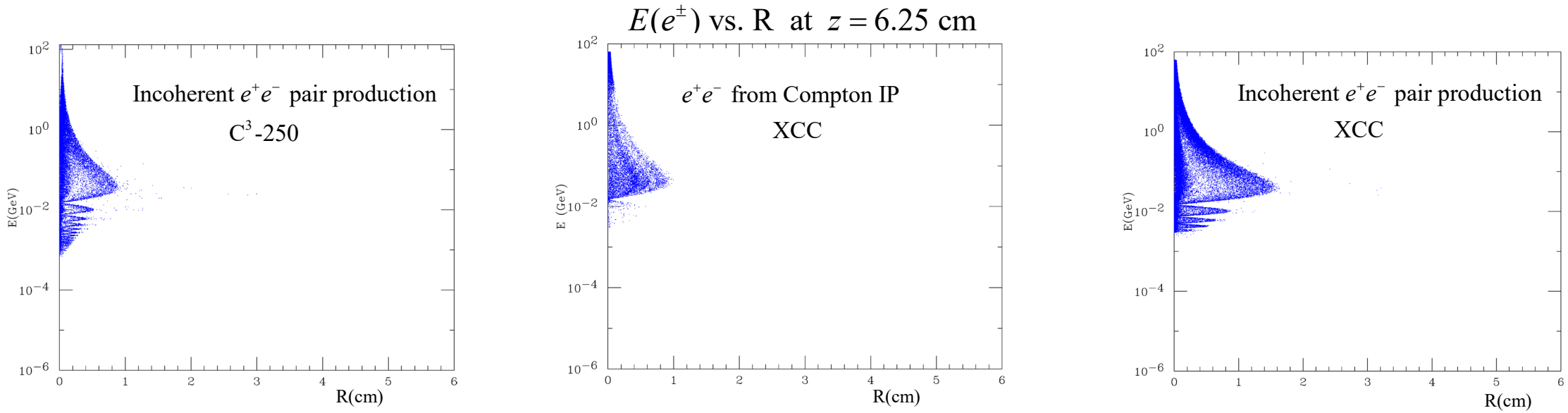
G. White

Example beam layout of KB mirror and electron beam final triplet QD0.
 This KB mirror example consists of two 5 m long mirrors (one
 horiz and one vertical). Mirrors are contained in the KB mirror vacuum chamber
 with movers and cooling. Electron beam must pass through this chamber(?)

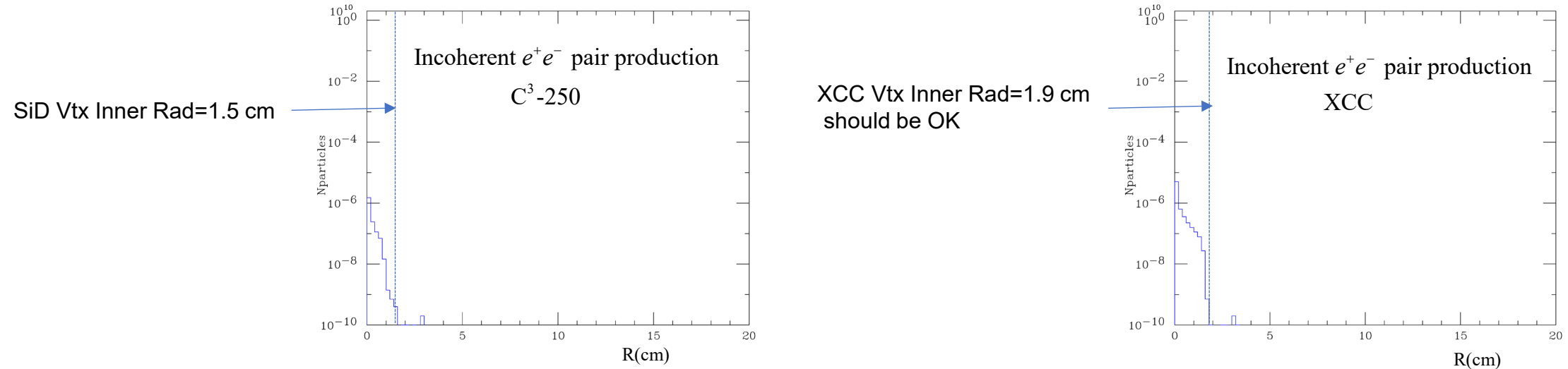


Vertex Detector Inner Radius

CAIN Simulation assuming 5 T Solenoid



$N(e^\pm)$ vs. R at $z = 6.25$ cm

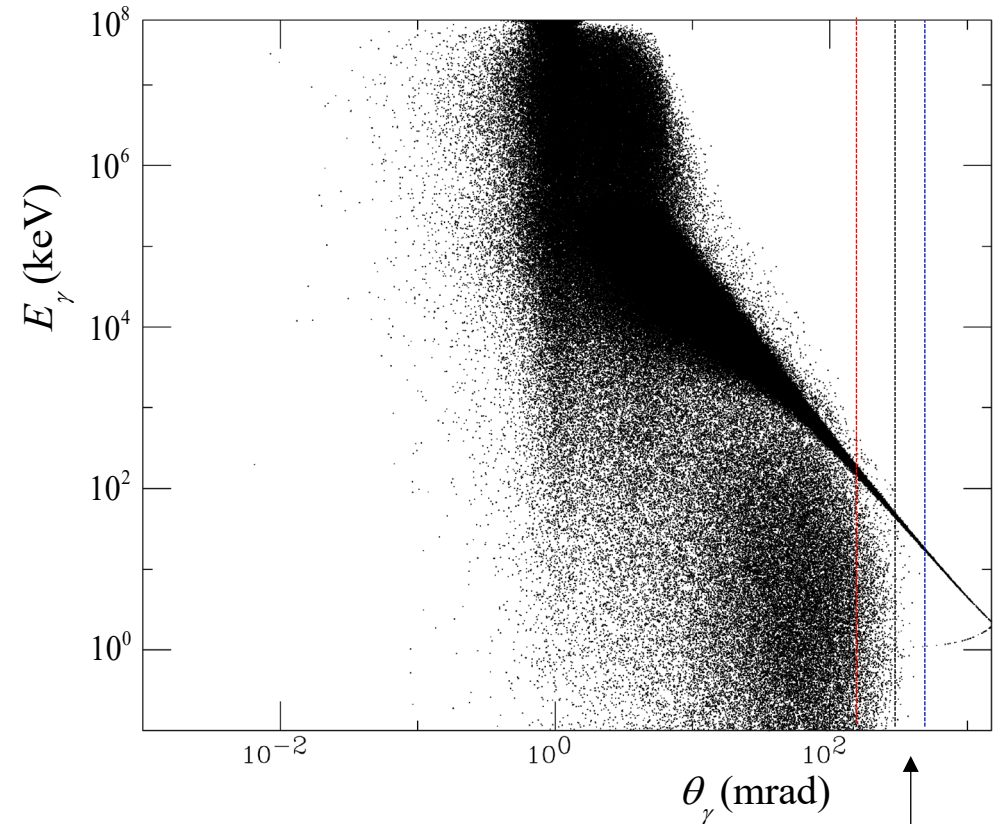
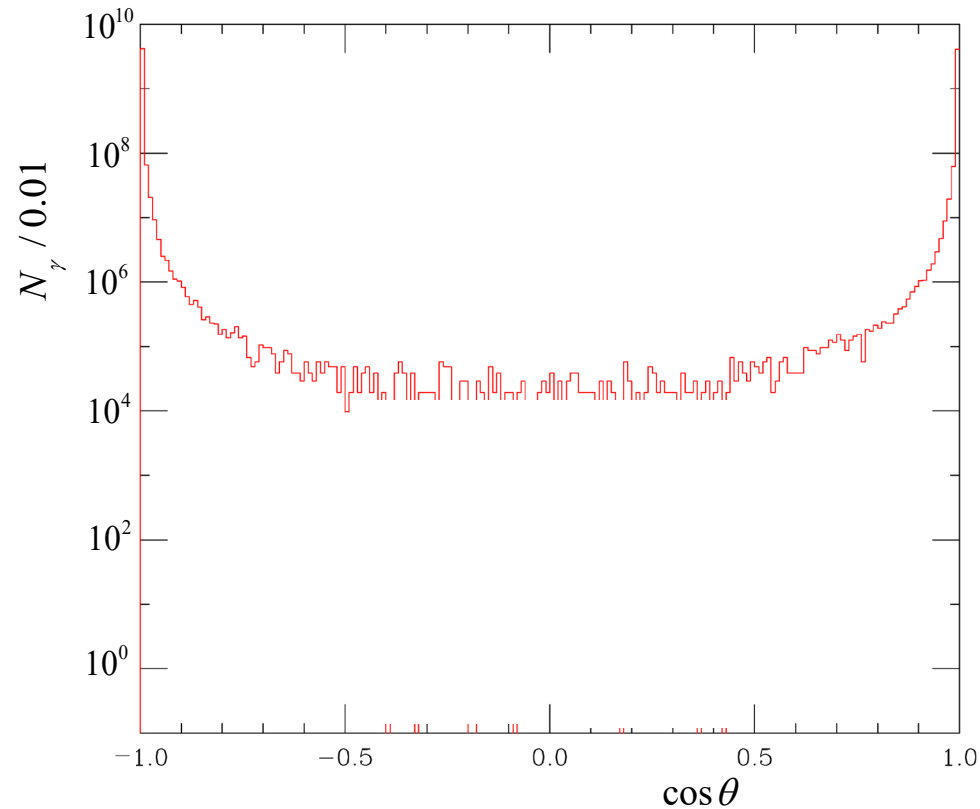


X-rays from Compton IP's

CAIN Simulation

Moderate flux of soft (few keV) X-rays in central region

Number and energy of Compton IP X-rays increases rapidly in the forward region



X-rays handled by adding 0.1% - 1.0% X_0 heavy element to Beampipe for $|\cos \theta| < 0.8$

Required absorber increases to 5.0% X_0 at $|\cos \theta| = 0.93$

Complicated design for $0.95 < |\cos \theta| < 0.99$; probably can't instrument for $|\cos \theta| > 0.99$

$|\cos \theta| = (0.99, 0.95, 0.90)$

Summary - Beam Delivery and Machine Detector Interface at XCC

BDS Accelerator Issues Related to Getting Four Particle Beams In and Out of IP Region

- (1) Crossing angle and Aperture of final quad (for 2 mrad crossing angle choice, e^+ , e^- , γ from primary & Compton IP's must pass through this aperture; for 20 mrad angle need collimators to protect final quad)
- (2) L^* , KB mirror length and location
- (3) Shared vacuum pipe: point of entry of XFEL beam into e^- beampipe, passing of electron beam through KB mirror chamber (?), beam dump design

Detector issues due to backgrounds from e^+ , e^- , γ produced at Compton IP's and primary IP:

- (1) Vertex detector inner radius (incoherent e^+e^- pairs from primary IP - same situation as e^+e^- linear colliders)
- (2) Beampipe X_0 (moderate soft X-ray flux from Compton IP's $|\cos \theta| < 0.95$)
- (3) Forward boundaries of the main tracker/calorimeter and solid angle coverage of forward detector (large hard X-ray flux from Compton IP's $|\cos \theta| > 0.95$)

XCC Accelerator Challenges

Electron beam:

- For the 280/380 GeV upgrade: e^- accelerator with 90 – 120 MV/m (common with $C^3 e^+e^-$ collider)
- Polarized low emittance e^- injector (common with $C^3 e^+e^-$, except flat beams not needed)
- Focusing of round e^- beams to $\sigma_{x,y} = 5.5$ nm

XFEL beam and Compton IP:

- Production of 1 keV γ XFEL with 700 mJ/pulse
- Focusing of 1 keV, 700 mJ/pulse XFEL beam to 70 nm FWHM waist
- XFEL and e^- beamline layouts around the IP
- Timing and position stability of the XFEL laser beam and e^- beam at Compton IP.

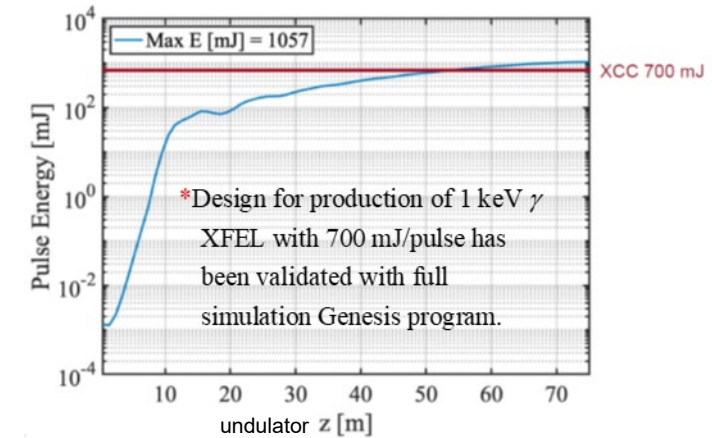
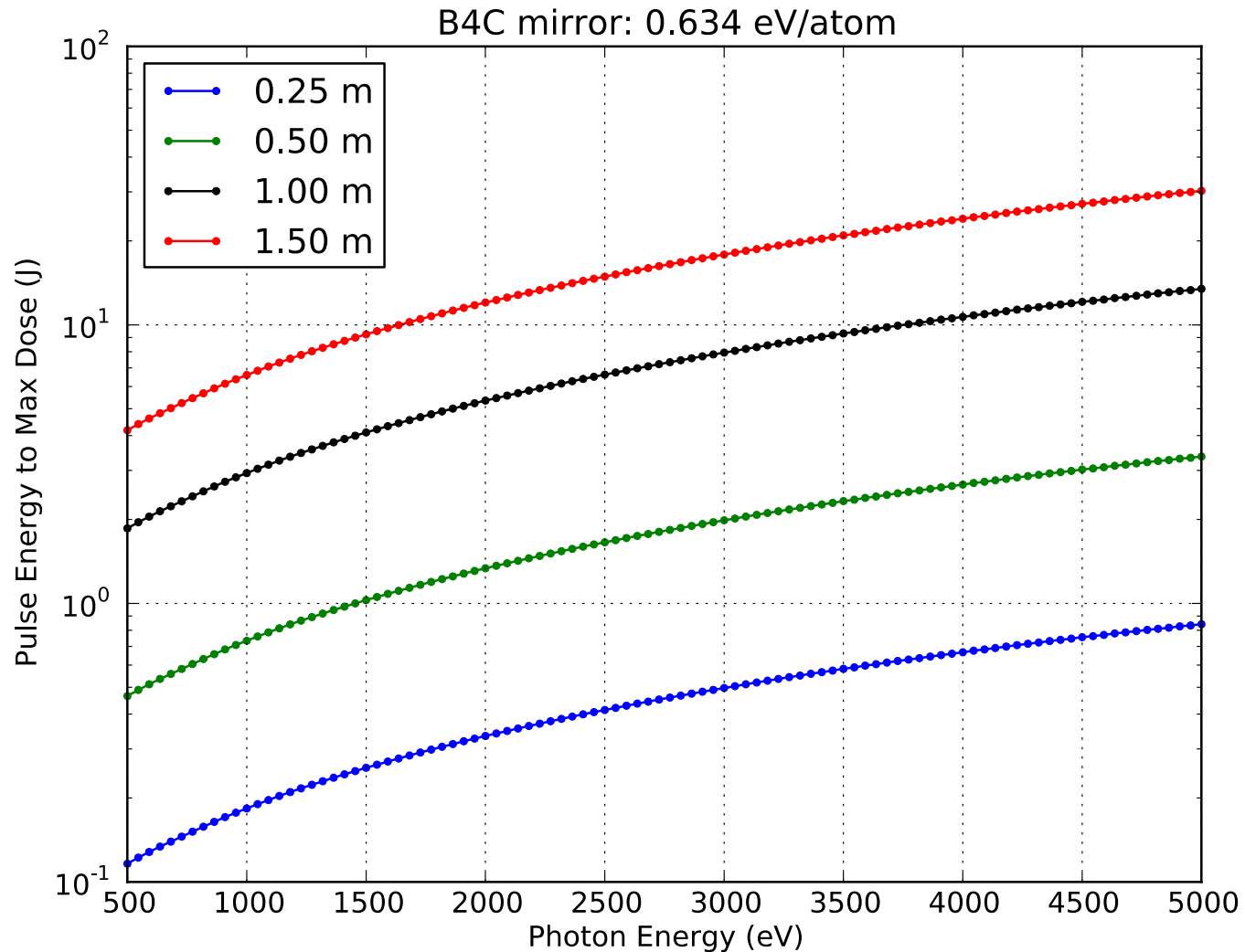


Table of XCC KB mirror parameters

Focal Size (nm)	Photon Energy (eV)	Rayleigh Range (μm)	RMS Source Size (μm)	AOI (deg)	Max E w/ 10x SF (J)	Substrate Length (m)	Unfocused Beam Size (mm)	Source Distance (m)	Reflectivity	Focal Length (m)	IP Distance from Mirror (m)
50	1000	4.5	10	1.30	0.31	1.00	11.34	487	0.872	1.032	0.532
100	1000	18.2	10	0.90	0.68	1.50	11.78	505	0.926	2.144	1.394
50	2000	9.1	10	0.80	0.54	1.00	6.98	600	0.933	1.27	0.770
100	2000	36.4	10	0.60	1.05	1.40	7.33	629	0.967	2.668	1.968
50	2000	9.1	10	0.65	1.21	1.50	8.51	731	0.962	1.548	0.798
100	2000	36.4	10	0.50	2.14	2.00	8.73	750	0.976	3.176	2.176
40	4000	11.6	10	0.4	1.06	1.13	3.93	675	0.982	1.143	0.581
70	4000	35.7	10	0.3	2.40	1.50	3.93	675	0.992	2.001	1.251
40	4000	11.6	10	0.4	2.39	1.50	5.24	899	0.982	1.525	0.775
70	4000	35.7	10	0.3	4.27	2.00	5.24	899	0.992	2.668	1.668

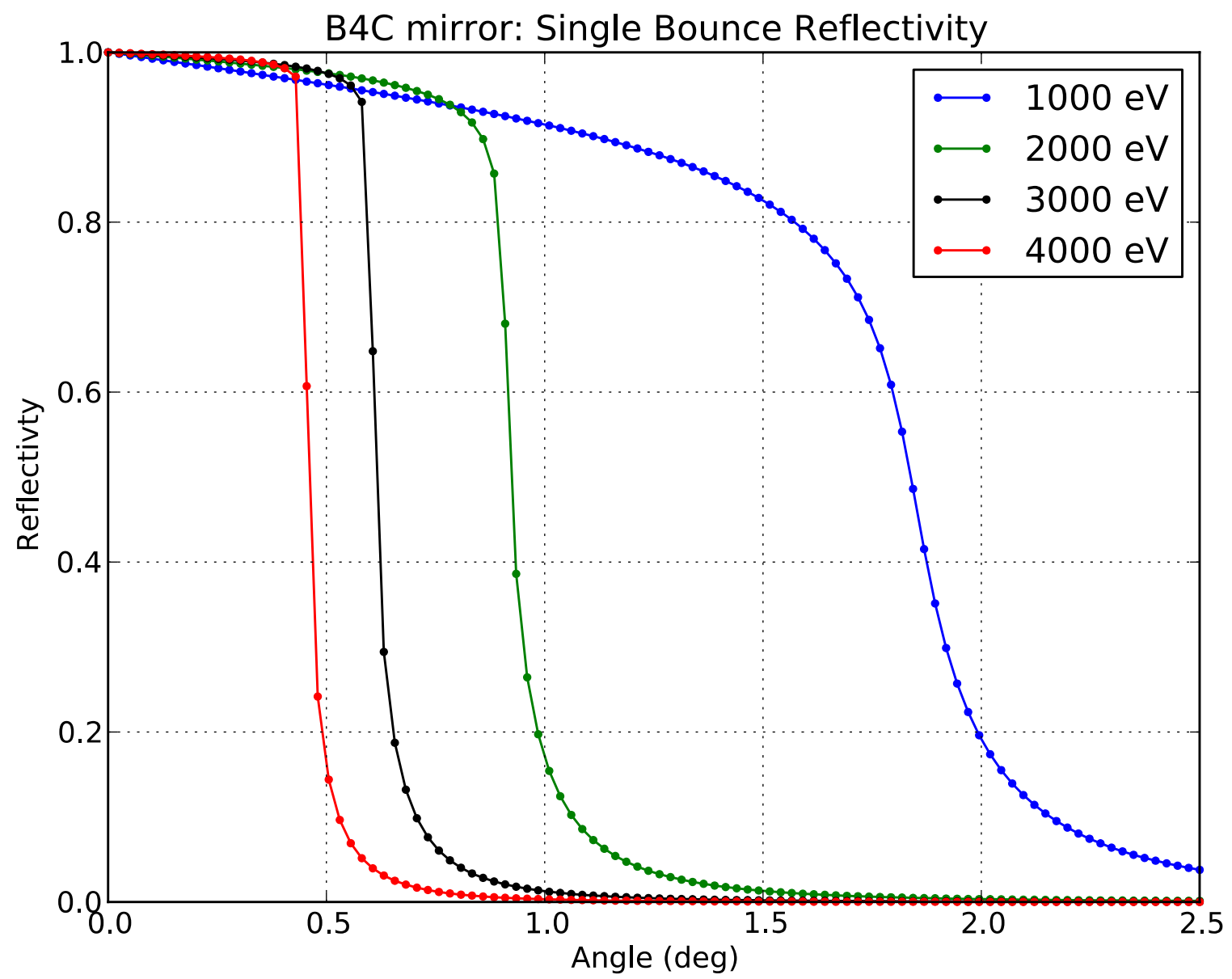
Mirror Damage Limit (single pulse)



- Boron carbide is the highest damage threshold coating and is used for this calculation
- Assumes the incident fwhm beam size is $\frac{1}{2}$ the substrate length
- No safety factor is included in these calculations – 5-10x below this value should be planned for
- Calculation is weakly dependent on incident angle below the mirror cutoff (0.3 deg AOI used)

A large mirror (> 1 m) is needed to survive ~ 1 J pulse energies

Mirror Reflectivity



X-ray Focusing summary following initial study

- Large mirrors (> 1 m) are needed for 1 J per pulse energy
 - 1 m FEL quality substrates produced today
 - 1.5 m substrates produced for synchrotrons
 - > 1 m FEL quality substrates would require development with industry but not R&D
- > 1 km source to KB optic distance is desirable
- FEL average power is a new regime (6.5 kW)
 - This requires an engineering study
 - Very grazing angles help since the most straight forward approach is to absorb less in the substrate
 - Another reason to consider beyond state-of-the-art substrates sizes (e.g. 2 m or beyond)

Replace 62.5 GeV e- beam w/ 5000 GeV WFA e- beam and simulate $\gamma\gamma$ Collisions using CAIN MC

PWFA parameters & $\beta^*=0.030$ mm

Technology	$\gamma\gamma$ PWFA
Aspect Ratio	Round
CM Energy	10.0
Single beam energy (TeV)	5.0
Gamma	1.0E+07
Emittance X (mm mrad)	0.12
Emittance Y (mm mrad)	0.12
Beta* X (m)	0.30E-04
Beta* Y (m)	0.30E-04
Sigma* X (nm)	0.61
Sigma* Y (nm)	0.61
N_bunch (num)	5.00E+09
Freq (Hz)	7725
Sigma Z (um)	5
Geometric Lumi (cm ² s ⁻¹)	6.58E+36

LWFA parameters & $\beta^*=0.100$ mm

$$E_0 = 5 \text{ TeV}$$

$$N_e = 1.2 \times 10^9$$

$$\beta_x = 0.1 \text{ mm}$$

$$\beta_y = 0.1 \text{ mm}$$

$$\epsilon_x = 240/\gamma \text{ nm}$$

$$\epsilon_y = 240/\gamma \text{ nm}$$

$$\sigma_z = 8.5 \text{ } \mu\text{m}$$

$$\text{Repetition Rate} = 47 \text{ kHz}$$

$$L_{e^-e^-, \text{ geo}} = 2.2 \times 10^{35}$$

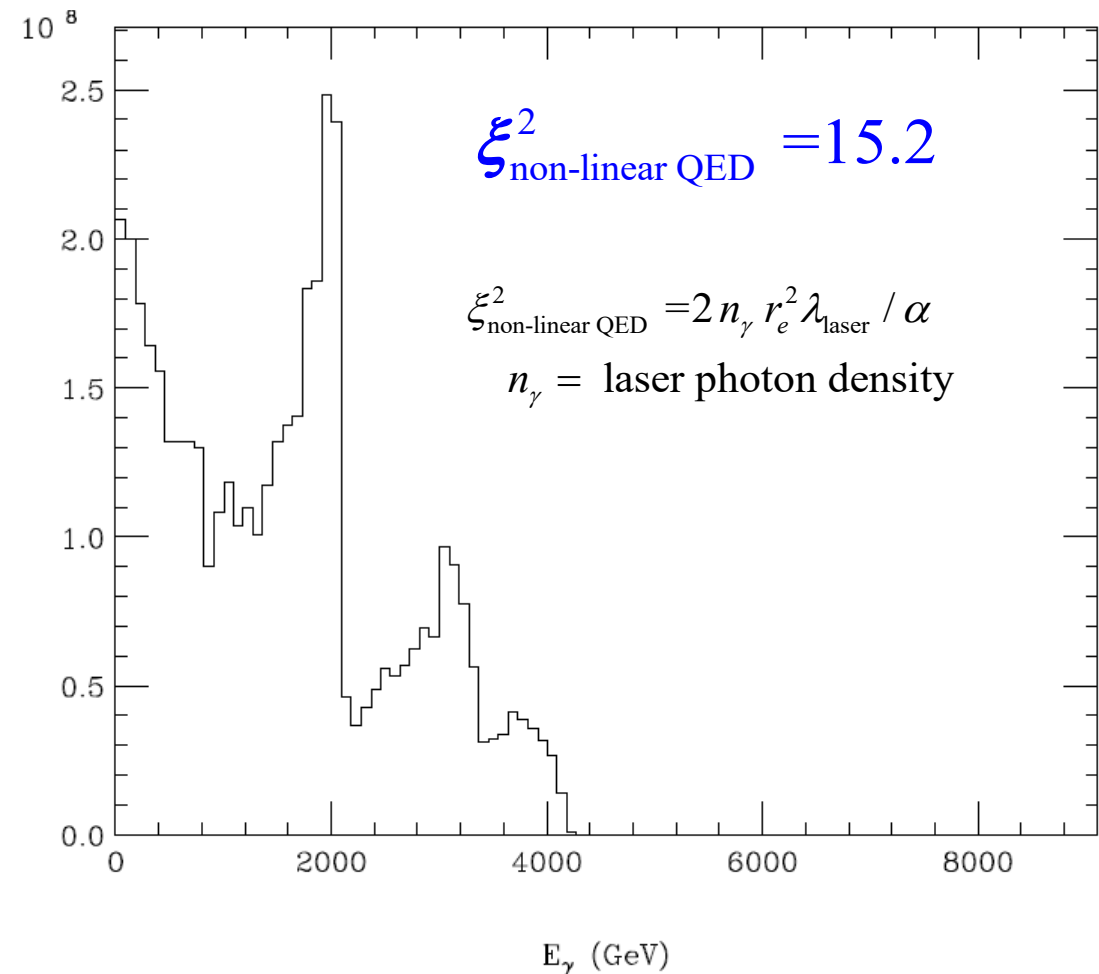
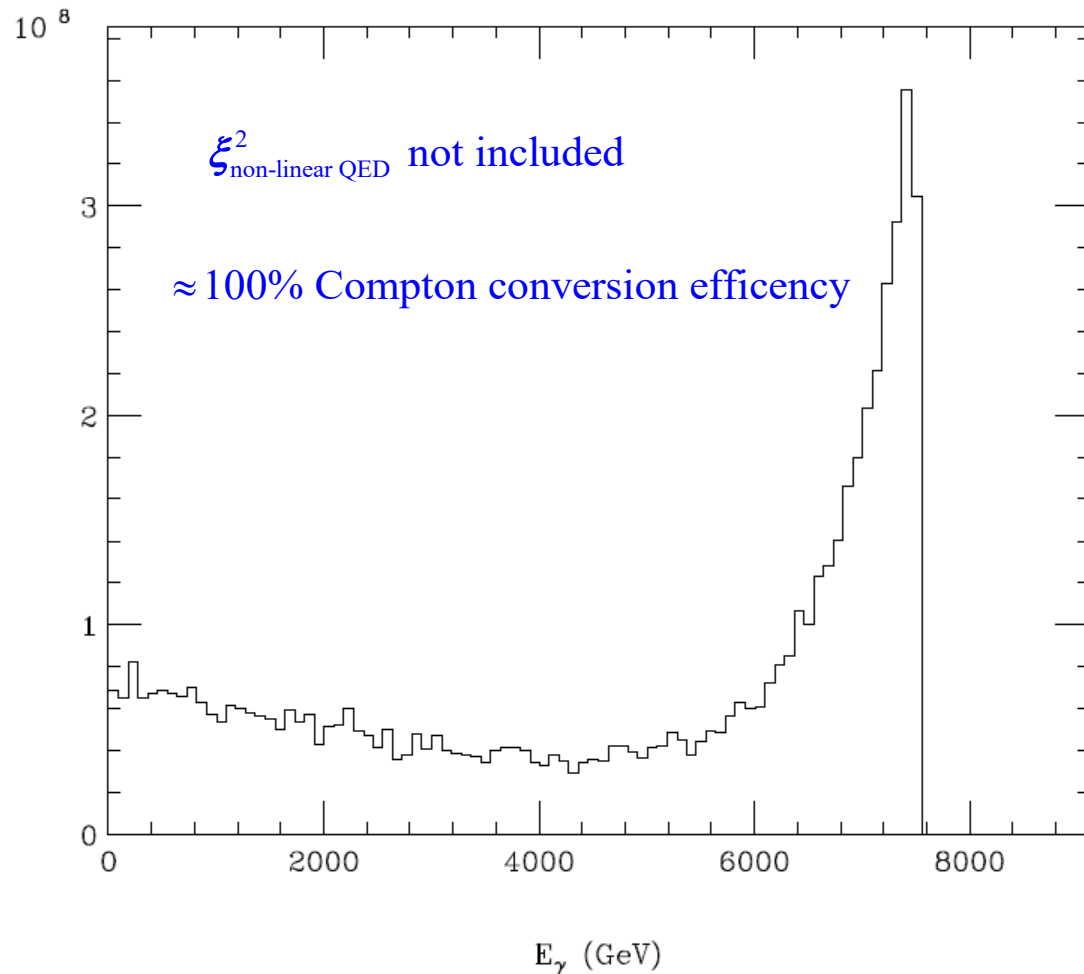
Note: a lot of the discussion that follows uses examples with $E_{\text{cm}}=15$ TeV

Start with $\beta^* = 0.030$ mm parameter set

$x=4.8$ adjust parameters to get $\sim 100\%$ conversion w/ linear QED

$x = 4.8 \Rightarrow 9100 \text{ GeV } e^- + 0.034 \text{ eV } \gamma \text{ } (\lambda=36 \mu\text{m}) \quad a_{\gamma FWHM} = 2.1 \text{ mm} \quad \sigma_{\gamma z} = 0.79 \text{ mm} \quad d_{cp} = 2.4 \text{ mm}$
 $\sigma_{ez} = 5 \mu\text{m} \quad N_{e^-} = 1 \text{ nC} \quad \gamma \epsilon_{x,y} = 120 \text{ nm} \quad 2P_c \lambda_e = -0.9 \quad E_{\text{pulse}} = 4400 \text{ J}$

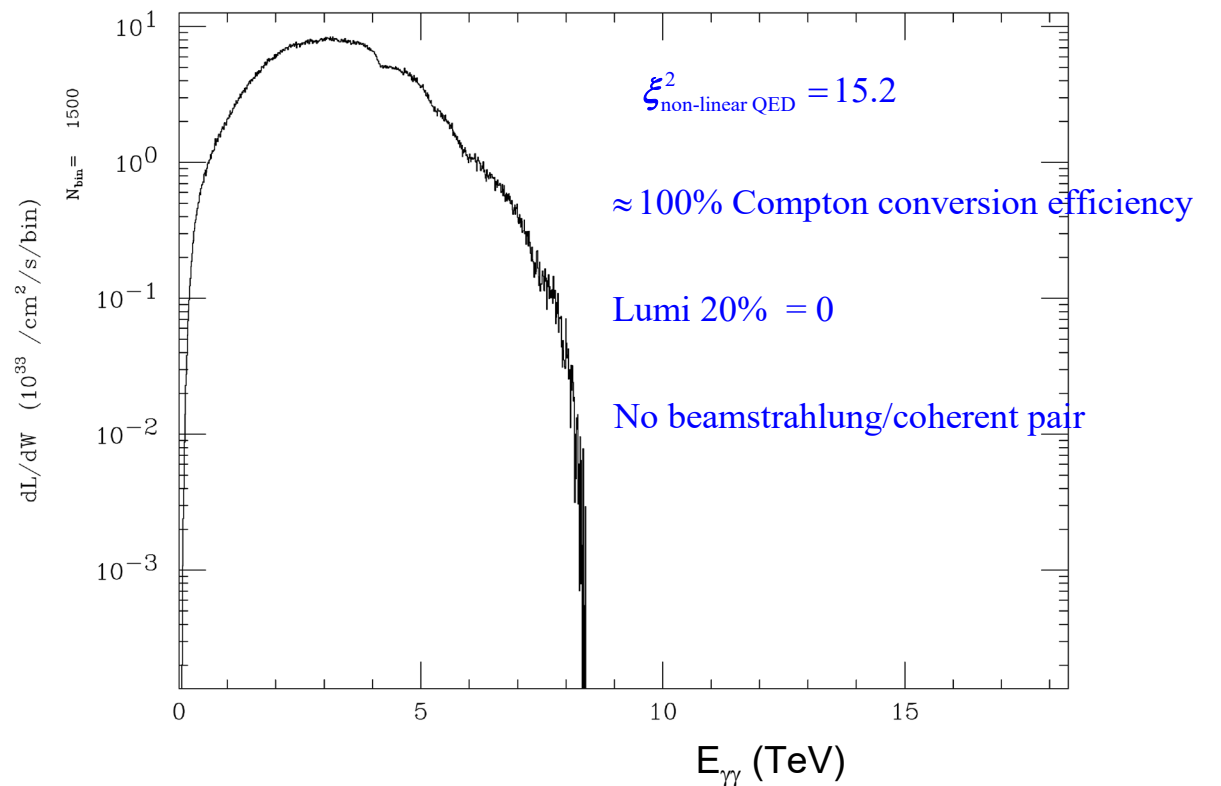
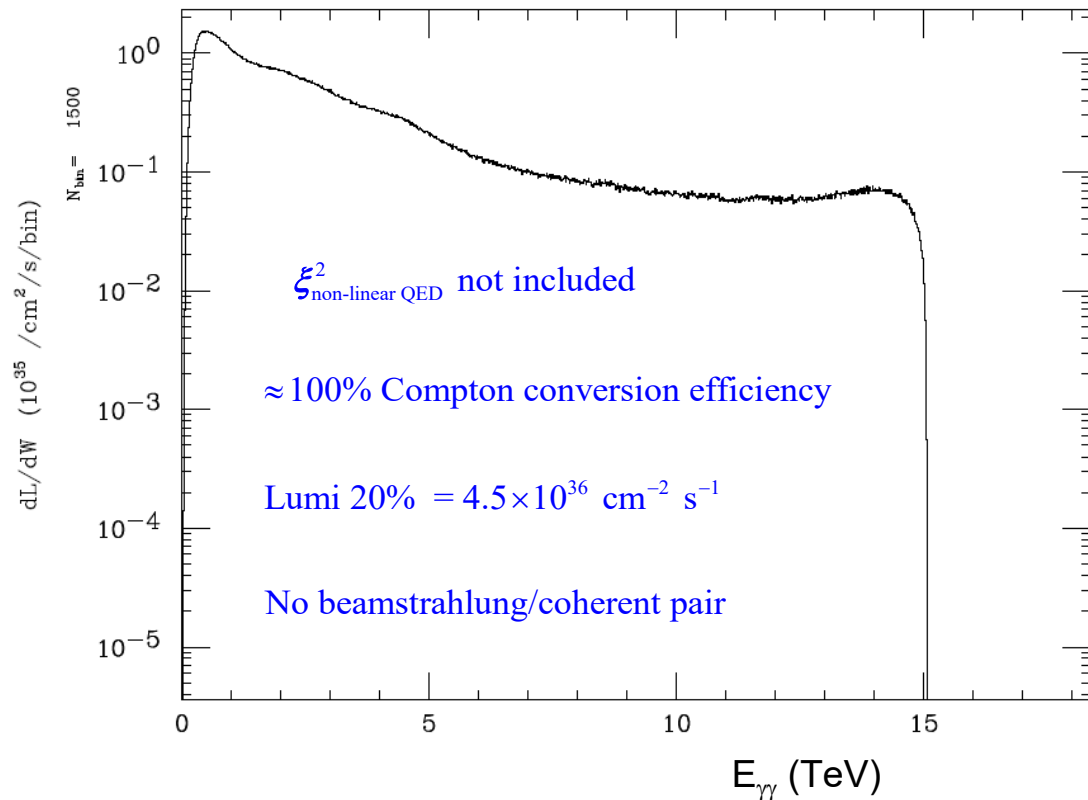
γ Energy Spectra



$x=4.8$, parameters with $\sim 100\%$ conversion w/ linear QED

$x = 4.8 \Rightarrow 9100 \text{ GeV } e^- + 0.034 \text{ eV } \gamma \text{ } (\lambda=36 \mu\text{m})$ $a_{\gamma FWHM} = 2.1 \text{ mm}$ $\sigma_{\gamma z} = 0.79 \text{ mm}$ $d_{cp} = 2.4 \text{ mm}$
 $\sigma_{ez} = 5 \mu\text{m}$ $N_{e^-} = 1 \text{ nC}$ $\gamma\epsilon_{x,y} = 120 \text{ nm}$ $2P_c\lambda_e = -0.9$ $E_{\text{pulse}} = 4400 \text{ J}$

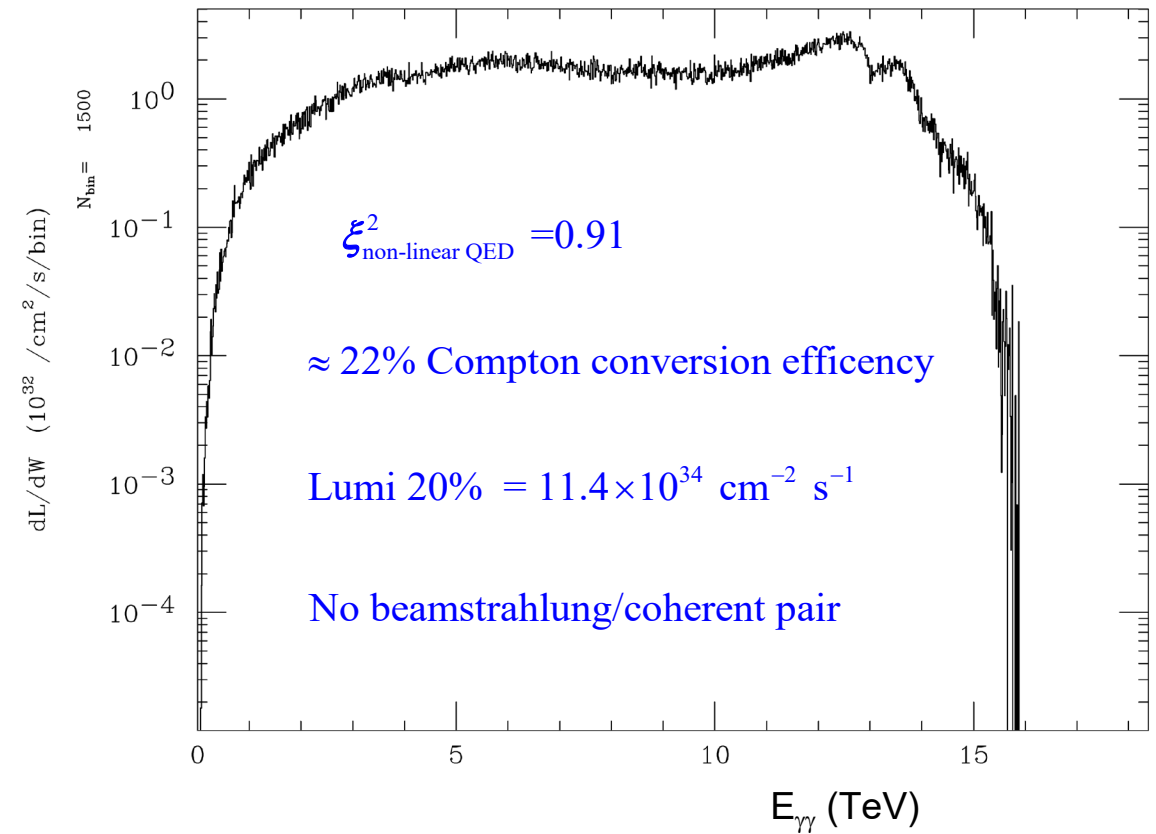
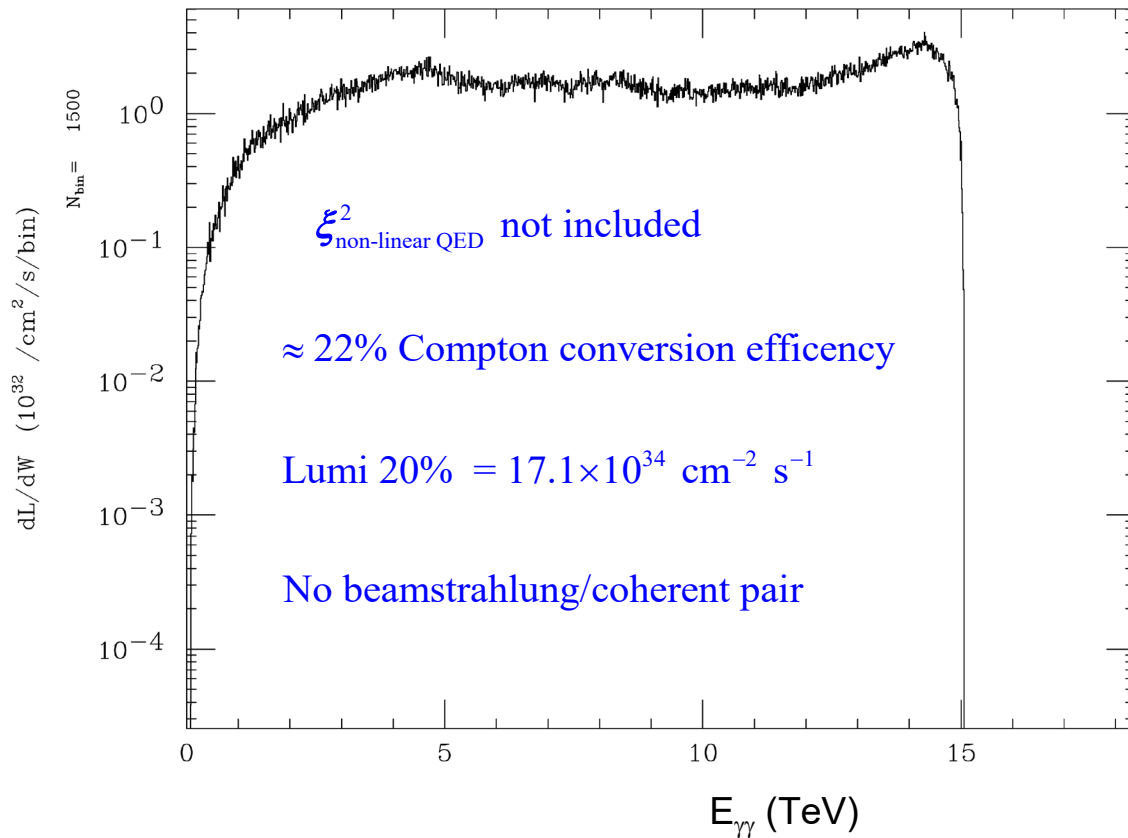
$\gamma\gamma$ Luminosity Spectra



$x=4.8$ dial back E_{pulse} to get $\xi^2 < 1$

$x = 4.8 \Rightarrow 9100 \text{ GeV } e^- + 0.034 \text{ eV } \gamma \text{ } (\lambda=36 \text{ } \mu\text{m}) \quad a_{\gamma FWHM} = 2.1 \text{ mm} \quad \sigma_{\gamma z} = 0.79 \text{ mm} \quad d_{\text{cp}} = 2.4 \text{ mm}$
 $\sigma_{ez} = 5 \text{ } \mu\text{m} \quad N_{e^-} = 1 \text{ nC} \quad \gamma \epsilon_{x,y} = 120 \text{ nm} \quad 2P_c \lambda_e = -0.9 \quad E_{\text{pulse}} = 260 \text{ J}$

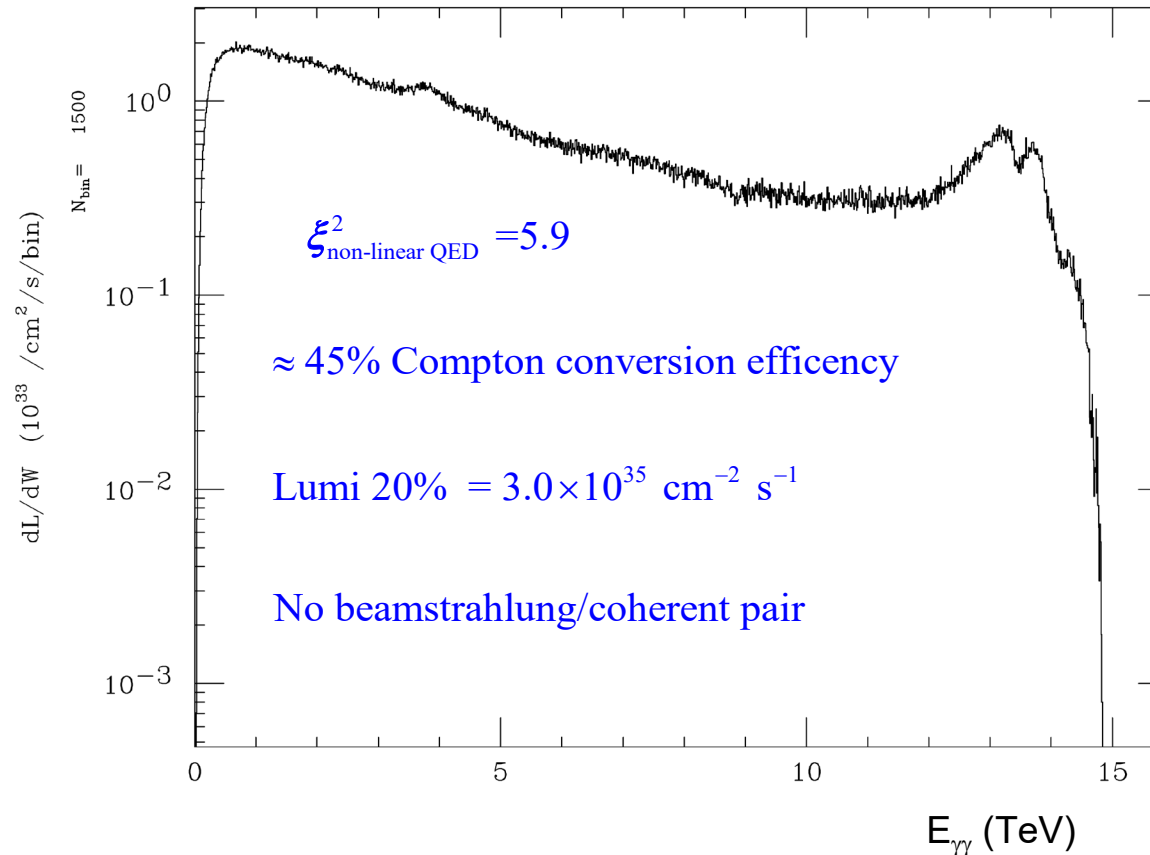
$\gamma\gamma$ Luminosity Spectra



Try $x=40$ to get more of a peak in the spectrum

$$x = 40 \Rightarrow 7875 \text{ GeV } e^- + 0.33 \text{ eV } \gamma \quad (\lambda = 3.7 \text{ } \mu\text{m}) \quad a_{\gamma FWHM} = 0.24 \text{ mm} \quad \sigma_{\gamma z} = 270 \text{ } \mu\text{m} \quad d_{cp} = 0.82 \text{ mm}$$
$$\sigma_{ez} = 5 \text{ } \mu\text{m} \quad N_{e^-} = 5 \times 10^9 \quad \gamma \epsilon_{x,y} = 120 \text{ nm} \quad 2P_c \lambda_e = -0.9 \quad E_{\text{pulse}} = 590 \text{ J}$$

$\gamma\gamma$ Luminosity Spectrum



15 TeV and x=40 Turn on coherent processes

$$x = 40 \Rightarrow 7875 \text{ GeV } e^- + 0.33 \text{ eV } \gamma \text{ } (\lambda = 3.7 \text{ } \mu\text{m}) \quad a_{\gamma FWHM} = 0.24 \text{ mm} \quad \sigma_{\gamma z} = 270 \text{ } \mu\text{m} \quad d_{cp} = 0.82 \text{ mm}$$
$$\sigma_{ez} = 5 \text{ } \mu\text{m} \quad N_{e^-} = 5 \times 10^9 \quad \gamma \epsilon_{x,y} = 120 \text{ nm} \quad 2P_c \lambda_e = -0.9 \quad E_{pulse} = 590 \text{ J}$$

Halfway through the collision CAIN complains:

(SUBR.COHPAR) Algorithm of coherent pair generation wrong.

Call the programmer prob,pmaxco= 8.309E-01 8.000E-01

Solution:

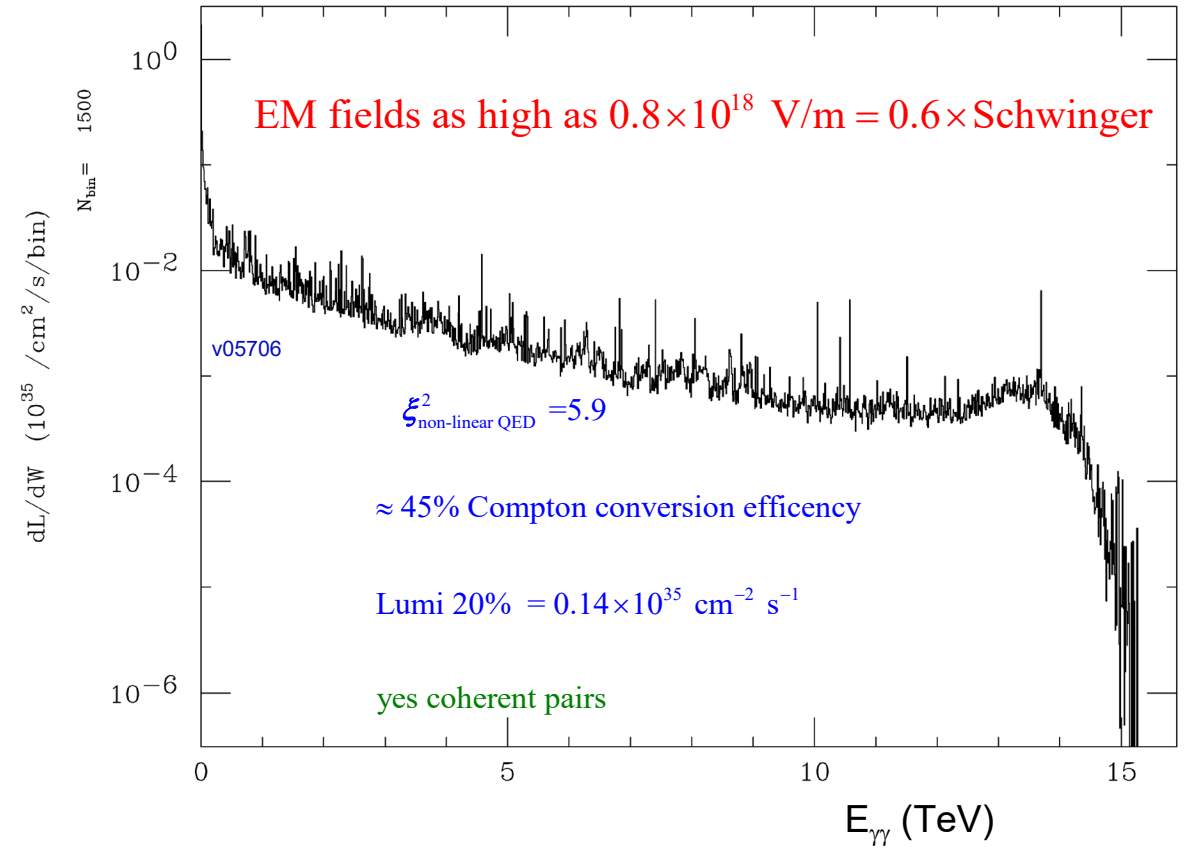
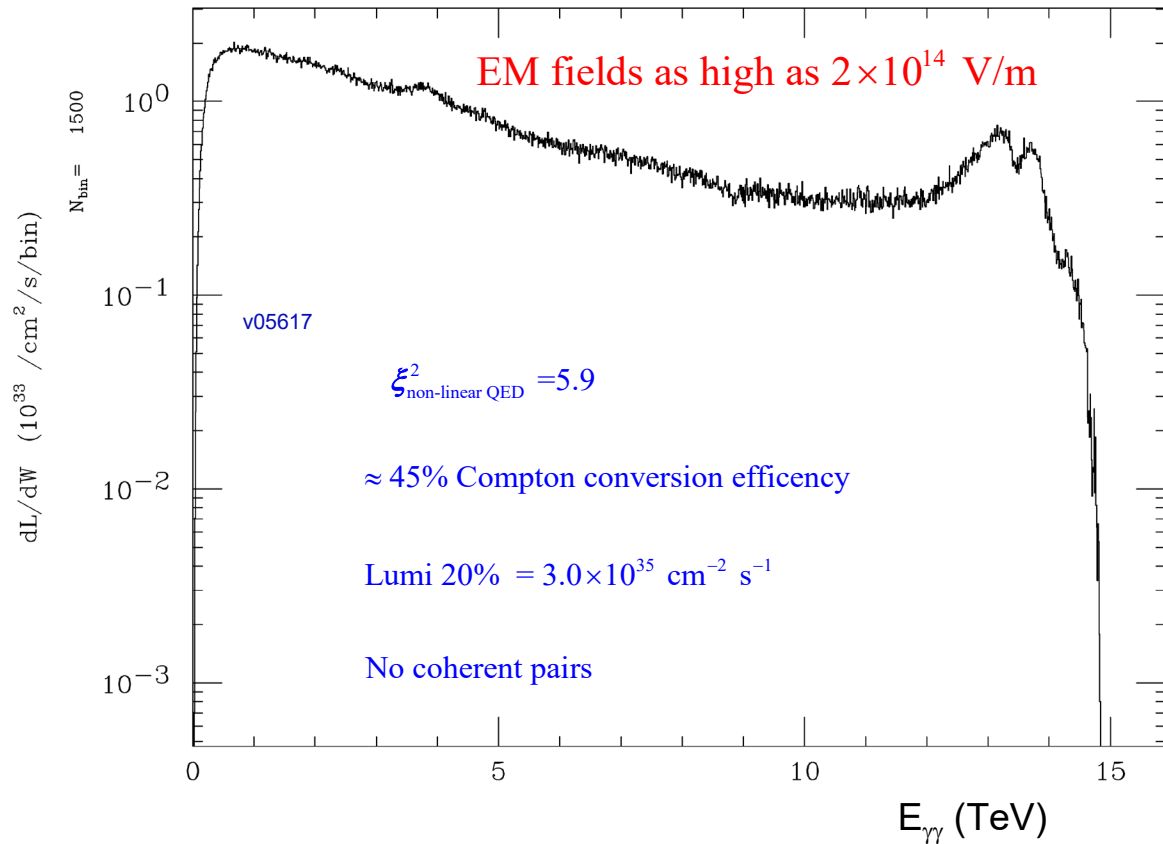
number of macro particles produced per coherent beamstrahlung photon = 1 \rightarrow 0.01

number of pairs of macro particles produced per coherent e+e- pair = 1 \rightarrow 0.0001

number of macro particles produced per incoherent particle = 1 \rightarrow 0.01

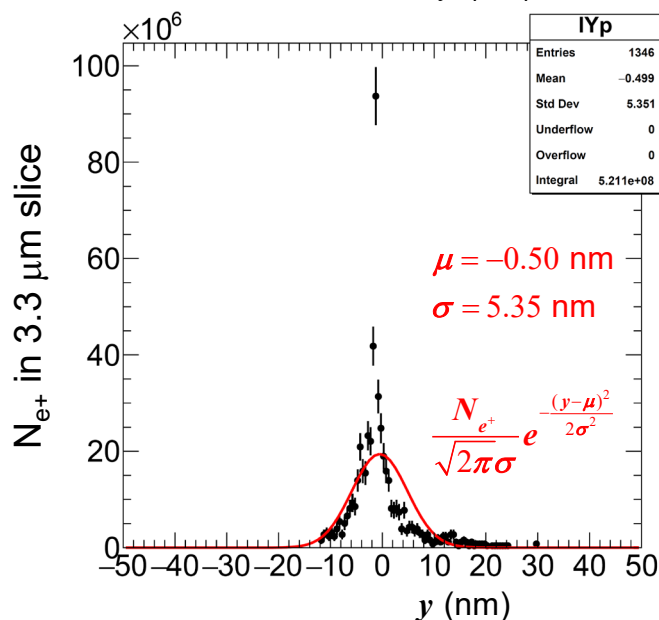
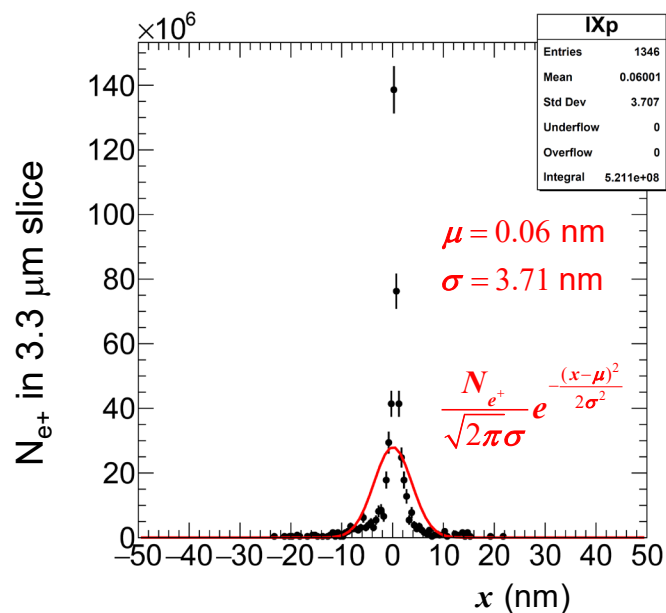
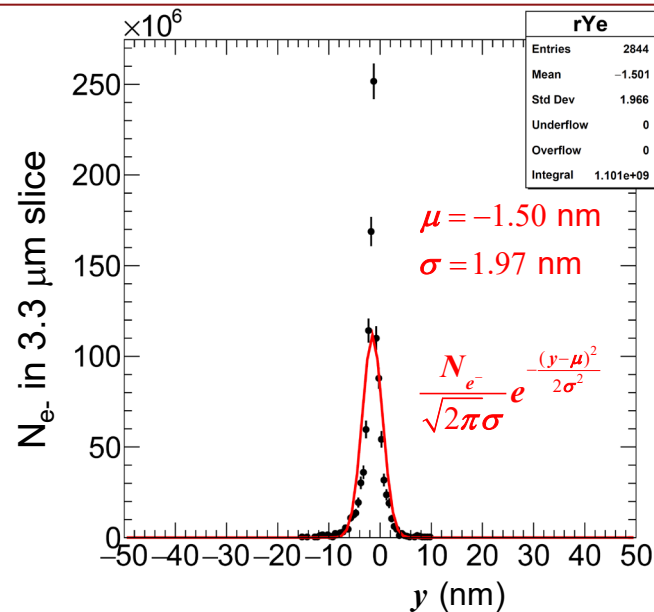
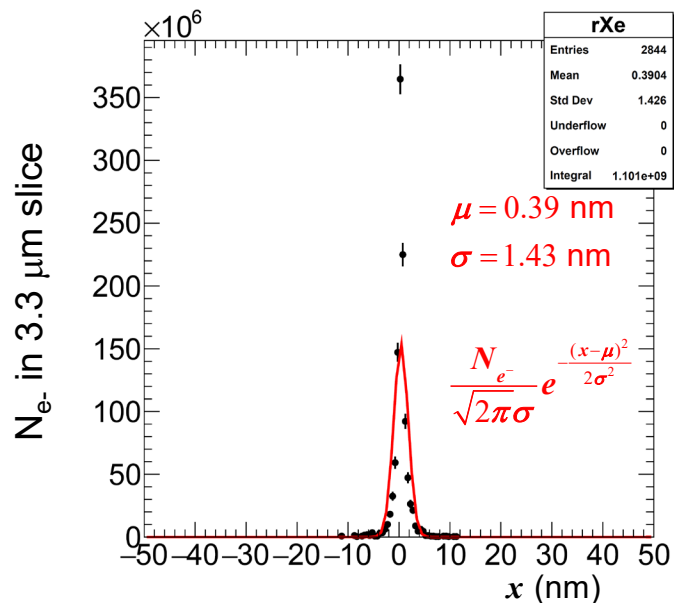
15 TeV and x=40 Turn on coherent processes

$x = 40 \Rightarrow 7875 \text{ GeV } e^- + 0.33 \text{ eV } \gamma \text{ } (\lambda = 3.7 \text{ } \mu\text{m})$ $a_{\gamma FWHM} = 0.24 \text{ mm}$ $\sigma_{\gamma z} = 270 \text{ } \mu\text{m}$ $d_{cp} = 0.82 \text{ mm}$
 $\sigma_{ez} = 5 \text{ } \mu\text{m}$ $N_{e^-} = 5 \times 10^9$ $\gamma \mathcal{E}_{x,y} = 120 \text{ nm}$ $2P_c \lambda_e = -0.9$ $E_{\text{pulse}} = 590 \text{ J}$



Coherent pair production eats up the 7.5 TeV photons and produces many e^+ that pinch the e^- beam leading to higher fields and even more coherent pair production.

$e^- \gamma$ collisions at $E_{e\gamma}=140$ GeV I.P. geometric $e^- \sigma_x, \sigma_y=5.1$ nm



During the collision, the e^+ from coherent e^+e^- production are focused by the EM field of the oncoming e^- beam. This leads to focusing (pinching) of the e^- beam.

This pinching creates very high fields which leads to even more coherent pair production and even higher fields.

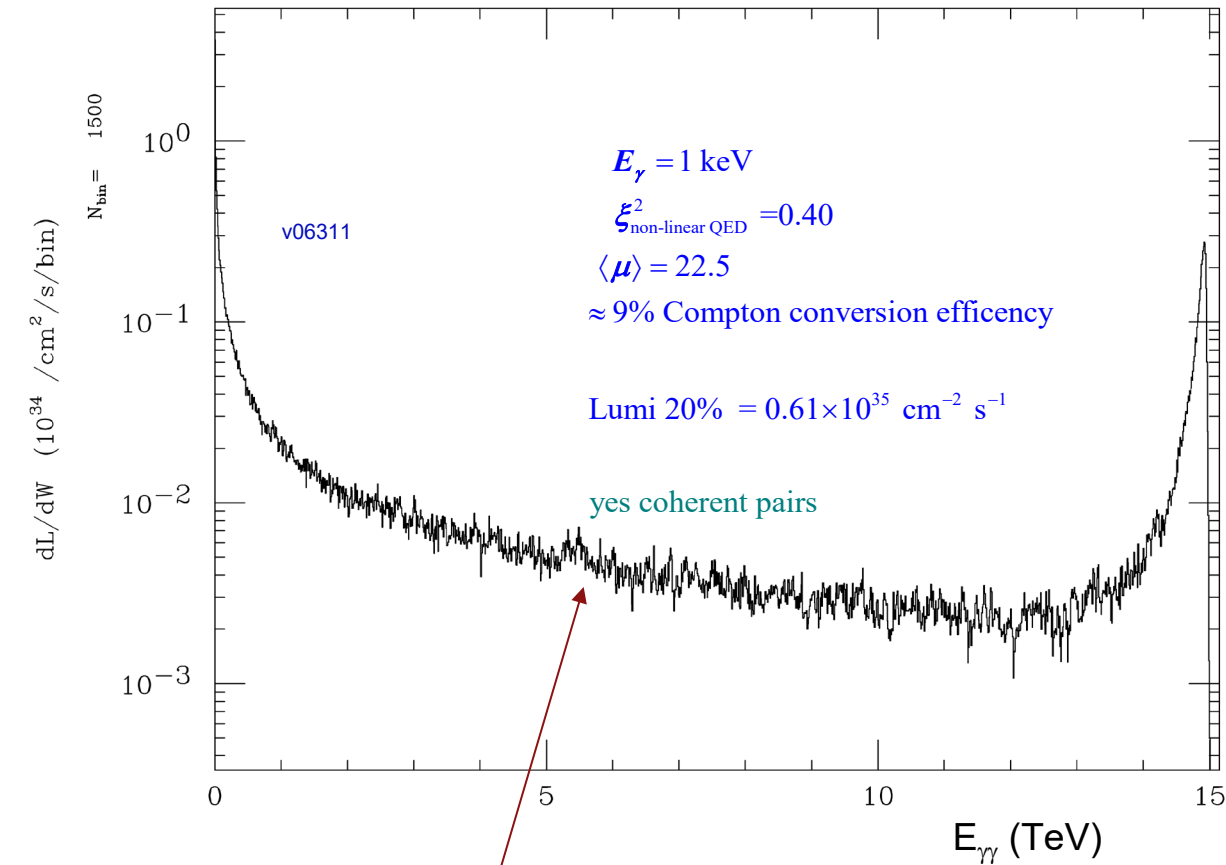
$x=1.2 \times 10^5$ (1 keV γ) not affected as much by coherent processes

$$x = 1.2 \times 10^5 \Rightarrow 7500 \text{ GeV } e^- + 1 \text{ keV } \gamma \quad (\lambda = 1.2 \text{ nm})$$

$$a_{\gamma FWHM} = 70 \text{ nm} \quad \sigma_{\gamma z} = 5 \text{ } \mu\text{m} \quad d_{cp} = 15 \text{ } \mu\text{m}$$

$$\sigma_{ez} = 5 \text{ } \mu\text{m} \quad N_{e^-} = 6 \times 10^9 \quad \gamma \epsilon_{x,y} = 120 \text{ nm}$$

$$2P_c \lambda_e = +0.9 \quad E_{\text{pulse}} = 0.72 \text{ J}$$

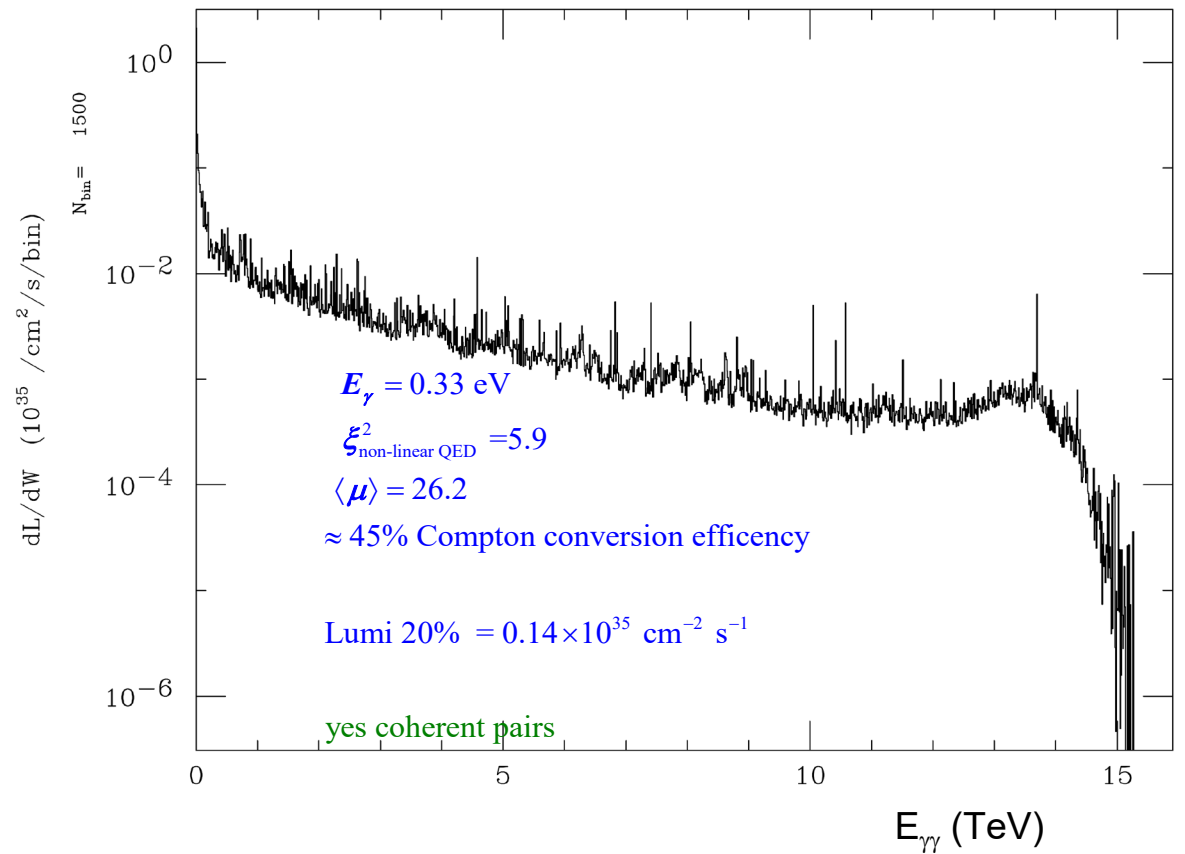


$$x = 40 \Rightarrow 7875 \text{ GeV } e^- + 0.33 \text{ eV } \gamma \quad (\lambda = 3.7 \text{ } \mu\text{m})$$

$$a_{\gamma FWHM} = 0.24 \text{ nm} \quad \sigma_{\gamma z} = 270 \text{ } \mu\text{m} \quad d_{cp} = 0.82 \text{ mm}$$

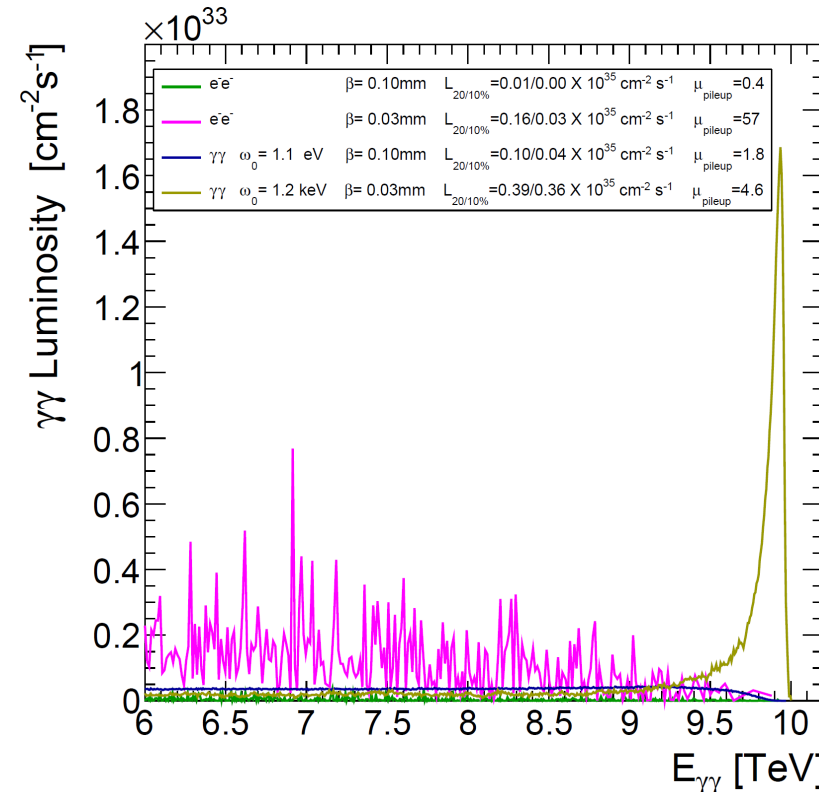
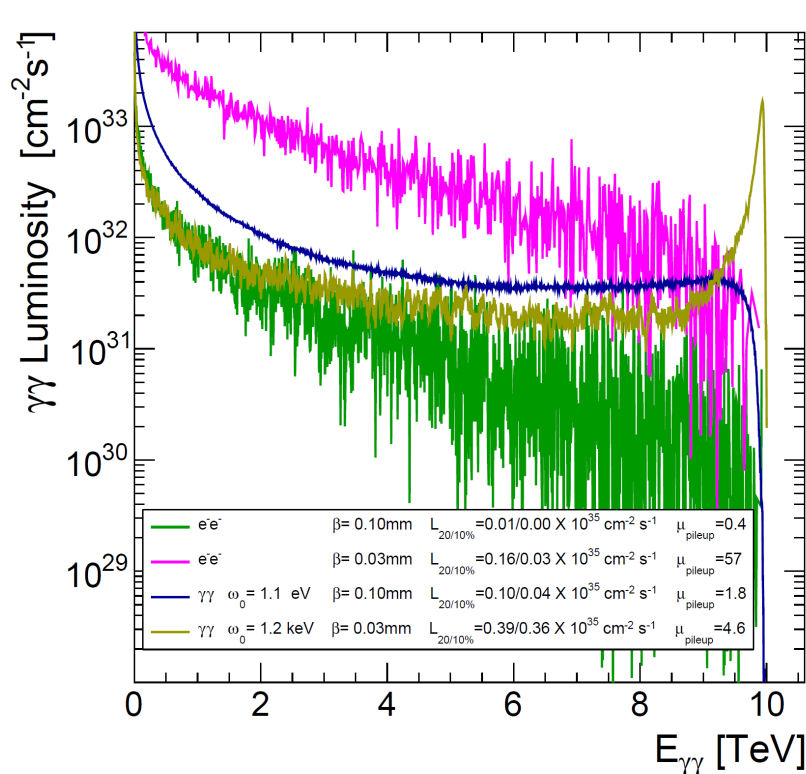
$$\sigma_{ez} = 5 \text{ } \mu\text{m} \quad N_{e^-} = 5 \times 10^9 \quad \gamma \epsilon_{x,y} = 120 \text{ nm}$$

$$2P_c \lambda_e = -0.9 \quad E_{\text{pulse}} = 590 \text{ J}$$



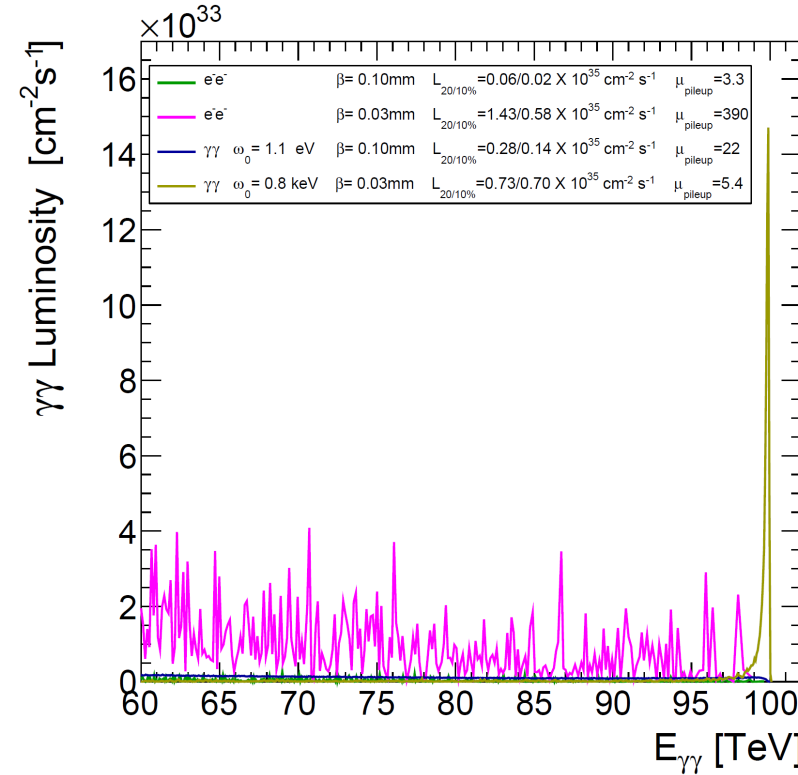
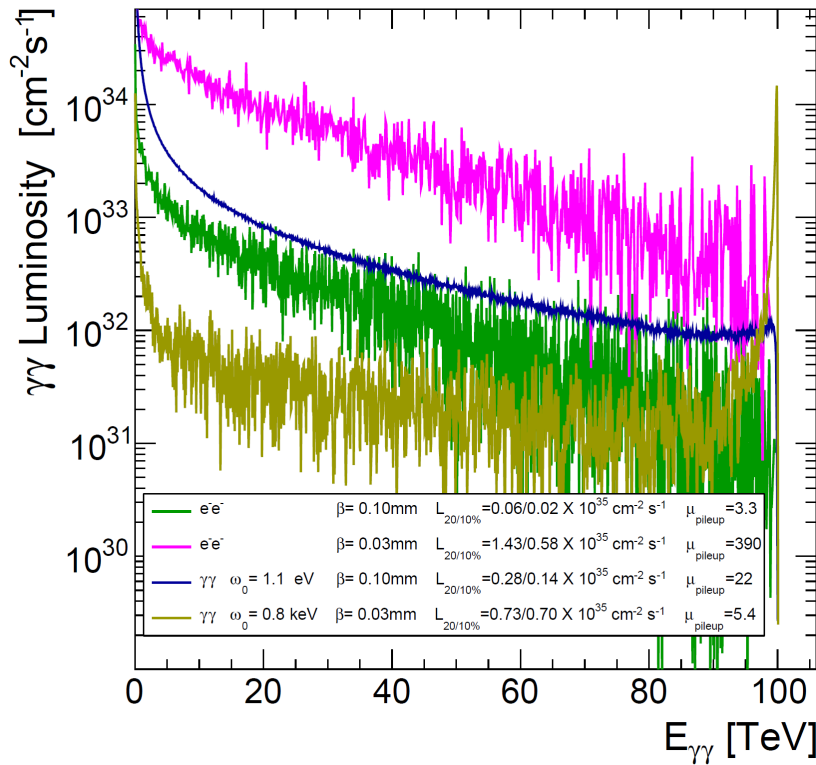
e^- from Compton IP have much reduced energy due to multiple trident $e^- \gamma \rightarrow e^- e^+ e^-$. EM fields are 3 orders of magnitude smaller.

$\gamma\gamma$ Luminosity Spectra at 10 TeV



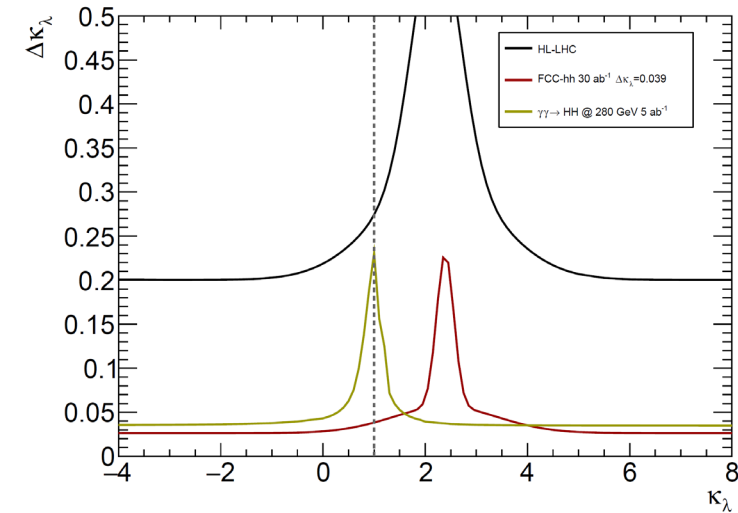
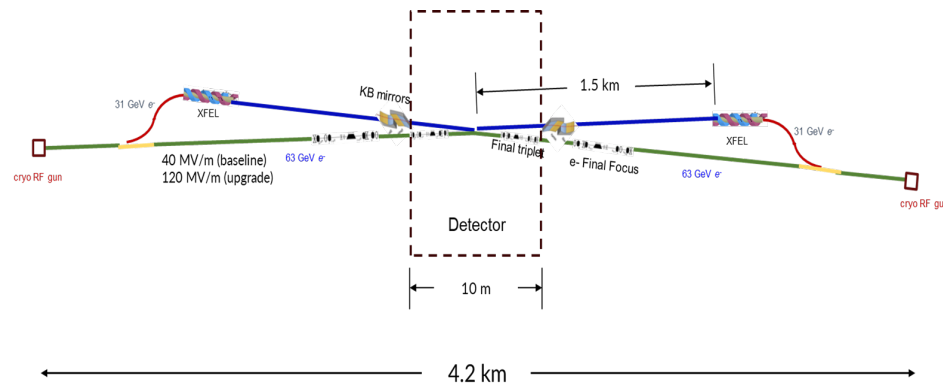
For $\beta^* = 0.03 \text{ mm}$, a minimum value of x is required to minimize final e^- energies through multiple $e^- \gamma \rightarrow e^- e^+ e^-$ interactions (without these interactions the large number of full energy e^- create too strong an EM field $\Rightarrow e^- e^-$ pinching and runaway pair production). After that the optimum value of $x = 90,000$ ($\omega_0 = 1 \text{ keV}$) is determined by the Compton IP evolution of $e^- \gamma \rightarrow e^- \gamma$, $e^- \gamma \rightarrow e^- e^+ e^-$ & $\gamma\gamma \rightarrow e^+ e^-$. Note that very different x but same ω_0 provide optimum peak luminosity.

$\gamma\gamma$ Luminosity Spectra at 100 TeV



Same story as w/ 10 TeV: for tight e^- focusing w/ $\beta^* = 0.03 \text{ mm}$, a minimum value of x is required to minimize final e^- energies through multiple $e^- \gamma \rightarrow e^- e^+ e^-$ interactions. After that the optimum value of $x = 600,000$ is determined by the Compton IP evolution of $e^- \gamma \rightarrow e^- \gamma$, $e^- \gamma \rightarrow e^- e^+ e^-$ & $\gamma\gamma \rightarrow e^+ e^-$. However, here the laser pulse energy has increased from 1 Joule to 20 Joules due to the extremely small cross-sections at this value of x . Also, other processes beyond $e^- \gamma \rightarrow e^- e^+ e^-$ probably come into play which have not been considered here. Again, optimum peak luminosity with very different x but same $\omega_0 \sim 1 \text{ keV}$.

Summary



The XCC has a compelling Higgs physics case with a minimal 4 km footprint, and could serve as a prototype for 10 - 100 TeV $\gamma\gamma$ PWFA colliders.

In the XCC the problem of cost and size has been transformed into a series of technological challenges:

- High brightness polarized e^- source, focusing of round beams to 5 nm x 5 nm, ...
- Layout of e- and XFEL beamlines with 2 e^- and 2 XFEL beams entering and exiting the IR.
- The accelerator R&D unique to XCC -- production and focusing of 1 Joule/pulse XFEL beams -- is unique not only within particle physics, but also within the broader x-ray science community. XCC is the first science project to require 1 Joule/pulse soft x-ray beams, which could ultimately have broader applications.
- The required R&D for XCC aggressively pushes both high brightness e^- acceleration and high power XFEL development.

$\gamma\gamma$ -Collider Path

Complete Higgs Factory Program, Comparable to ILC, LCF

125 GeV

280/380 GeV

10 TeV

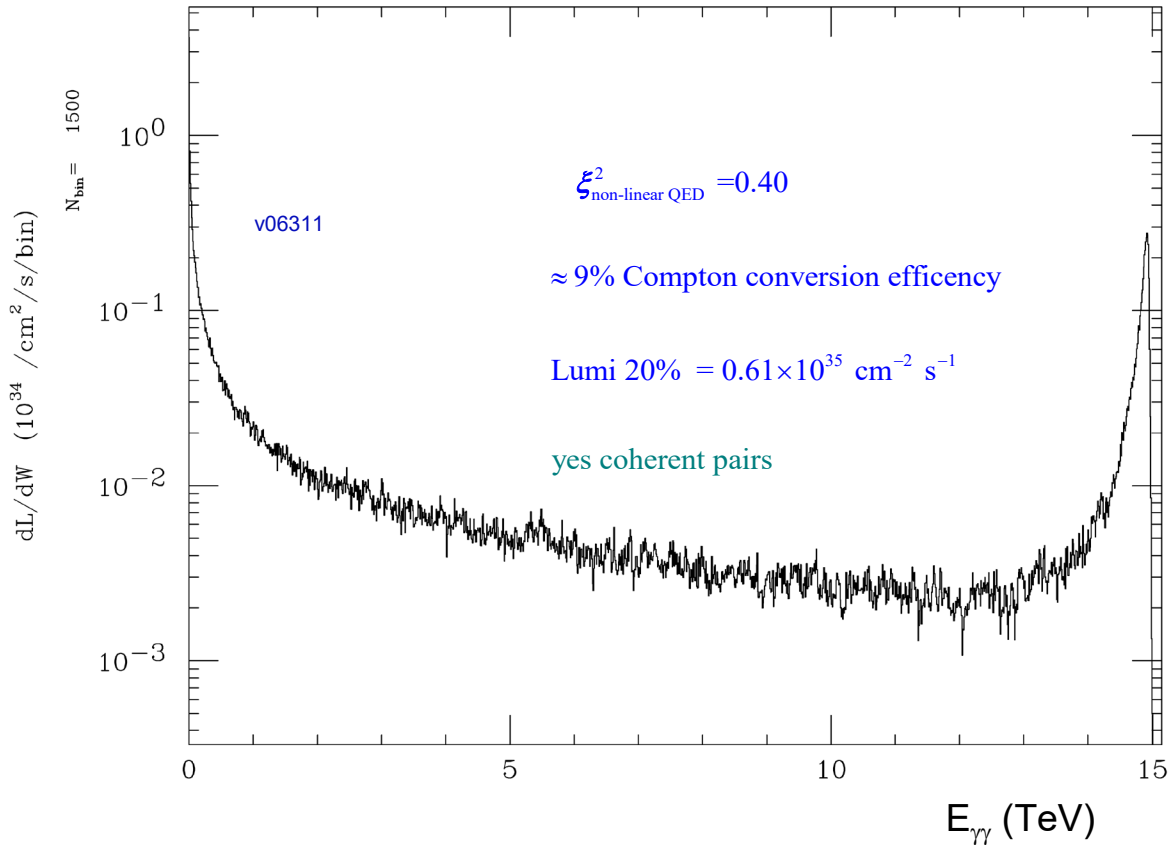
- Standalone project (XCC)
- Second interaction region of a linear collider facility at CERN (**LCVISION** proposal to European Strategy)
- Future 10 TeV plasma wakefield collider

Backup

$$\gamma\gamma \rightarrow N \times e^+e^-, \quad e^-\gamma \rightarrow e^- + N \times e^+e^-, \quad N = 2, 3, \dots$$

$$x = 1.2 \times 10^5 \Rightarrow 7500 \text{ GeV } e^- + 1 \text{ keV } \gamma \quad (\lambda = 1.2 \text{ nm}) \quad a_{\gamma FWHM} = 70 \text{ mm} \quad \sigma_{\gamma z} = 5 \mu\text{m} \quad d_{cp} = 15 \mu\text{m}$$

$$\sigma_{ez} = 5 \mu\text{m} \quad N_{e^-} = 1 \text{ nC} \quad \gamma\epsilon_{x,y} = 120 \text{ nm} \quad 2P_c\lambda_e = +0.9 \quad E_{\text{pulse}} = 0.72 \text{ J}$$



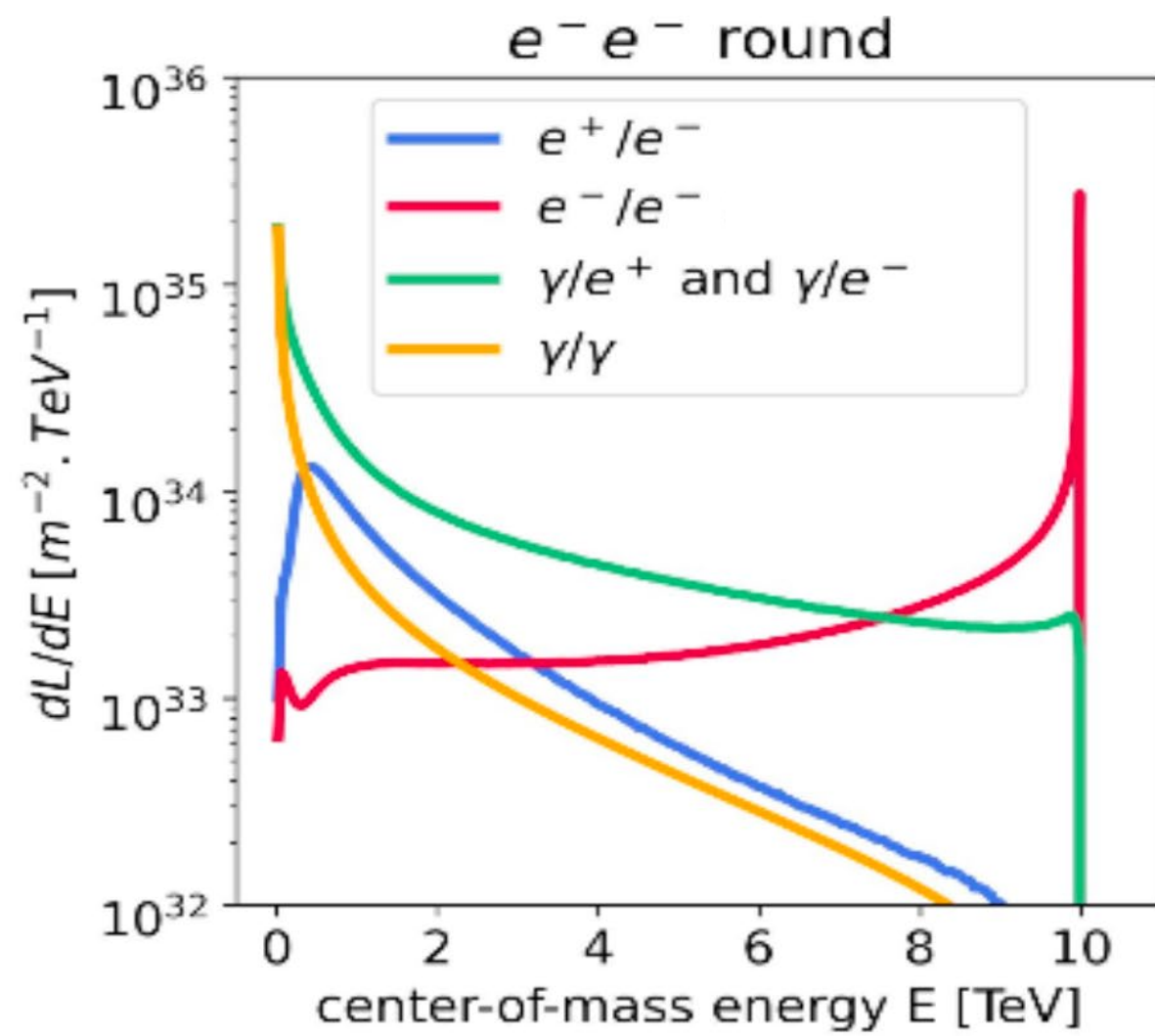
$\gamma\gamma \rightarrow N \times e^+e^-, \quad e^-\gamma \rightarrow e^- + N \times e^+e^-, \quad N = 2, 3, \dots$ are not simulated by CAIN.
 $N \geq 2$ cross sections relatively small for $x \leq 1000$, but what about at $x \sim 10^5$?

Cross section Table for 1 keV laser γ calculated using Tree-level MC Integration:

Note: processes colored red are included in the CAIN MC

process	$E_{e^-} \text{ (GeV)}/x = 62.6 / 1000$	$E_{e^-} \text{ (GeV)}/x = 5000 / 80,000$	$E_{e^-} \text{ (GeV)}/x = 7500 / 120,000$
$\gamma\gamma \rightarrow e^+e^-$	$2.16 \times 10^{12} \pm 0.03\%$	$2.68 \times 10^{10} \pm 0.07\%$	
$\gamma\gamma \rightarrow e^+e^-e^+e^-$	$3.26 \times 10^9 \pm 0.27\%$	$5.70 \times 10^9 \pm 0.92\%$	
$\gamma\gamma \rightarrow e^+e^-e^+e^-e^+e^-$		$2.33 \times 10^4 \pm 11.9\%$	
$e^-\gamma \rightarrow e^-e^+e^-$	$8.22 \times 10^{12} \pm 0.22\%$	$9.55 \times 10^{11} \pm 13.4\%$	$4.61 \times 10^{10} \pm 30.4\%$
$e^-\gamma \rightarrow e^-e^+e^-e^+e^-$	$1.63 \times 10^7 \pm 0.78\%$	$5.68 \times 10^6 \pm 21.1\%$	$7.47 \times 10^5 \pm 17.4\%$

The relative MC integration statistical error increases for $x \sim 10^5$ but it is good enough to demonstrate that the $N = 1$ processes still dominate at $x \sim 10^5$ and therefore the current CAIN MC is valid.



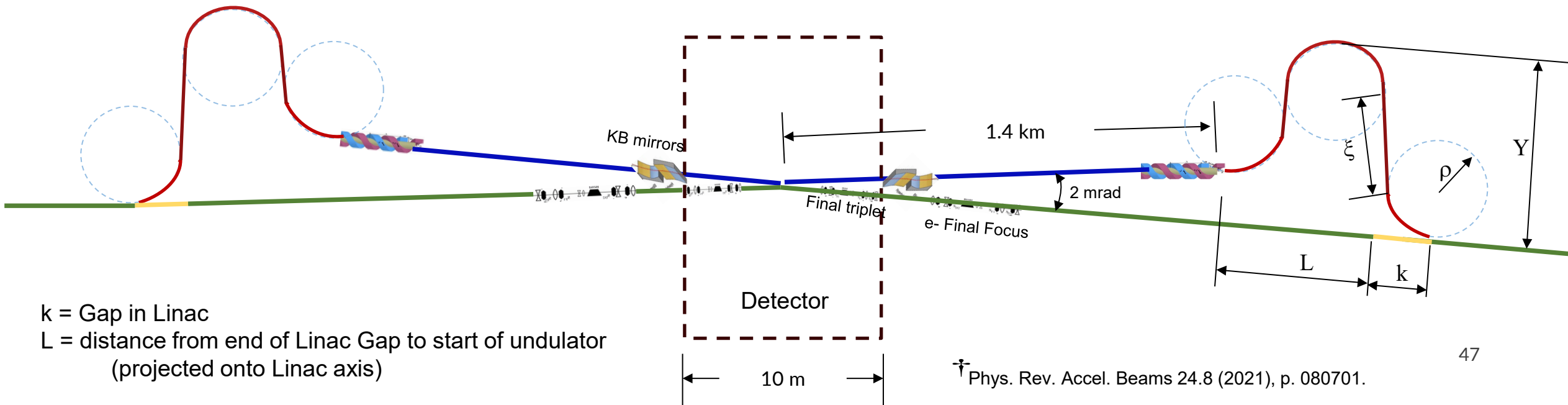
Trombone-like configuration for extraction line

Δs = difference in path lengths for the 31 GeV and 62.6 GeV beams (should be 0.63 m for $\Delta t = 2.1$ ns bunch spacing)

job	L[m]	k[m]	ξ [m]	Y[m]	ρ [m]	Δt [ns]	Δs [m]	σ_{CSR} [%]	B_{field} [T]	Magnetic length [m]
v00052	199	282	255	26	1.0	2.1	0.63	0.005	102	0.40
v00054	108	139	136	16	0.5	2.1	0.63	0.005	205	0.22
v00060	377	117	255	40	3.1	2.1	0.63	0.012	9.9	1.9
v00061	426	68	254	45	4.4	2.1	0.63	0.015	7.0	3.2
v00064	272	123	203.19	40.33	4.4	2.1	0.63	0.017	7.0	3.5
v00064	272	123	203.39	40.37	4.4	3.4	1.02	0.017	7.0	3.5

$$\dagger \sigma_{CSR} = 0.246 \frac{Nr_e L_B}{\gamma \rho^{2/3} \sigma_z^{4/3}}$$

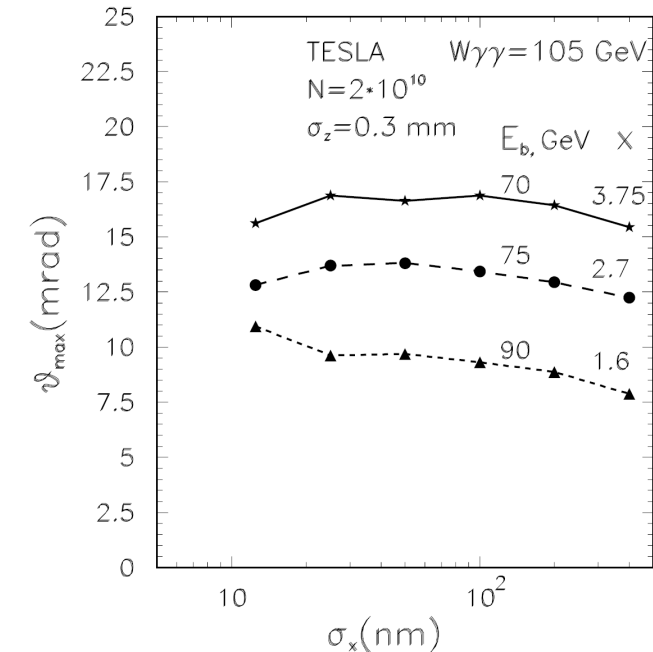
Should also check incoherent synchrotron radiation



TESLA TDR $\gamma\gamma$ Collider Specifies 34 mrad Crossing Angle

The crossing angle for the TESLA $\gamma\gamma$ collider is discussed in section 1.4.4.2 of TESLA TDR, Part VI, Chapter 1: The Photon Collider at TESLA

The concern is low energy, large angle particles striking the quads. For fixed $\sqrt{s_{\gamma\gamma}}$ the maximum disruption angle ϑ_{\max} is given by $\vartheta_{\max} \propto \frac{x}{\sqrt{(1+x)\sigma_c(x)}}$ where $\sigma_c(x)$ is the Compton cross section with leading term $\sigma_c(x) \propto \frac{1}{x}$.



They conclude that for a fixed laser $\lambda=1.06 \mu\text{m}$ and $200 \text{ GeV} \leq \sqrt{s_{\gamma\gamma}} \leq 500 \text{ GeV}$, the the maximum disruption angle is $\vartheta_{\max} \approx 14$ mrad, and they set the crossing angle at $\theta_c = 34$ mrad.

Let's check this with CAIN. Calculate energy incident on 6 cm dia. cryostat at L*=3m.

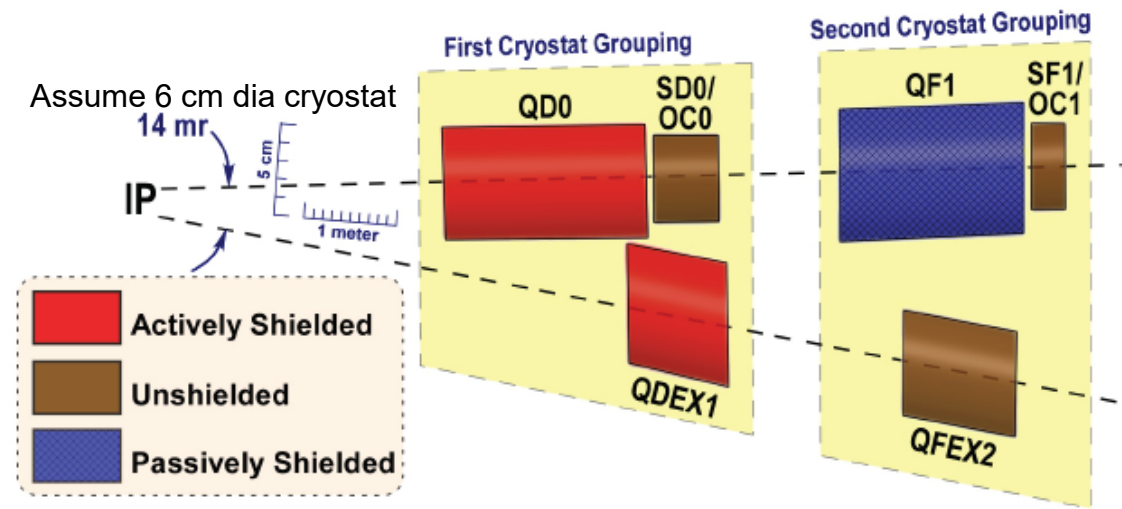
Use parameters for TESLA TDR $\sqrt{s_{\gamma\gamma}} = 500 \text{ GeV}, \quad x = 4.5$

TESLA-500, $\gamma\gamma$		
Repetition rate	f_{rep} [Hz]	5
Beam pulse length	T_P [μ s]	950
RF-pulse length	T_{RF} [μ s]	1370
No. of bunches per pulse	n_b	2820
Bunch spacing	Δt_b [ns]	337
Charge per bunch	N_e [10^{10}]	2
Emittance at IP	$\gamma\epsilon_{x,y}$ [10^{-6} m]	3, 0.03
Beta at IP	$\beta_{x,y}^*$ [mm]	4, 0.4
Beam size at IP	$\sigma_{x,y}^*$ [nm]	157, 5
Bunch length at IP	σ_z [mm]	0.3
Geometric luminosity	L_{geom} [$10^{34}\text{cm}^{-2}\text{s}^{-1}$]	5.8
Effective $\gamma\gamma$ luminosity	$L_{\gamma\gamma}$ [$10^{34}\text{cm}^{-2}\text{s}^{-1}$]	0.6

Table 1.3.2: Beam parameters for the $\gamma\gamma$ option. The effective luminosity takes into account only the high energy peak of the luminosity spectrum ($E_{cm,\gamma\gamma} \approx 400 \text{ GeV}$), see part VI, chapter 1 for details.

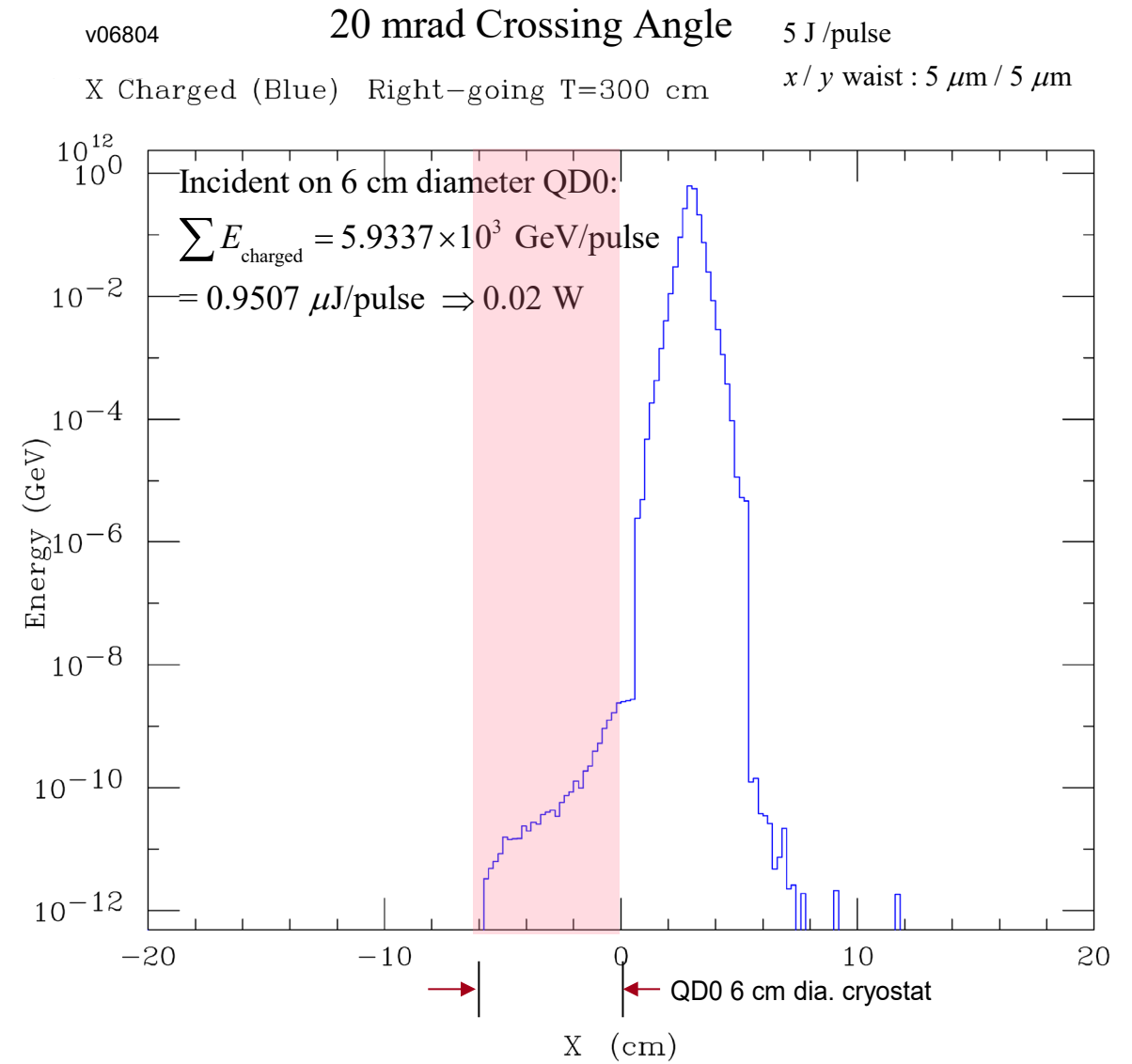
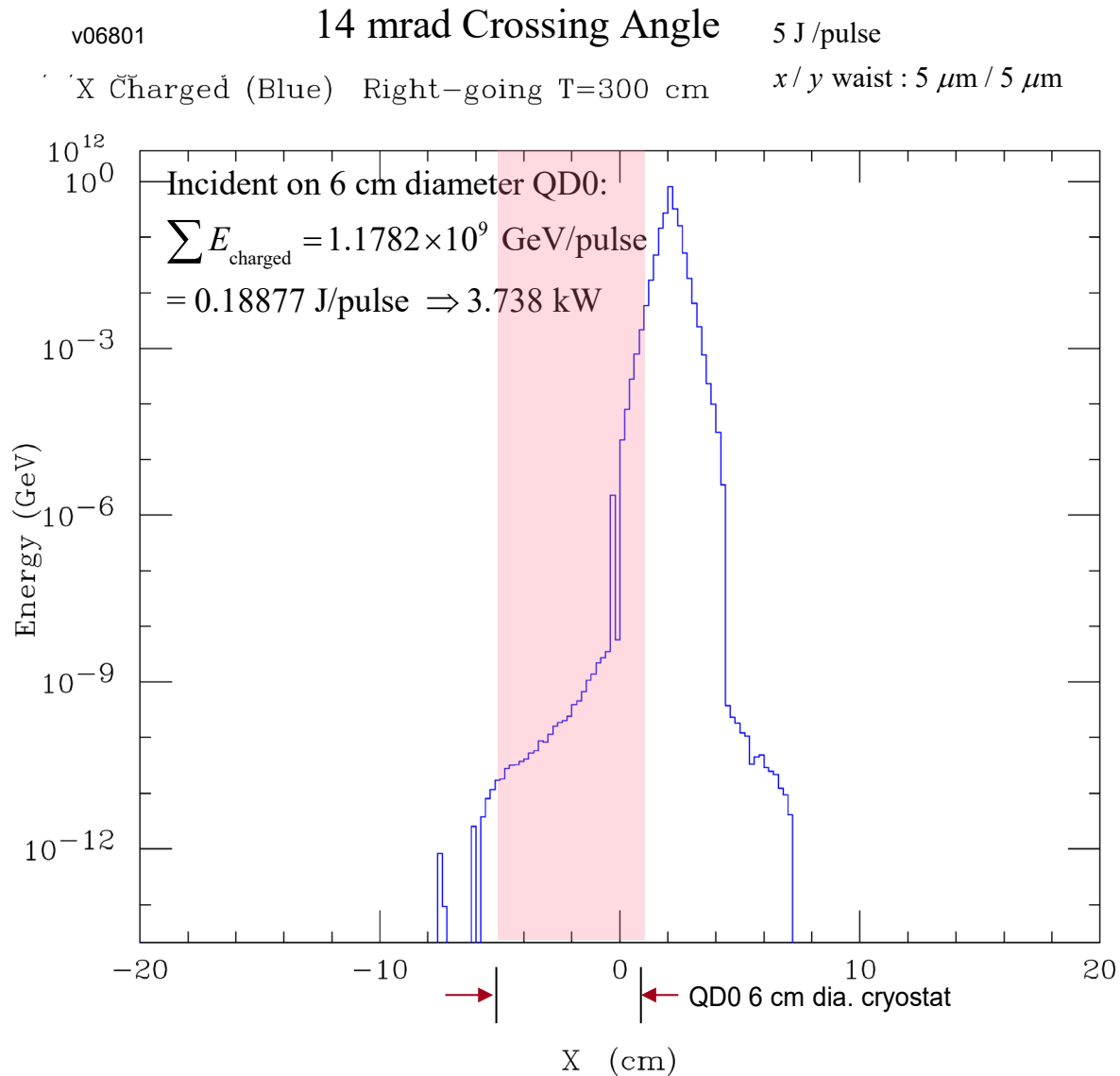
$2E_0$ [GeV]	200	500	800
λ_L [μ m]/ x	1.06/1.8	1.06/4.5	1.06/7.2
t_L [λ_{cont}]	1.35	1	1
$N/10^{10}$	2	2	2
σ_z [mm]	0.3	0.3	0.3
$f_{rep} \times n_b$ [kHz]	14.1	14.1	14.1
$\gamma\epsilon_{x/y}/10^{-6}$ [m·rad]	2.5/0.03	2.5/0.03	2.5/0.03
$\beta_{x/y}$ [mm] at IP	1.5/0.3	1.5/0.3	1.5/0.3
$\sigma_{x/y}$ [nm]	140/6.8	88/4.3	69/3.4
b [mm]	2.6	2.1	2.7
$L_{ee}(geom)$ [$10^{34} \text{ cm}^{-2}\text{s}^{-1}$]	4.8	12	19
$L_{\gamma\gamma}(z > 0.8z_{m,\gamma\gamma})$ [$10^{34} \text{ cm}^{-2}\text{s}^{-1}$]	0.43	1.1	1.7
$L_{\gamma e}(z > 0.8z_{m,\gamma e})$ [$10^{34} \text{ cm}^{-2}\text{s}^{-1}$]	0.36	0.94	1.3
$L_{e^+e^-}(z > 0.65)$ [$10^{34} \text{ cm}^{-2}\text{s}^{-1}$]	0.03	0.07	0.095

Table 1.4.1: Parameters of the $\gamma\gamma$ collider based on TESLA. two options.



As discussed in Section 1.3.2.1 the 5 μ m spot size of the laser beam matches the effective crabbed horizontal beam size of $\sigma_x = \sigma_z \alpha_c / 2 = 5 \mu\text{m}$ for $\sigma_z = 300 \mu\text{m}$ and $\alpha_c = 34 \text{ mrad}$ Hence there is little luminosity degradation for $0 < \alpha_c < 34 \text{ mrad}$ Not the case for XCC where laser spot size is 21 nm and $\sigma_x = \sigma_z \alpha_c / 2 = 340 \mu\text{m}$ for $\sigma_z = 20 \mu\text{m}$ and $\alpha_c = 34 \text{ mrad}$

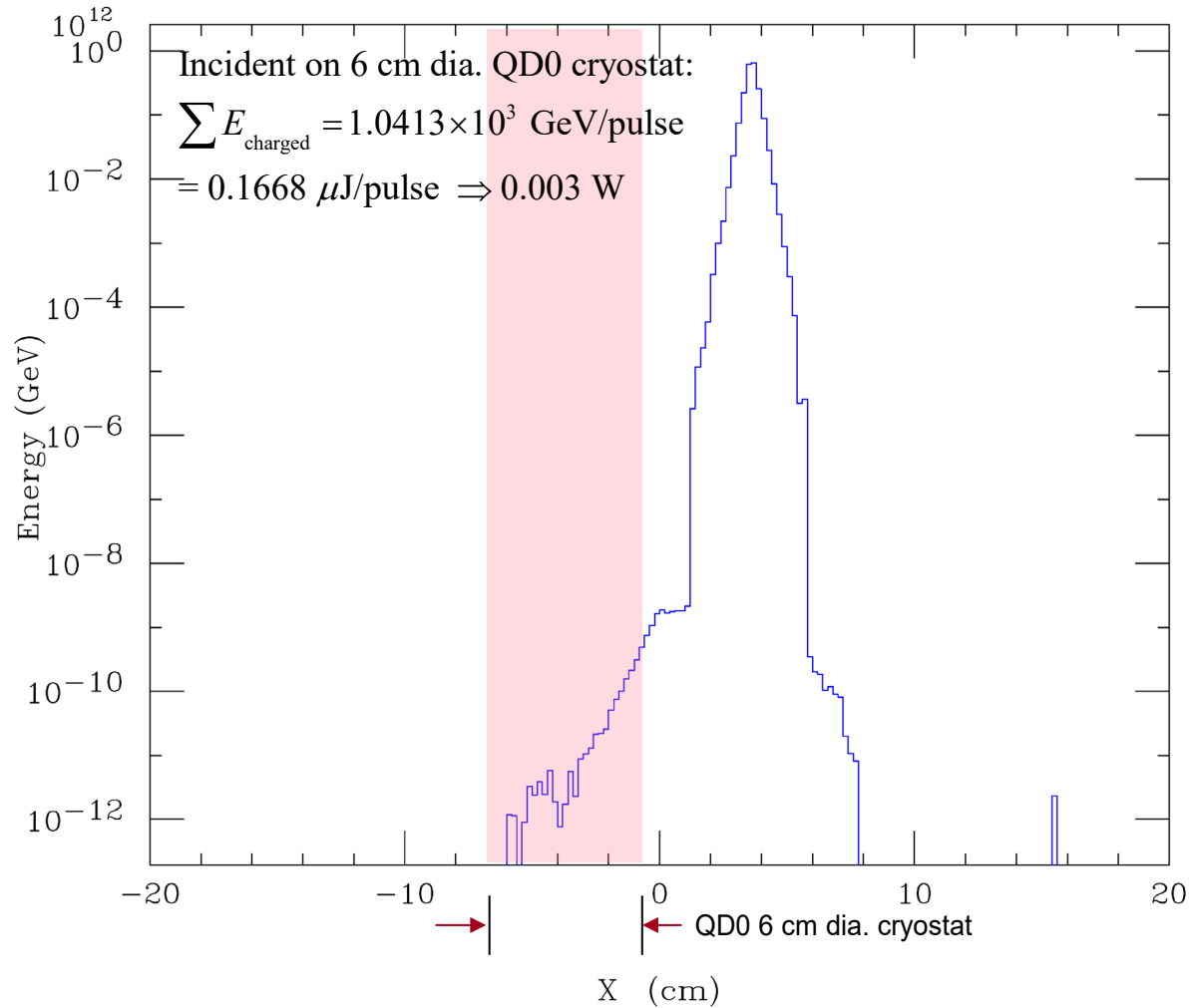
TESLA TDR $\gamma\gamma$ Collider $\sqrt{s} = 500$ GeV



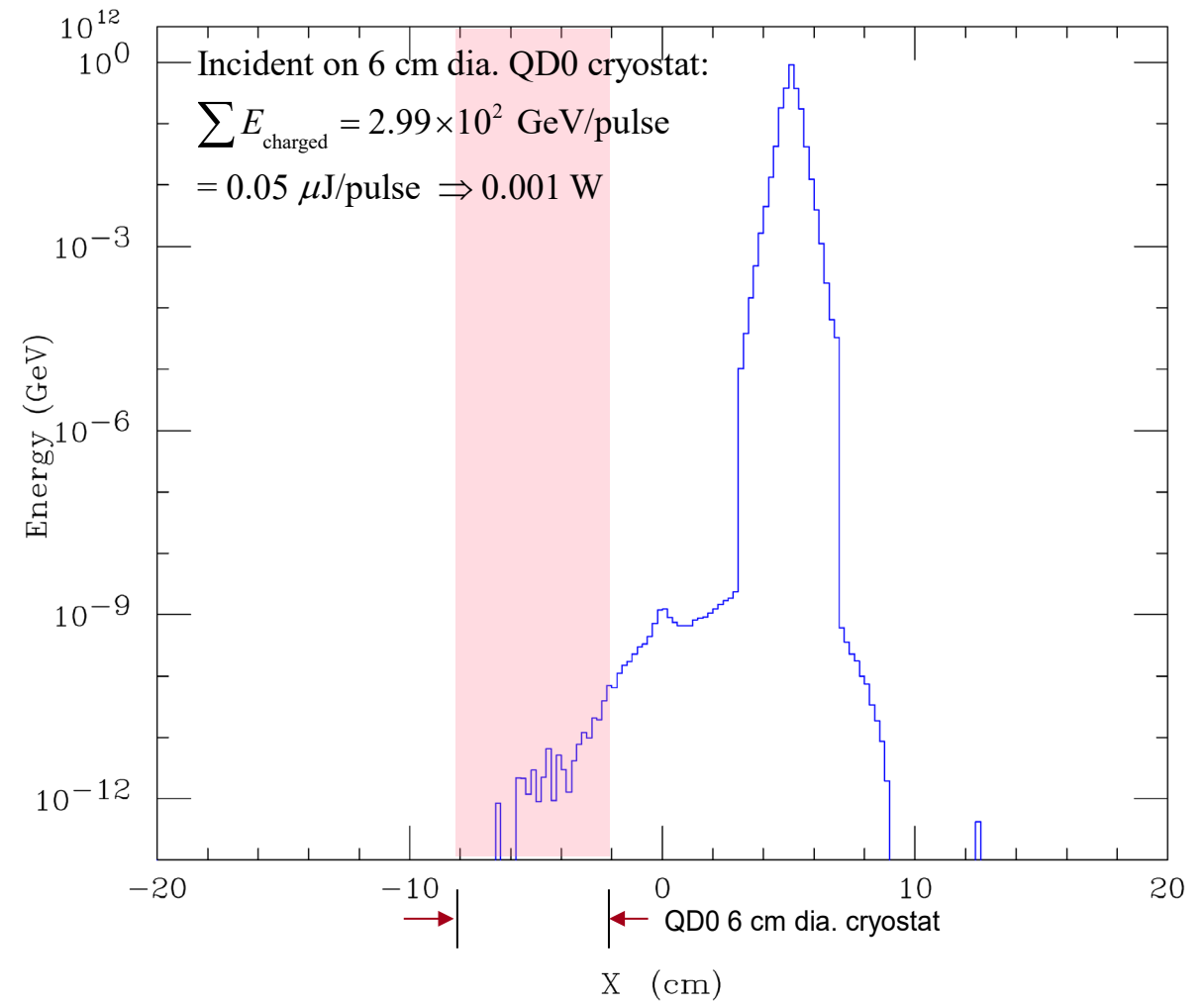
Assuming only few Watts on QD0 is tolerable, we conclude that 14 mrad is insufficient and 20 mrad is the minimum crossing angle. 50

TESLA TDR $\gamma\gamma$ Collider $\sqrt{s} = 500$ GeV

v06802 24 mrad Crossing Angle 5 J/pulse
X Charged (Blue) Right-going T=300 cm x/y waist : 5 μm / 5 μm



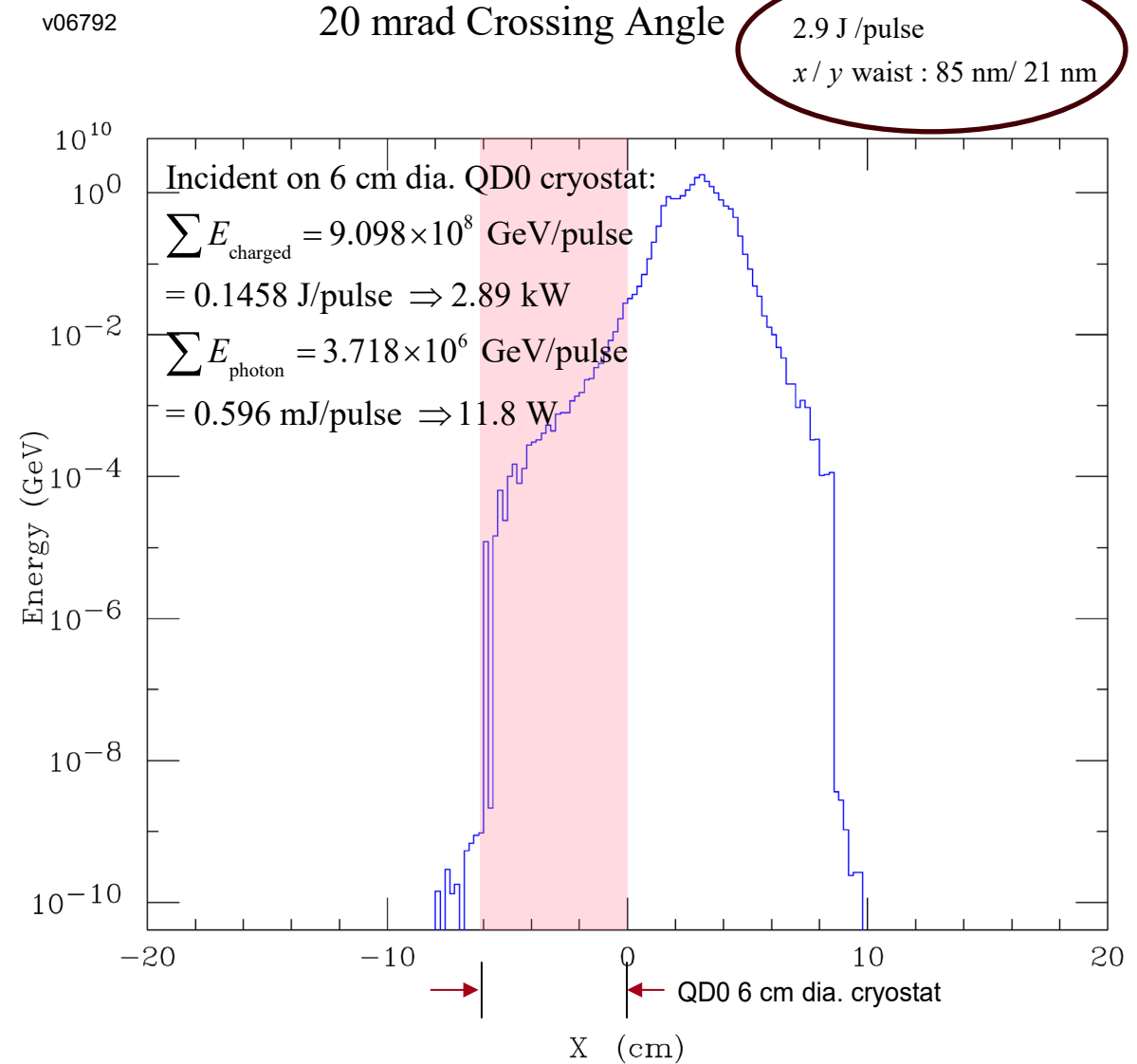
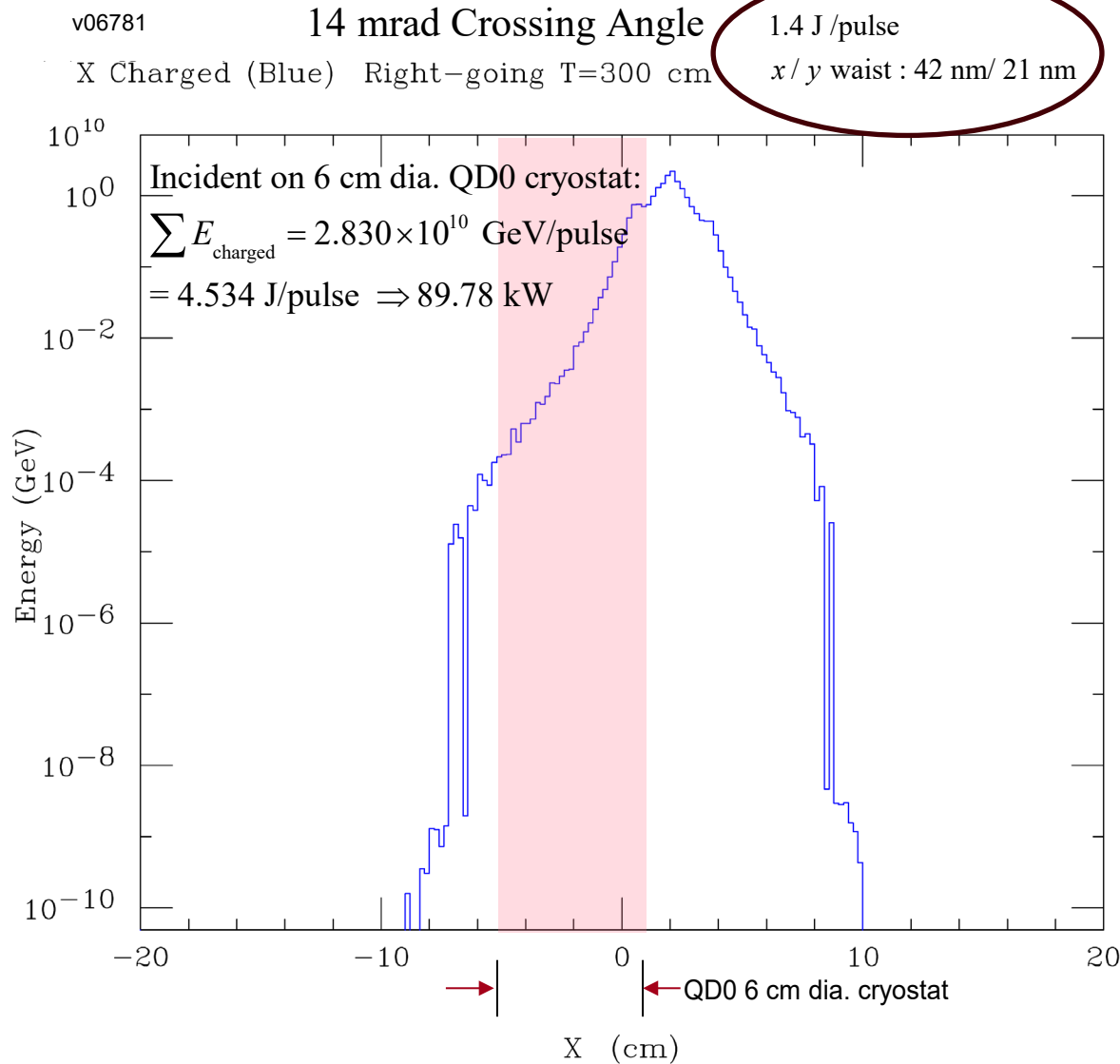
v06803 34 mrad Crossing Angle 5 J/pulse
X Charged (Blue) Left-going T=300 cm x/y waist : 5 μm / 5 μm



Conclude from CAIN that 24 mrad is more comfortable than 20 mrad and 34 mrad is overkill

XCC $\gamma\gamma$ Collider $\sqrt{s} = 125$ GeV

Increase horizontal laser spot size from 21 nm to 42 (85) nm to better match
 $\sigma_x = \sigma_z \alpha_c / 2$. Increase pulse energy to maintain laser photon density



20 mrad will work if collimators are installed to protect QD0; must study size of collimator backscatter into detector

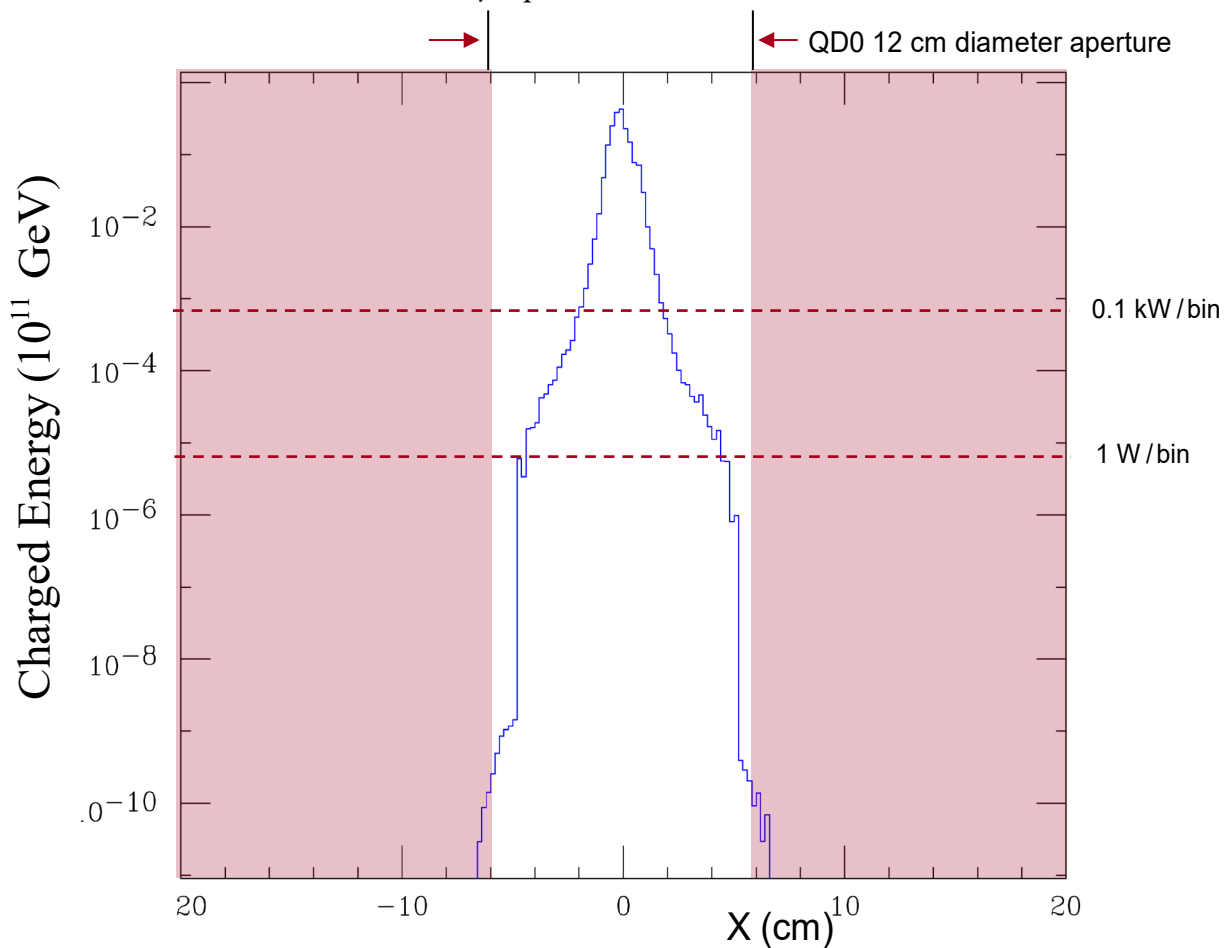
2 mrad crossing angle, $L^*=1.5$ m

CAIN Simulation from IP to Face of Quad at $L^*=1.5$ m, Assume 5 T Solenoid

Incident on Triplet Cryostat:

$$\sum E_{\text{charged}} = 4.2306 \times 10^2 \text{ GeV/pulse}$$

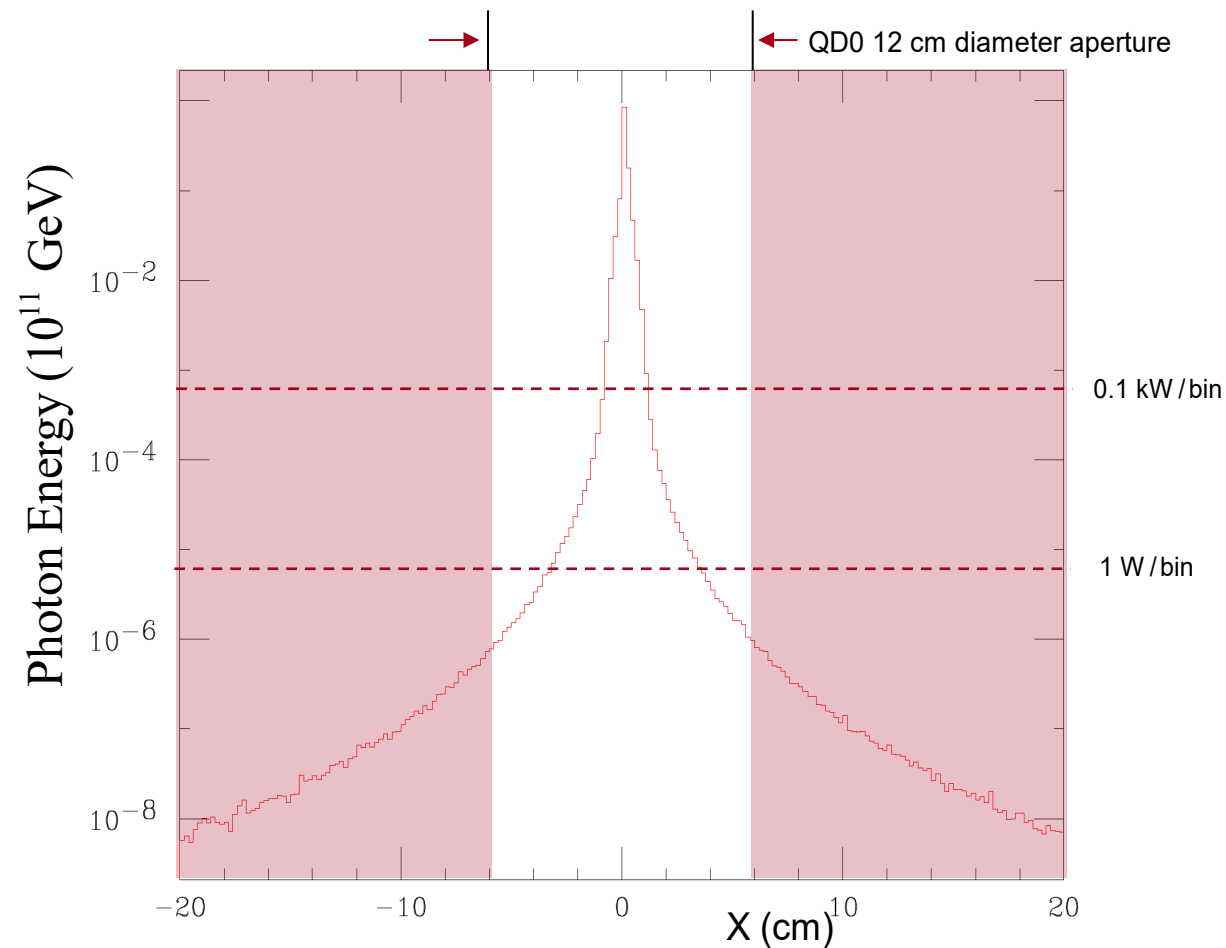
$$= 0.07 \text{ } \mu\text{J/pulse} \Rightarrow 0.001 \text{ W}$$



Incident on Triplet Cryostat:

$$\sum E_{\text{photon}} = 4.2306 \times 10^2 \text{ GeV/pulse}$$

$$= 0.29 \text{ mJ/pulse} \Rightarrow 5.8 \text{ W}$$



Solution requires large aperture HL-LHC-like final triplet. Significant departure from usual e+e- collider design